Schizophrenia: Effect of Fluanxol® treatment on redox status

Jenna Fay Annandale

Thesis presented in partial fulfillment of the requirements for the degree of Master of Science (Physiology) in the Faculty of Natural Science at Stellenbosch University.

Supervisor: Prof Carine Smith

March 2021

Declaration

By submitting this thesis electronically, I declare that the entirety of the work contained therein is my own, original work, that I am the sole author thereof (save to the extent explicitly otherwise stated), that reproduction and publication thereof by Stellenbosch University will not infringe any third party rights and that I have not previously in its entirety or in part submitted it for obtaining any qualification.

Signature: Date: 25/02/2021

Abstract

Oxidative stress has been implicated in the pathology of schizophrenia, with impaired antioxidant mechanisms observed in these patients. The modulatory role of oxidative stress on the activity of NMDA receptors on GABA interneurons impacts neurotransmitter signalling, leading to hyperdopaminergic dysfunction (directly associated with the disease symptoms), microglial activation and a pro-inflammatory shift, rendering these patients susceptible to inflammatory comorbidities. It is therefore important to investigate therapeutic drugs prescribed to schizophrenia patients for their effect on redox status. Flupentixol dihydrochloride (Fluanxol®) is prescribed to patients with schizophrenia and has known antipsychotic effects. However, the mechanisms by which this drug exerts those effects are not yet fully elucidated, particularly in terms of its effect on redox status and inflammation.

We aimed to investigate the effect of the antipsychotic, Fluanxol®, on redox status *in vitro* using BE(2)-M17 neuroblastoma cells, to simulate the target site, and CaCo2 gut epithelial carcinoma cells, to simulate the site of absorption, in the presence or absence of an inflammatory challenge (LPS). Cell viability (WST-1) validated the prescribed doses of Fluanxol® in our cellular models. Oxidant production (H_2O_2 assay kit), oxidative damage (TBARS (MDA) assay) and antioxidant capacity (TEAC) were assessed to probe the drug's effect on redox status. Further investigation *in vivo* in zebrafish was used to assess effect of Fluanxol® on redox at whole organism complexity. After confirming non-toxicity of treatment doses *in vivo*, zebrafish were subjected to induced seizures using the pentylenetetrazole (PTZ) model, to determine therapeutic dose of Fluanxol® treatment in zebrafish. Activity monitoring was performed using a Daniovision activity tracker and Ethovision software. Optimal therapeutic dose of Fluanxol® treatment was assessed in terms of potential effects on redox status in zebrafish larvae at 4 days post-fertilisation (dpf), using the fluorescent ROS marker CM-H_2DCFDA and live organism microscopy.

No detrimental effects of Fluanxol® were observed *in vitro,* in terms of redox status. Dosage adjusted for bioavailability, confirmed that Fluanxol® does not display mitochondrial toxicity at the prescribed doses (3 mg/day to 12 mg/day), but mitochondrial toxicity was observed at an overdose concentration equivalent to 30 mg/day ($p<0.0001$). In the zebrafish model of psychosis, potential GABAergic effects of Fluanxol® was observed ($p<0.0001$). In addition, a novel finding was an antioxidant effect of Fluanxol®, as illustrated by reduced ROS (fluorescent intensity ($p<0.01$) and fluorescent area ($p<0.05$)) in 5 dpf zebrafish larvae.

We conclude that Fluanxol® exhibited *in vitro* mitochondrial toxicity only at a dose equivalent to human overdose concentration, but that little to no toxicity is present within the prescribed doses. In line with this *in vitro* data, doses of Fluanxol® showing maximal antipsychotic effect in a zebrafish larval model, also reduced ROS levels, suggesting its therapeutic effect to include a positive outcome in terms of

redox status. Finally, the observed antipsychotic effect of Fluanxol® in the PTZ model in zebrafish additionally suggest GABAergic modulation as a potential additional mechanism of action of this drug.

Uittreksel

Oksidatiewe stress word geïmpliseer in skisofrenie patologie, met ingekorte teen-oksidant meganismes in pasiënte. Die modulerende rol van oksidatiewe stress op dieaktiwiteit van NMDA reseptore on GABA interneurone wat neurologiese seinoordrag beïnvloed, en lei sodoende na hiperdopaminergiese wanfunksie (direk geassosieer met siekte simptome), mikrogliale aktevering en ‘n pro-inflammatoriese skuif, wat hierdie pasiënte meer vatbaar vir inflammatoriese ko-morbiditeite maak. Dit is daar belangrik om terapeutiese middels wat aan skisofrenie lyers voorgeskryf word, te ondersoek en hul effek op redoksstatus te bepaal. Flupentixol dihydrochloride (Fluanxol®) word aan skisofrenie pasiënte voorgeskryf en het bekende anti-psigotiese effekte, maar die meganismes waardeur hierdie middel sy effekte uitoefen, is nog nie heeltemal duidelik nie. In terme van sy effek op redoksstatus en inflammasie spesifiek, is geen inligting bekend nie.

Ons het beoog om die effek van die anti-psigotiese middel Fluanxol®, op *in vitro* redoksstatus te bepaal. Om hierdie doel te bereik, is BE(2)-M17 neuroblastoomselle, om die teikenwerf voor te stel, en CaCo2 kolonepiteelkarsinoomselle, om die absorpsieplek voor te stel, in die teenwoordigheid of afwesigheid van 'n inflammatoriese uitdaging (LPS). Sel lewensvatbaarheid (WST-1) het die voorgeskrewe dosisse Fluanxol® in ons sellulêre modelle gevalideer. Oksidatiewe stres (H_2O_2), oksidatiewe skade (TBARS (MDA) toets) en teen-oksidant kapasiteit (TEAC) is bepaal om die effek op die redoksstatus te ondersoek. Verdere ondersoek in vivo in sebravisse is gebruik om die effek van Fluanxol® op redoks by die hele organisme se kompleksiteit te bepaal. Na die bevestiging van nie-toksiese doserings *in vivo*, is sebravisse aan eksperimentele psigose in die pentileentetrasol (PTZ) model blootgestel, om terapeutiese dosis te bepaal van Fluanxol® behandeling in sebravisse. Aktiwiteit is met ‘n Daniovision aktiwiteitspoorder en Ethovision sagteware gemeet. Optimale terapeutiese doserings van Fluanxol® is ook in terme van die effek op redoksstatus in zebravislarwes teen 4 dae na bevrugting (dnb), gemeet, deur gebruik te maak van die RSS merker CM-H_2DCFDA en lewende organisme mikroskopie.

Geen nadelige effekte is *in vitro* vir Fluanxol® waargeneem in terme van redoksstatus nie. Nadat dosis aangepas is vir biobeskikbaarheid, is vasgestel dat Fluanxol® nie mitokondriale vergiftiging by voorgeskrewe dosisse (3 mg/dag tot 12 mg/dag) tot gevolg gehad het nie, maar wel by ‘n oordosering gelykstaande aan 30 mg/dag ($p<0.0001$). In die zebravismodel van psigose is moontlike GABAergiese effekte van Fluanxol® gemeet ($p<0.0001$). ‘n Verdere nuwe bevinding was ‘n teen-oksidant effek van Fluanxol®, soos geïllustreer deur verlaagde RSS (fluoresensie intensiteit ($p<0.01$) en area van fluoresensie ($p<0.05$)) in 5 dnb zebravislarwes.

Ons bevind dat Fluanxol® slegs in ‘n dosering gelykstaande aan menslike oordosering, *in vitro* mitokondriale vergiftiging veroorsaak, maar dat min of geen vergiftiging by doserings gelykstaande aan voorgeskrewe terapeutiese doserings voorkom nie. In lyn met hierdie *in vitro* data, het doserings van

Fluanxol® wat goeie terapeutiese effek in die zebravismodel van psigose gehad het, ook laer RSS vlakke tot gevolg gehad, wat aandui dat die terapeutiese effekte van hierdie middel ook positiewe effekte op redoksstatus insluit. Laastens suggereer die waargenome teen-psigotiese effekte van Fluanxol® in die PTZ model in zebravisse dat GABAergiese modulering ‘n moontlike addisionele meganisme van aksie van hierdie middel mag wees.

Acknowledgements

The National Research Foundation (NRF) – For financial support of this study.

The Stellenbosch post graduate support office and the Adele Searll 100 Club for funding.

The Central Analytic Facilities (CAF) Microscopy Unit at Stellenbosch University for assistance with acquisition of imaging data.

Professor Carine Smith – There are no words to hold the gravitas of my gratitude for such a phenomenal supervisor and an incredibly inspiring woman.

Hannes van der Merwe – Thank you for all the insight, guidance and support with the zebrafish work.

MSB research group; especially Dr Kelly Ross, Dr Yigael Powrie, Tracey Ollewagen, Lesha Pretorius and Rohan Benecke

My friends and family for all their love and support.

Research Output

Southern African Neuroscience Society (SANS) 2020 Symposium (October 2020). Online. Oral Presentation: “Probing mechanisms of action of the antipsychotic Fluanxol® in cell culture and zebrafish”.

Contents

List of Abbreviations

Abbreviation	Meaning
5-HT	Serotonin
ABTS	2,2'-Azino-bis(3-ethylbenzothiazoline-6-sulfonic acid)
ATP	Adenosine triphosphate
BBB	Blood-brain barrier
BDNF	Brain-derived neurotrophic factor
BHT	Butylated hydroxytoluene
CaCl	Calcium chloride
CAT	Catalase
CCL2	Chemokine ligand 2
CD80	Cluster of differentiation 80
CD86	Cluster of differentiation 86
CM-H_2DCFDA	5-(and 6-)chloromethyl-2',7'-dichlorodihydrofluorescein diacetate
CNS	Central nervous system
COX-2	Cyclooxygenase-2
CSF	Cerebral spinal fluid
CYP	Cytochrome P450
DA	Dopamine
dH_2O	Distilled water
DMEM	Dulbecco's modified eagle's medium
DNA	Deoxyribonucleic acid
Dpf	Days post fertilisation
DRD	Dopamine receptor
EPC	Equivalent plasma concentration
FBS	Foetal bovine serum
Fe	Iron
FEP	First-episode psychosis
FGA	First generation antipsychotic
Fpn1	Ferroportin1

GABA	Gamma-Aminobutyric acid
GM-CSF	Granulocyte–macrophage colony-stimulating factor
GPx	Glutathione peroxidase
GR	Glutathione reductase
GSH	Reduced glutathione
GSSG	Glutathione disulphide
GWAS	Genome-wide association study
H_2O_2	Hydrogen peroxide
HBSS	Hank's balanced salt solution
HIF-1α	Hypoxia inducible factor-1 alpha
HNO_3	Nitric acid
HO-1	Heme oxygenase 1
Iκβ	Inhibitor of kappa beta
IL	Interleukin
IRP2	Iron regulatory protein 2
KCl	Potassium chloride
KYNA	Kynurenic acid
LIP	Labile iron pool
LPS	Lipopolysaccharide
LSD	D-lysergic acid diethylamide
MCP-1	Monocyte chemoattractant protein 1
MDA	Malondialdehyde
$MgSO_4$	Magnesium sulphate
MMP	Matrix metalloproteinases
mnSOD	Manganese superoxide dismutase
MTD	Maximum tolerated dose
NaCl	Sodium chloride
NADH	Nicotinamide adenine dinucleotide
NAE-086	(R)-3,4-dihydro-N-isopropyl-3-(N-isopropyl-N-propylamino)-2H-1-benzopyran-5-carboxamide
NaOH	Sodium hydroxide

NF-κβ	Nuclear factor kappa beta
NMDA	N-methyl-D-aspartate
NO	Nitric oxide
NO_3^-	Nitrate
NOS	Nitric Oxide Synthase
Nox	Nicotinamide adenine dinucleotide phosphate hydrogen oxidase
Nrf2	Nuclear factor erythroid 2-related factor
$O_2^{\cdot -}$	Superoxide radical
$OH^{\cdot}$	Hydroxyl radical
$ONOO^{\bullet}$	Peroxynitrite
OPA	Ortho-phosphoric acid
P53	Protein 53
PANSS	Positive And Negative Syndrome Scale
PBS	Phosphate buffered saline
PCP	Phencyclidine
PenStrep	Penicillin-Streptomycin
PET	Positron emission tomography
PTZ	Pentylenetetrazole
PV-positive	Parvalbumin-positive
ROS	Reactive oxygen species
RNS	Reactive nitrogen species
SGA	Second generation antipsychotic
SIRT1	Sirtuin 1
SLC	Solute carrier
SNP	Single nucleotide polymorphism
SOD	Superoxide dismutase
TBA	Thiobarbituric acid
TBARS	Thiobarbituric acid reactive substances
TEAC	Trolox Equivalent Antioxidant Capacity
Tf	Transferrin

TfR1	Transferrin receptor 1
T_H	T helper
TNF-α	Tumour necrosis factor alpha
TPH1	Tryptophan hydroxylase 1
TPH2	Tryptophan hydroxylase 2
Trypsin-EDTA	Trypsin ethylenediaminetetraacetic acid
VTA	Ventral tegmental area
WST-1	Water soluble tetrazolium salt 1

List of Figures

List of Tables

Chapter 1

Introduction

Schizophrenia is a well characterised psychiatric disorder affecting about 20 million people around the world (World health organisation, 2019) Schizophrenia is the 19th leading cause of disability globally (James *et al.*, 2018) and can be fatal (Sher and Kahn, 2019), with 50% of patients attempting suicide and 10% succeeding according to a global study, InterSePT, that takes statistics from 67 sites across 11 countries (Meltzer *et al.*, 2003). Reduced life expectancy, of about 20 years, in patients with schizophrenia is not only due to suicide but other comorbidities, preventable diseases, unhealthy lifestyle choices and side effects of antipsychotic medication (Laursen, Nordentoft and Mortensen, 2014; Schmitt *et al.*, 2018). Schizophrenia is a spectrum of disorders diagnosed based on the presence of positive symptoms and can be accompanied by cognitive as well as negative symptoms (Joyce and Roiser, 2007; Tandon *et al.*, 2013).

The cognitive, positive, and negative symptoms of schizophrenia are an effect of abnormal neurotransmitter signalling (Stahl, 2018). Other physiological mechanisms, such as the inflammatory response or redox status, modulate neurotransmitter signalling and neurotransmitter signalling effects other physiological mechanisms, adding complexity to the disease pathology (Perkins, Jeffries and Do, 2020). Inflammation and oxidative stress are also postulated to play a key role in the pathophysiology of schizophrenia (Khoury and Nasrallah, 2018). Oxidative stress is present before onset of first episode of psychosis in what is referred to as the prodromal phase of schizophrenia and is an indicator of probable progression to psychosis in high risk of psychosis patients (Perkins, Jeffries and Do, 2020). Redox status is intricately linked with inflammatory status (Gill, Tsung and Billiar, 2010; El Assar, Angulo and Rodríguez-Mañas, 2013; Biswas, 2016) and plays a critical role in chronic diseases with an inflammatory component. Schizophrenia may be categorised as an inflammatory disease - as discussed in depth in the next chapter with regards to the cytokine hypothesis (Watanabe, Someya and Nawa, 2010). The modulatory effects that redox status has on neurotransmitter signalling and the effects that neurotransmitter signalling has on redox status will be discussed in greater depth in the next chapter.

In terms of treatment, according to Revier *et al.*, (2015) in a ten-year follow up study, only 13% of patients obtain pre-onset level of function with treatment with antipsychotics, with 64% showing some improvement of schizophrenia symptoms and 23% of patients experience drug resistance. This is in line with statistics reported in a review by Tamminga and Holcomb, (2005) with first episode patients who are treatment naïve observed as being more responsive than chronic multi-episode patients

with schizophrenia (Haddad and Correll, 2018). It is evident that current treatment has room for improvement. Further investigation of the mechanisms of the disease is required to elucidate new potential therapeutic targets to improve on current treatment. The mechanisms of action of current treatments needs to be investigated further to understand how treatment for patients with schizophrenia can be improved. Flupentixol dihydrochloride (Fluanxol®) is commonly prescribed to patients with schizophrenia, but its potential effects on redox status have not been fully elucidated. With redox status potentially playing a key role in schizophrenia pathology it is imperative to elucidate the effect treatment has on redox status as this would dictate treatment efficacy and risk of inflammatory co-morbidities. Redox response to treatment can be easily probed in cellular models and further investigated in animal models to further elucidate redox response in a multicellular environment while able to exclude confounding factors often present in clinical trials such as smoking status, substance use, comorbidities etc. Redox parameters are often investigated in isolation, with either oxidant production, oxidative damage or endogenous antioxidant capacity reported (Kowalski, Labuzek and Herman, 2003, 2004; Kropp *et al.*, 2005; Chittiprol *et al.*, 2010; Kim and J.-H. Song, 2016). All three parameters investigated allows for the effects on redox status to be inferred. Therefore, this thesis aimed to investigate the effect of Fluanxol® on redox status and to probe it in different human cellular models, in a manner relevant to site of absorption and target site of the drug *in vitro*, as well as investigate oxidative stress *in vivo* using *Danio rerio* animal models.

In the next chapter, I provide an overview of the most pertinent scientific literature on the topic of schizophrenia pathology, current treatment, and its effect on redox status.

Chapter 2

Literature Review

2.1. Introduction

The mechanisms of the pathogenesis of schizophrenia are complex involving multiple signalling pathways that interact, further complicated by the clinical heterogeny of patients with schizophrenia (Quednow, Geyer and Halberstadt, 2020). There are prominent hypotheses on the pathology of the disease, including the serotonergic hypothesis, the dopaminergic hypothesis, and the cytokine hypothesis, which will be discussed here as a starting point. Additionally, I will provide an overview of the literature on schizophrenia-associated neurotransmitter dysfunction and the mechanisms by which this dysfunction may negatively impact redox status. This will be followed by an overview of the role of inflammation and redox in the pathology of schizophrenia. Finally, in terms of treatment, the known effects of the antipsychotic Fluanxol® will be summarised, pointing out gaps in the literature, in particular pertaining to its effects on redox status and inflammation.

2.2. Neurotransmitter dysfunction hypotheses of Schizophrenia

2.2.1. Serotonergic Hypothesis

The serotonin hypothesis is the second oldest neurochemical hypothesis, second to the transmethylation of norepinephrine hypothesis (Osmond and Smythies, 1952), but is still highly relevant in the pathology of schizophrenia (Quednow, Geyer and Halberstadt, 2010). The hypothesis was first based on the serotonin (5-HT) antagonistic effects of D-lysergic acid diethylamide (LSD), which suggested that decreased serotonin signalling is responsible for the hallucinations experienced by patients with schizophrenia (Gaddum and Hameed, 1954; Woolley and Shaw, 1954). This was then revised to attribute increased serotonin signalling to schizophrenia pathology when LSD was noted to also mimic some 5-HT effects (De Gregorio *et al.*, 2016) while antagonising others. The serotonergic pathway begins at the dorsal and median raphe nuclei and projects to the cerebellum as well as innervates limbic structures such as the thalamus, hypothalamus, amygdala, and hippocampus as well as the frontal cortex and other regions of the forebrain. Serotonergic signalling interacts with and modulates dopaminergic (Browne *et al.*, 2019) and glutamatergic signalling (Wang *et al.*, 2019), resulting in linked dysfunction within the pathology of schizophrenia.

Serotonin is a monoamine neurotransmitter derived from tryptophan (Curran and Chalasani, 2012). Serotonin quenches reactive oxygen species (ROS) through its ROS-scavenging activity and reduces inflammatory cytokine production from macrophages (Vašíček, Lojek and Číž, 2020) and when it binds to receptor 5-HT_{1A} receptors in the brain increases cortisol secretion from the adrenal

gland in the periphery (Ronaldson *et al.*, 2018) which has been observed to be elevated in patients with schizophrenia (Yildirim *et al.*, 2011; Sun *et al.*, 2016). Chronically elevated cortisol secretion leads to glucocorticoid receptor insensitivity (glucocorticoid resistance) resulting in a pro-inflammatory shift which is coupled with a pro-oxidant shift (Barnes and Adcock, 2009). This suggests a link between the serotonin hypothesis and the cytokine hypothesis (and redox).

A detailed discussion on all the serotonin receptor subtypes is beyond the scope of this thesis. Focus will be limited to 5-HT receptors most relevant to informing my study rationale. Treatments such as tandospirone, that act as 5-HT_{1A} receptor agonists, have shown efficacy in improving cognitive symptoms of schizophrenia such as verbal memory and executive functions, when administered on its own or in conjunction with typical antipsychotics that lack serotonergic effects (Huang *et al.*, 2017). 5-HT_{1A} receptor agonist, (R)-3,4-dihydro-N-isopropyl-3-(N-isopropyl-N-propylamino)-2H-1-benzopyran-5-carboxamide (NAE-086), affected control volunteers negatively by inducing hallucinations and nightmares (Rënyi *et al.*, 2001) which is also supported by 5-HT_{1A} agonist, LSD, which induces hallucinations (De Gregorio *et al.*, 2016). This indicates that upregulation of 5-HT_{1A} receptor activity within a narrow range, that should be individually optimised, may benefit schizophrenic patients. It is possible, however, that the hallucinogenic effects of LSD and NAE-086 are attributed to agonism and sensitisation, respectively, of the 5-HT_{2A} receptor as Buspirone, a 5-HT_{1A} agonist, is an anxiolytic that does not induce psychosis (Rënyi *et al.*, 2001). Buspirone has dopamine receptor antagonistic effects, however, which could account for the absence of hallucinogenic effects. 5-HT_{1A} receptors are therefore still suspect in schizophrenia pathology but further investigation is required to elucidate the divergent results observed in positron emission tomography (PET) studies (Quednow, Geyer and Halberstadt, 2020).

Decreased levels of serotonin and 5-HT_{2A} receptor density was observed centrally in post-mortem studies (Quednow, Geyer and Halberstadt, 2010) and elevated 5-HT_{1A} receptor density prefrontal cortex (Weinberger and Laruelle, 2002; Bantick *et al.*, 2004; Selvaraj *et al.*, 2014) which has been challenged by PET studies in younger subjects that are treatment naïve which record that no difference in 5-HT_{2A} receptor density was observed in the cortex of these patients compared to controls (Trichard *et al.*, 1998; Okubo *et al.*, 2000; Verhoeff *et al.*, 2000; Bantick *et al.*, 2004; Erritzoe *et al.*, 2008). Contradictory results in CNS levels of 5-HT and density of 5-HT_{1A} and 5-HT_{2A} receptors in schizophrenia patients have been reviewed by Quednow and Geyer (2020). These discrepancies are multifactorial and include potential degradation of receptors and aging effects in older subjects in post-mortem studies, confounding effects of antipsychotic treatment (Trichard *et al.*, 1998), lack of specificity of the radio ligands used in PET studies, receptor occupancy in immunohistochemistry studies and broad phenotypic variance of the disease (Quednow, Geyer and Halberstadt, 2020). Single nucleotide polymorphisms A-1438G - found in the promotor region of the gene (Parsons *et al.*, 2004)- and T102C for the 5-HT_{2A} serotonin receptor have been identified as potential factors in

reduced receptor expression by reducing transcription of the 5-HT_{2A} receptor gene (Quednow, Geyer and Halberstadt, 2010).

Both 5-HT_{2A} and 5-HT_{2C} receptors show a modulatory role on dopamine (DA) signalling, however, their effects are inverse to each other. When serotonin binds to 5-HT_{2A} it signals an increase of dopamine release into the synaptic cleft (Aghajanian and Marek, 2000) whereas 5-HT_{2C} signalling inhibits synaptic dopamine release (Alex and Pehek, 2007). SNPs of 5-HT_{2C} receptors associated with patients with schizophrenia may result in decreased receptor expression (Reynolds, Zhang and Zhang, 2002) which would provide a potential explanation of hyperdopaminergic signalling implicated in schizophrenia pathology, which induces an increase in oxidative stress as discussed below (Figure 2.1).

Together, these findings seem to suggest that the decreased levels of at least some sub-types of serotonin receptors such as 5-HT_{2A} and increased levels of 5-HT_{1A} in psychosis may be a downstream effect, rather than a primary cause of the psychosis. The largest Genome-wide association study (GWAS) study to date supports this, with 108 most significant variants associated with schizophrenia found to not include any SNPs related to serotonergic pathways (Ripke *et al.*, 2014). Serotonergic dysfunction in schizophrenia may be a downstream effect of other transmitter signalling innervating its pathway, modulated by oxidative stress and inflammation, as will be elucidated further in the sections to follow.

2.2.2. Dopaminergic Hypothesis

The dopaminergic pathways are affected by serotonergic signalling and is evident to be implicated in schizophrenia pathology as shown in studies reviewed by McCutcheon, Abi-Dargham and Howes (2019). The dopaminergic hypothesis of schizophrenia suggests the pathology of this disorder to be linked to hyperactive dopamine signalling in the mesolimbic pathway from the ventral tegmental area (VTA) innervating the ventral striatum, the nucleus accumbens, amygdala and hippocampus (Stahl, 2018) potentially the cause of positive symptoms. Indeed, in patients with schizophrenia, elevated presynaptic dopamine synthesis capacity has been observed, but in the associative striatum and sensorimotor striatum and not significantly elevated in the limbic striatum (McCutcheon *et al.*, 2018). Presynaptic dopamine synthesis capacity measures in the ventral striatum may be confounded by small volume size of this region and close proximity to other regions that may allow for overspill of radiotracer (McCutcheon *et al.*, 2018) and therefore ruling out this region for elevated dopamine signalling requires further investigation. Furthermore, negative symptoms are ascribed to hypoactive dopamine signalling within the prefrontal cortex (da Silva Alves *et al.*, 2008; Quednow, Geyer and Halberstadt, 2010; Yoon *et al.*, 2013; Slifstein *et al.*, 2015). These abnormalities may be linked as diminished cortical dopamine signalling from lesions in frontotemporal regions in animal studies have been associated with an induced elevated striatal dopamine signalling (Howes and Kapur, 2009).

The dopamine hypothesis is further supported by the efficacy of dopamine-antagonistic antipsychotics in reducing psychosis in patients with schizophrenia (Kapur and Mamo, 2003; Brisch *et al.*, 2014; Remington *et al.*, 2016). Another dopaminergic pathway implicated in schizophrenia is the nigrostriatal pathway which starts at the substantia nigra and projects into the striatum, including the caudate and putamen (McCutcheon, Abi-Dargham and Howes, 2019). Hyperdopaminergic signalling, compared to matched controls, has been observed in the striatum in the rostral and dorsal parts of the caudate in patients with schizophrenia (Kegeles *et al.*, 2010; Howes *et al.*, 2012). Extrapyramidal side effects from antipsychotics are more prevalent in antipsychotics that occupy more than 68% of striatal D_2 dopamine receptors (Uchida *et al.*, 2011). When a patient is treated with antipsychotics, an overcompensating decrease in dopamine signalling in the nigrostriatal pathway can result in Parkinsonism (Shin and Chung, 2012) if striatal D_2 receptor occupancy is too high.

Dopamine is a monoamine neurotransmitter that binds to D_1, D_2, D_3, D_4 and D_5 receptors (Mishra, Singh and Shukla, 2018). Antipsychotic tolerance is observed in patients with schizophrenia which is not surprising as receptor adaptation has been observed in cases of cocaine and amphetamine use (Ashok *et al.*, 2017). With chronic D_2 dopamine receptor antagonism from antipsychotic treatment, a possible compensation mechanism of an increase in dopamine receptors on the postsynaptic neuron is suspected. This is supported by super-sensitivity psychosis which occurs at the abrupt halt of antipsychotic treatment (Seeman *et al.*, 2005; Chouinard *et al.*, 2017). Of particular relevance to the current thesis, elevated levels of dopamine induce oxidative stress in neurons (Miyazaki and Asanuma, 1999). Dopamine metabolism results in reactive dopamine quinones adding to ROS (Grima *et al.*, 2003; Blesa *et al.*, 2015). Metabolism of dopamine by monoamine oxidase produces hydrogen peroxide (H_2O_2) as a by-product (Youdim, 2018). Oxidative stress can be caused by elevated dopamine levels facilitating intracellular iron accumulation in macrophages as seen in Figure 2.1.

Elevated dopamine levels in the extracellular environment can form a complex with iron which are then transported into cells, such as macrophages, via dopamine receptors or potentially solute carriers (Dichtl *et al.*, 2018). Intracellularly these iron complexes induce upregulation of ferritin translation which then induces oxidative stress and upregulated transcription of nuclear factor erythroid 2-related factor (Nrf2) and hypoxia inducible factor-1α (HIF-1α). Upregulated HIF-1α induces an increase in transferrin receptor 1 (TfR1) expression (Yang *et al.*, 2018) increasing intracellular iron influx. Upregulated Nrf2 and HIF-1α transcription, however, simultaneously increase iron exporter ferroportin1 (Fpn1) (Dichtl *et al.*, 2018) balancing iron efflux and preventing intracellular iron accumulation and therefore oxidative stress. Nrf2 induces the antioxidant response element including heme-oxygenase-1 which counteract oxidative stress through breakdown of heme into biliverdin which is converted into a potent antioxidant bilirubin by biliverdin reductase (Loboda *et al.*,

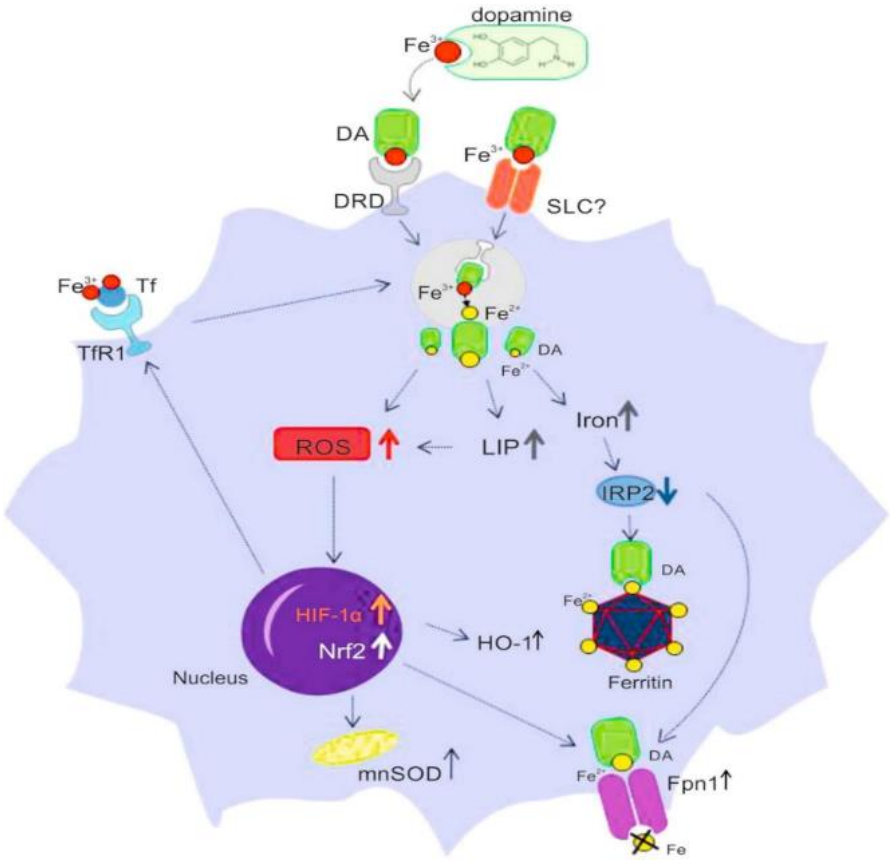

Figure 2.1: Dopamine-induced intracellular iron accumulation and oxidative stress. *Elevated extracellular dopamine facilitates iron accumulation in macrophages leading to ROS production and oxidative stress. DA: dopamine, DRD: dopamine receptor, Fe: iron, Fpn1: ferroportin1, HIF-1α: hypoxia inducible factor-1α, HO-1: heme oxygenase-1, IRP2: iron regulatory protein 2, LIP: labile iron pool, mnSOD: mitochondrial superoxide dismutase, Nrf2: nuclear factor erythroid 2-related factor, ROS: reactive oxygen species, SLC: solute carrier, Tf: transferrin, TfR1: transferrin receptor 1. (Dichtl et al., 2018)*

2016). In schizophrenia pathology, however, Nrf2 signalling is dysfunctional resulting in attenuation of compensatory redox mechanisms to counteract the effects of elevated dopamine resulting in intracellular iron accumulation and oxidative stress (Genc and Genc, 2009). Oxidative stress modulates N-methyl-D-aspartate (NMDA) receptor function resulting in hyperactive dopamine signalling. These elevated dopamine levels could therefore be a downstream effect of serotonergic hyperdrive or NMDA hypoactivity resulting in glutamatergic dysfunction from (gamma-Aminobutyric acid) GABA attenuation (Stahl, 2018) as will be discussed below in the next section.

2.2.3 Glutamatergic dysfunction

Psychotic symptoms have been observed to be exacerbated in patients suffering from schizophrenia who consumed ketamine or phencyclidine (PCP). Ketamine and PCP are both glutamate antagonists at the NMDA receptor (Tamminga and Holcomb, 2005) indicating a role of glutamatergic dysfunction in schizophrenia pathology. Ketamine exposure reduced NMDA signalling and resulted in hallucinations in control subjects and PCP-induced pre-pulse inhibition deficits in rodents which is an indicator of cognitive deficits present in psychotic disorders such as schizophrenia (Geyer and Ellenbroek, 2003). Antagonism of NMDA receptors has been observed to increase serotonin release

in the brain (Martin, Carlsson and Hjorth, 1998; Amargós-Bosch *et al.*, 2006; Adell, 2020). This is supported by a model by Carlsson (1995) showing that the effects of NMDA antagonism can be reversed by antagonism of the 5-HT_{2A} receptors, indicating that NMDA signalling has downstream effects on serotonergic signalling via the 5-HT_{2A} receptor. This can potentially be explained by hypoactivation of NMDA receptors observed in the GABA interneurons, in the cerebral cortex of patients with schizophrenia, which attenuates inhibition on the pathways these GABA interneurons innervate. In Figure 2.2 consulted literature has been illustrated to provide insight on how signalling of multiple neurotransmitters may be involved in schizophrenia pathology and leads to oxidative stress as well as how oxidative stress modulates this connected neurotransmitter dysfunction. Figure 2.2 shows hypoactivation of NMDA on GABA interneurons, particularly parvalbumin-positive (PV-positive) fast-spiking interneurons, decreases GABA signalling resulting in downstream upregulated glutamate signalling innervating dopaminergic neurons in the VTA (Stahl, 2018). Upregulated glutamatergic signalling and dopaminergic signalling may induce excitotoxicity and oxidative stress

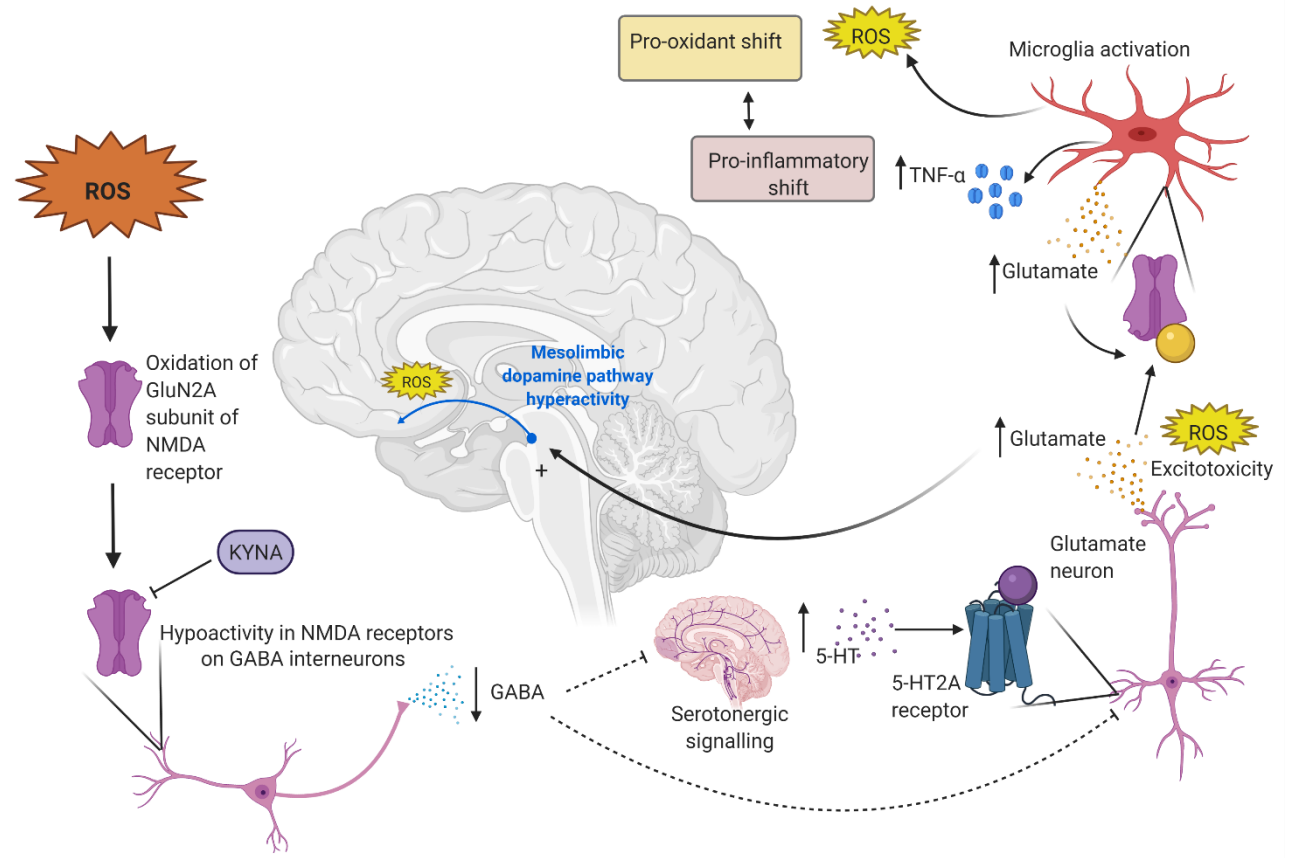

Figure 2.2: Oxidative stress-induced neurotransmitter dysfunction in schizophrenia leading to further oxidative stress and inflammation. *Oxidation of GluN2A subunits of NMDA receptor result in hypoactivity of this receptor on GABAergic interneurons which results in hyperdopaminergic signalling in the mesolimbic pathway. Glutamate neurons in the ventral tegmental area activate dopamine neurons along this pathway. Overproduction of glutamate results in excitotoxicity and ROS production as well as overactive dopamine signalling which upregulates ROS production leading to oxidative stress. Elevated glutamate results in microglia activation via extra-synaptic NMDA receptors which induce TNF-α release and ROS production. Inflammation results in a shift in the kynurenine pathway and KYNA production which is an NMDA receptor antagonist. 5-HT: serotonin, GABA: gamma-Aminobutyric acid, KYNA: kynurenic acid, NMDA: N-methyl-D-aspartate, ROS: reactive oxygen species, TNF-α: tumour necrosis factor alpha (Created with BioRender.com).*

(Newell *et al.*, 1995; Aghajanian and Marek, 2000; Platt, 2007; Perkins, Jeffries and Do, 2020) as seen in Figure 2.1.

Oxidative stress modulates NMDA activity (Nakazawa and Sapkota, 2020) potentially via ROS oxidizing the cysteine residues on GluN2A subunits supported by the decreased currents of NMDA receptors with mutated cysteine subunits indicating decreased activity of these receptors via cysteine residue oxidation resulting in a disulphide bond (Choi, Chen and Lipton, 2001). Under physiological conditions, NMDA activity is kept at an optimal level for neurotransmitter signalling. Whereas under pathological conditions with elevated ROS levels, such as in schizophrenia, NMDA activity is suppressed. GWAS data suggests a genetic link to glutamatergic dysfunction within this receptor sub-type, with mutations in gene *GRIN2A* associated with schizophrenia patients (Ripke *et al.*, 2014). This genetic disposition in these patients renders them more susceptible to oxidative stress as decreased NMDA activity can in turn add to oxidative stress as NMDA receptor activation upregulates transcription of antioxidant genes increasing reduced glutathione (GSH) levels (Baxter *et al.*, 2015), which are notably reduced in patients with schizophrenia (Nucifora *et al.*, 2017), and NMDA activity also enhances the thioredoxin-peroxiredoxin antioxidant mechanism (Papadia *et al.*, 2008).

Psychosis in schizophrenia may therefore be linked to hypoactivation of NMDA receptors on PV-positive GABAergic interneurons, with GluN2D (specific to these neurons) or GluN2A subunits (Nakazawa and Sapkota, 2020). Synaptic and extra-synaptic NMDA receptors have different outcomes once glutamate is bound to these receptors (Hardingham and Bading, 2010). This difference in signalling is likely due to the different subunits these receptors have. The synaptic NMDA receptors predominantly include GluN2A subunits whilst GluN2B is predominant in the extra-synaptic receptors. Elevated levels of extra-synaptic levels of glutamate can trigger a pro-inflammatory shift. Microglia have extra-synaptic glutamate receptors that induce tumour necrosis factor alpha (TNF-α) release when stimulated (Pocock and Kettenmann, 2007) suggesting a link between altered glutamate signalling in schizophrenia and inflammation. Tumour necrosis factor alpha (TNF-α) induces monocyte and dendritic cell activation (Esposito and Cuzzocrea, 2011) upregulating ROS production. Stimulation of microglia by lipopolysaccharide (LPS), amyloid-β or chromogranin A peptide triggered glutamate release from microglia which further drives TNF-α production (Pocock and Kettenmann, 2007). Inflammation results in a shift in the kynurenine pathway towards greater kynurenic acid production which is an antagonist of the NMDA receptor adding to decreased activity in NMDA receptors in patients with schizophrenia (Nakazawa and Sapkota, 2020).

2.2.4 GABAergic dysfunction

GABAergic dysfunction is also a downstream effect of inflammation as TNF-α downregulates $GABA_A$ receptor density through activating endocytosis of these receptors in rodent models (Pribiag and Stellwagen, 2013). TNF-α levels are elevated in patients with schizophrenia (Luo *et al.*, 2019) potentially exacerbating GABAergic signalling abnormalities. Rodent models have displayed

oxidative stress being implicated in prefrontal cortex and anterior cingulate cortex deficits of parvalbumin containing GABAergic interneurons (Cabungcal *et al.*, 2006; Steullet *et al.*, 2017) which are decreased in patients with schizophrenia compared to healthy controls observed in a post-mortem study by (Steullet *et al.*, 2018). Despite this information, few studies have investigated GABA dysregulation in schizophrenia and inconsistencies are likely attributed to small effect sizes, lack of binding specificity in the marker used for GABA, insufficient overlap of brain areas studied and methodological limitations as reviewed by (Egerton *et al.*, 2017) and further investigation is required to elucidate fully this gap in research.

Of specific interest to the thesis topic, a zebrafish model of psychosis is based on GABA receptor antagonism (Afrikanova *et al.*, 2013). The high throughput and availability of zebrafish as a research tool provides the opportunity to probe the effects of Fluanxol® on GABA receptor interaction as a potential mechanism of action as will be discussed further at the end of this chapter.

2.3 The impact of inflammatory role players on disease severity and longer-term clinical outcome

Oxidative stress and inflammation are intricately linked and pro-inflammatory cytokines are elevated, in the central nervous system and in circulation, in patients with schizophrenia (Watanabe, Someya and Nawa, 2010; Rodrigues-Amorim *et al.*, 2018; Luo *et al.*, 2019). The cytokine hypothesis suggests a gene-environment interaction where inflammation results in the epigenetic modification and alternative expression of genes associated with schizophrenia pathology (Momtazmanesh *et al.*, 2019). Since redox was the focus of this thesis, and not inflammation directly, I will limit my discussion on inflammation to a brief contextualisation for the sake of brevity.

Pro-inflammatory cytokines are key players in the inflammatory response. Cytokines such as tumour necrosis factor-alpha (TNF-α), Interleukin-6 (IL-6) and interleukin-1 (IL-1) are pro-inflammatory and orchestrate cell death, increase permeability of vascular endothelium, recruit immune cells to the sight of inflammation and induce acute-phase protein production (Takeuchi and Akira, 2010). Pro-inflammatory cytokines increase the permeability of the blood-brain barrier (BBB) by altering the integrity of tight junctions between astrocytes and endothelial cells (Wong, Dorovini-Zis and Vincent, 2004; Terrando *et al.*, 2011). Polymorphisms in the genes of pro-inflammatory cytokines such as IL-1 and IL-6 as well as upregulated plasma levels of these cytokines have been associated with schizophrenia (Debnath and Berk, 2014). Serum levels of TNF-α, IL-6 and IL-18 are elevated in patients with schizophrenia (Luo *et al.*, 2019) supporting that genetic mutations in inflammatory genes in these patients may upregulate protein expression shifting to a pro-inflammatory state. These pro-inflammatory cytokines trigger cell death in neural progenitor cells in the hippocampus and the amygdala, leading to an inhibition of neurogenesis (Bernier *et al.*, 2002; Liu, Lin and Tzeng, 2005) and impairs synaptic function (Avital *et al.*, 2003). Elevated TNF-α levels also activate

microglia and monocytes resulting in ROS production and a pro-oxidant shift (see Figure 2.3) (Esposito and Cuzzocrea, 2011).

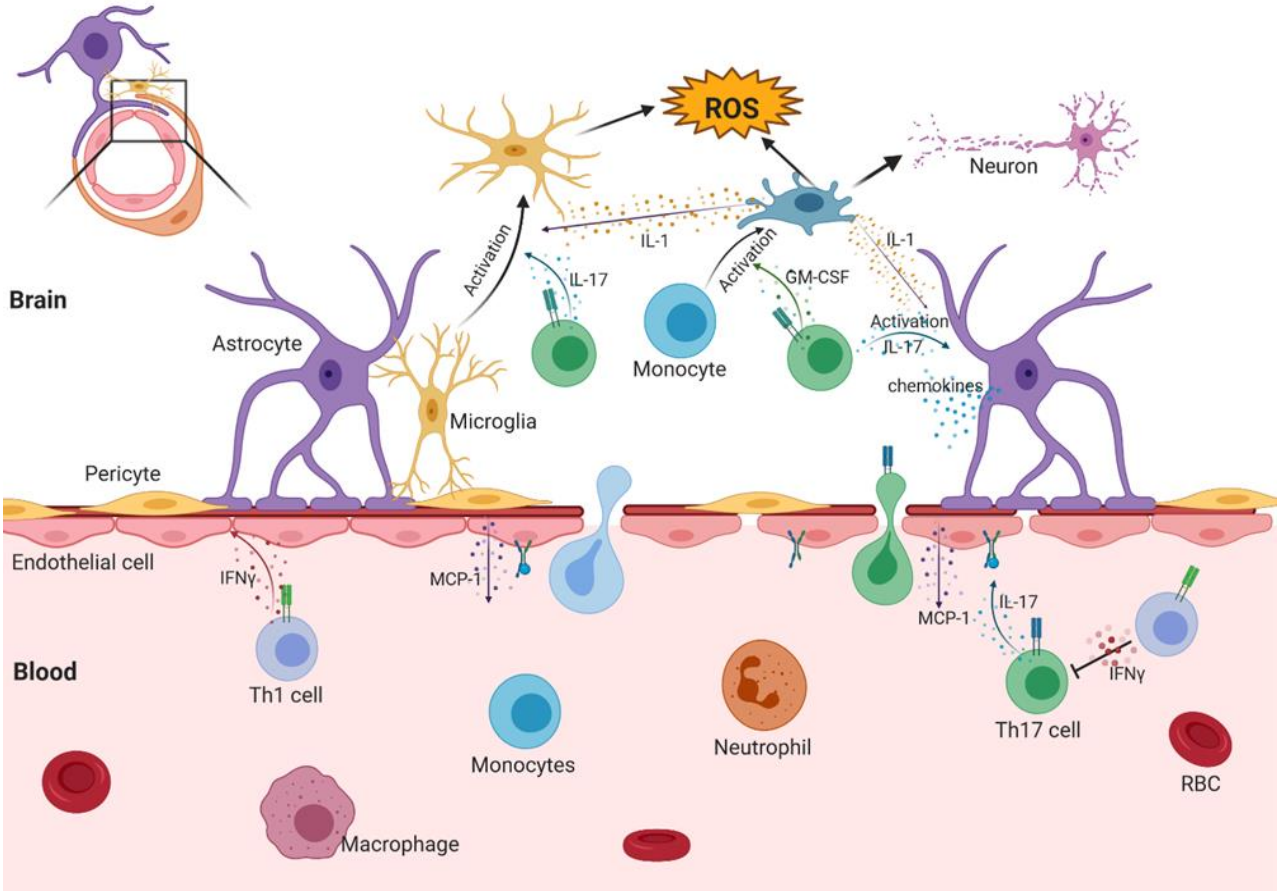

Figure 2.3: Systemic inflammation to neuroinflammation via the BBB and the link to oxidative stress. *Elevated pro-inflammatory cytokine levels in systemic inflammation activate various T helper (T_H) cells. T helper 1 (T_H1) cells release interferon-γ which has a direct impact on the integrity of the blood–brain barrier (BBB). T helper 17 (T_H17) cells secrete IL-17 which binds to IL-17 receptors on endothelial cells resulting in a release of monocyte chemoattractant protein-1 (MCP-1). MCP-1 recruits monocytes and macrophages to the BBB. IL-17 activates astrocytes. Activated glial cells such as astrocytes secrete chemokines including chemokine ligand 2 (CCL2) which recruit leukocytes to the BBB and potentiate their migration into the neural space. Chemokines are also produced by invading leukocytes. Secretion of granulocyte–macrophage colony-stimulating factor (GM-CSF) by T_H cells triggers monocytes and monocyte-derived cells to develop into pro-inflammatory phagocytic cells. These cells are destructive and produce reactive oxygen species (ROS) and cytokines such as interleukin-1 (IL-1), which further fuel the inflammation through glial cell activation. (Created with BioRender.com).*

The inflammatory response in the CNS is mediated by glial cells, (which includes astrocytes, microglia, oligodendrocytes, ependymal cells, Schwann cells, and satellite cells) as well as leukocytes that migrate from the periphery after permeabilization of the BBB (DiSabato, Quan and Godbout, 2016; Becher, Spath and Goverman, 2017). Pro-inflammatory cytokines that cross the BBB from systemic circulation activate microglia and astrocytes (Watanabe, Someya and Nawa, 2010; Calcia *et al.*, 2016). In a chronic state when inflammation is unresolved, however, neuroinflammation can itself inflict damage to brain tissue that it is designed to protect (Tewari and Seth, 2016; Becher, Spath and Goverman, 2017). Overexpression of these cytokines through

genetic polymorphisms in schizophrenia patients or prenatal infection activate toll-like receptors which potentiates further pro-inflammatory cytokine production and T-helper 17 (Th17)-cell differentiation. Th17 cells then remain as effector memory T cells which proliferate. Activation of these cells drives chronic inflammation through production of pro-inflammatory cytokines, IL-17A, IL-17F, IL-21 and IL-22, as well as through activation of microglia (from colony-stimulating factor 2 production), alterations of gut permeability and disruption of the BBB (Tewari and Seth, 2016; Becher, Spath and Goverman, 2017). Th17 cells therefore provide a link between systemic inflammation, gut-inflammation, neurodegeneration, and oxidative stress in the brain seen in schizophrenia pathology .

Apart from their action on microglia, Th17 also affects astrocytes directly. Migrated Th17 cells secrete IL-17 which stimulates neutrophil-attracting chemokines production from type A1 astrocytes (Becher, Spath and Goverman, 2017). Briefly, type A2 astrocytes have neuroprotective effects and stimulate an increase in neurotrophic factors such as brain-derived neurotrophic factor (BDNF). In contrast, type A1 astrocytes, when activated, release chemokines which attract T-lymphocytes to migrate into the CNS from the periphery (Tewari & Seth, 2016) (See Figure 2.3). Neutrophils migrate into the CNS and exacerbate the inflammatory response. Pro-inflammatory cytokines are also released from activated type A1 astrocytes, adding to the inflammatory shift in the CNS to a pro-inflammatory state (Cekanaviciute and Buckwalter, 2016). The increase in pro-inflammatory cytokines will stimulate an increase in ROS production (see Figure 2.3) and lipid peroxidation, in the lipid-rich environment of the brain, producing thiobarbituric acid reactive substances (TBARS) which are a by-product of lipid peroxidation. Left unresolved, the shift to a pro-inflammatory state in a chronic setting will lead to astrocytosis (Blasko *et al.*, 2004). A deficit in supporting cells will lead to decreased viability of neurons and result in neuronal dysfunctions. Although Th17 cells and glial cells were not specifically probed in this thesis, this literature illustrates the complexity of ROS related maladaptation and the intricate link with inflammation and serves to highlight the importance of understanding the effect of antipsychotic effects on redox status.

The entire CNS extracellular space is monitored by microglia every few hours through the process of immuno-surveillance (Ousman and Kubes, 2012). If the protrusions on microglia come into contact with pathogens, protein aggregates such as amyloid beta, endotoxins such as LPS, tissue damage, pro-inflammatory cytokines or noxious stimuli, the activation of the microglial cell is triggered (Thameem Dheen, Kaur and Ling, 2007; Hanisch, 2013) and ROS is produced. Activated microglia undergo a transformation into what is referred to in literature as the M1 phenotype and release pro-inflammatory cytokines further adding to microglia activation and neuroinflammation (Tang and Le, 2016; Zhang, 2019). More specifically, nuclear factor kappa beta (NF-κβ) signalling pathways are activated in microglia of the M1 phenotype (Hanisch, 2013). A transcriptome-wide association study indicated elevated NF-κβ signalling in patients with schizophrenia (Gandal *et al.*, 2018) which upregulates transcription of pro-inflammatory cytokines such as tumour necrosis factor-alpha (TNF-

α), interleukin-6 (IL-6), interleukin-23 (IL-23) and interleukin-1β (IL-1β) but also cyclooxygenase-2 (COX-2), inducible nitric oxide synthase, ROS, chemokines (including CCL2, CCL3 and CCL5), matrix metalloproteinases (including MMP-1, -2, -7, -9, and -12) and molecules involved in antigen presentation major histocompatibility complex class II and CD80 (cluster of differentiation 80) and CD86 (cluster of differentiation 86) (Hanisch, 2013; DiSabato, Quan and Godbout, 2016; Shabab *et al.*, 2017; Dubbelaar *et al.*, 2018), allowing microglia to interact with T cells that enter the CNS from the peripheral circulation across the BBB (Pocock and Kettenmann, 2007). The proteinases produced by activated microglia upregulate protein degradation, protein aggregation, axonal transport deficiencies and mitochondrial dysfunctions, leading to oxidative stress and apoptosis induction (Becher, Spath and Goverman, 2017). The pro-inflammatory cytokines and ROS produced by active microglia further drive inflammation and shift the redox status towards oxidative stress.

Microglia can also transform into a more phagocytic, pro-regenerative, phenotype which is more anti-inflammatory in nature - often referred to as the M2 phenotype in literature. Microglia are the resident macrophages of the brain (de Araújo Boleti *et al.*, 2020) and due to their phagocytic nature, they are able to remove dysfunctional cells, foreign material and debris (Perry and Teeling, 2013). M2 phenotype microglia release anti-inflammatory cytokines such as interleukin-4 (IL-4) and interleukin-13 (IL-13) as well as promote wound healing, clear cellular debris and restore neuronal homeostasis (Cherry, Olschowka and O'Banion, 2014). The protective effects of microglia are also achieved through the production of neurotrophins such as BDNF, neurotrophin-3, glial cell line-derived neurotrophic factor, ciliary neurotrophic factor and nerve growth factor (Ousman and Kubes, 2012). These cells play a role in regulating oxidative stress levels within the CNS (Perry and Teeling, 2013). Microglia play an important role in development of the brain through pruning of synapses (Yong *et al.*, 2019). Inflammatory events such as maternal infection during foetal development may disrupt this process and lead to altered pruning, possibly resulting in neurodevelopmental disorders such as schizophrenia. It is postulated that the M1/M2 transition of microglia elucidates relapse and remission in patients with schizophrenia (Nakagawa and Chiba, 2014). Activation and transition into M1 microglia secrete pro-inflammatory cytokines and is correlated with psychotic symptoms in schizophrenia patients (Figure 2.4). M1 microglia release CCL2 and IL-6 which induces transition of microglia to an M2 phenotype with anti-inflammatory effects of IL-10 production and these M2 microglia are suspected to be prominent during phases of remission in patients with schizophrenia

(Nakagawa and Chiba, 2014). These transitions can be modulated by redox status and inflammatory status further indicating importance of antipsychotic effect on oxidative stress and inflammation.

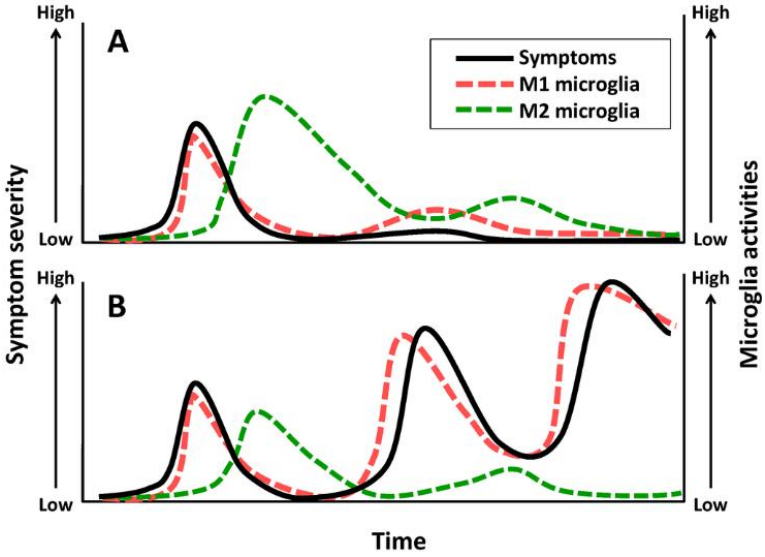

Figure 2.4: Phases of relapse and remission in patients with schizophrenia correlate with M1 and M2 microglia. *Increased pro-inflammatory cytokines released from M1 microglia are evident during schizophrenia psychosis. CCL2 and IL-6 secreted from M1 microglia initiates M2 microglia transition resulting in IL-10 production observed in schizophrenia patients suspected to be linked to the remission of their symptoms* (Nakagawa and Chiba, 2014)*. CCL2: chemokine ligand 2, IL-6: interleukin 6, IL-10: interleukin 10.*

Neuroinflammation induces ROS production which modulates NMDA receptors and GABA signalling, affecting serotonergic, glutamatergic, and dopaminergic signalling indicating that oxidative stress and inflammation may be the crux of schizophrenia pathology. Therefore, it is not unexpected that the cytokine hypothesis of schizophrenia is prominent as it ties all the previous hypotheses together. It is evident that redox and inflammatory status are linked and play a role in the pathology of schizophrenia through gene-environment interactions. Taken together these literature insights demonstrate the intricate interdependence of neurotransmitter function and inflammatory profile and redox status. Thus, a small deviation in any of these systems is likely to significantly affect the others and suggests a significant role in treatment. Redox and inflammation will therefore play a role in treatment efficacy and can dictate long term outcome of the treatment and co-morbidities that arise, dependent on the effect of treatments on redox status and inflammation and prevent relapse of symptoms through impact on redox and inflammation modulatory effects on NMDA receptors, neurotransmitter dysfunction and microglia modulation.

Prenatal and postnatal stress cause epigenetic modifications that alter the functioning of the HPA axis and can impair the stress response throughout life of the offspring (Weaver *et al.*, 2004; Adams and Smith, 2020). Parental stress during the gestation or neonatal period can impair the immune profile of the foetus or neonate (Watanabe, Someya and Nawa, 2010). Immunomodulatory drugs such as COX-2 inhibitors show beneficial outcomes in treatment of schizophrenia patients (Müller *et al.*, 2005; Akhondzadeh *et al.*, 2007) indicating that treatments that have an effect on inflammation

have therapeutic benefit and may alleviate the pro-inflammatory disposition induced from parental stress. Some atypical antipsychotics, such as risperidone and clozapine, have indicated anti-inflammatory effects with noted reduction in IL-2, IL-6 and TNF-α serum levels (Lü *et al.*, 2004) which would reduce activation of microglia, reducing the drive of neurotransmitter dysfunction (Figure 2.2). This is further supported by minocycline, inhibitor of microglial activation, reducing psychosis in patients with schizophrenia (Miyaoka *et al.*, 2007, 2008). Other antipsychotics such as chlorpromazine, haloperidol, olanzapine, quetiapine and aripiprazole as reviewed by Monji, Kato and Kanba (2009) show reduced release of pro-inflammatory cytokines and nitric oxide from microglia.

Lastly, stress is speculated to trigger psychotic episodes in patients with schizophrenia and possibly influence time of psychosis onset and rate of disease progression (Corcoran *et al.*, 2002; Berger *et al.*, 2018). Increased adrenaline (epinephrine), from activation of the sympathomedullary pathway due to psychological stress, upregulates IL-6 levels which are correlated severity of positive symptoms, negative symptoms and total PANSS score in patients with schizophrenia (Luo *et al.*, 2019). Elevated IL-6 levels from a stressful event may trigger onset of schizophrenia symptoms by inducing neuroinflammation and oxidative stress in the brain (see Figure 2.3) which modulates NMDA receptor activity leading to neurotransmitter signalling dysfunctions resulting in the symptoms seen in patients with schizophrenia (see Figure 2.2). Elevated IL-6 levels were correlated with kynurenic acid (KYNA) levels, an NMDA receptor antagonist (Pedraz-Petrozzi *et al.*, 2020) which can lead to neurotransmitter dysfunction, microglia activation and oxidative stress (Figure 2.2). Antipsychotic medication possessing anti-inflammatory, or antioxidant effects has potential to reduce NMDA receptor related dysfunction induced by psychological stress leading to oxidative stress and pathological outcome. Anti-inflammatory cytokine IL-4 suppresses KYNA production through inhibiting kynurenine aminotransferase (Papadimitriou *et al.*, 2018). IL-4 levels are reduced in patients with schizophrenia (Pedraz-Petrozzi *et al.*, 2020) which are secreted by M2 microglia (Cherry, Olschowka and O'Banion, 2014) indicating that an anti-inflammatory shift to M2 phenotype is a potential therapeutic benefit of antioxidant and anti-inflammatory effects in drugs used to treat schizophrenia. Persistent psychological stress results in chronic low-grade inflammation (Petersen and Smith, 2016) and is reported to result in the production of superoxide anion radical, hydroxyl radical, and hydrogen peroxide, especially in the brain (Salim, 2014). Rodent models have reported a causal link between oxidative stress and anxiety-like behaviours (Hovatta *et al.*, 2005; de Oliveira *et al.*, 2007; Masood *et al.*, 2008; Salim *et al.*, 2010). Oxidative stress inhibits sirtuin 1 (SIRT1) activity (a sirtuin with antioxidant effects through its antagonistic activity on NF-κβ signalling as well as enhancing antioxidant expression) which fuels inflammation (Salminen, Kaarniranta and Kauppinen, 2013). SIRT1 transcription was observed to be reduced in patients with schizophrenia with depressive symptoms (Wang *et al.*, 2020). With the modulatory effect of oxidative stress on SIRT1 it is potentially therapeutic for treatments to counteract this effect as shown by polyphenols which upregulate SIRT1 (Iside *et al.*, 2020). SIRT1 upregulation would decrease TNF-α production, through reduced NF-κβ signalling, decreasing TNF-α associated comorbidities of schizophrenia such as

cardiovascular disease (De Hert, Detraux and Vancampfort, 2018). Therefore, it is imperative to investigate the effect of antipsychotic treatment on redox status and inflammation as this will impact on the presence of inflammatory co-morbidities, disease progression and relapse of symptoms.

2.4 Oxidative Stress

Redox status has been observed to be out of balance in patients with schizophrenia (Bitanihirwe and Woo, 2011). Antioxidant defence mechanism abnormalities (Gysin *et al.*, 2007; Do *et al.*, 2009; Yao and Keshavan, 2011) have been associated with schizophrenia and oxidative stress has been observed in first-episode psychosis (FEP) patients with schizophrenia (Flatow, Buckley and Miller, 2013) indicating the link of oxidative stress to the disease pathology in the absence of antipsychotic treatment. Antioxidant effects of antipsychotics need to be further investigated to elucidate their efficacy in targeting oxidative stress driving disease outcome.

Oxidative stress is an imbalance of free radicals in the form of ROS and reactive nitrogen species (RNS) referred to as nitrosative stress. The imbalance can be due to over production of ROS and RNS, excessive exposure to pro-oxidant environmental factors or due to a decrease in antioxidant defences (Berg, Youdim and Riederer, 2004). RNS are chemically reactive, nitrogen containing molecules, such as nitric oxide (NO) and peroxynitrite ($ONOO^{\bullet}$). ROS are chemically reactive, oxygen-containing molecules, such as H_2O_2, superoxide radical ($O_2^{\cdot -}$), and hydroxyl radical ($OH^{\cdot}$) (Bitanihirwe and Woo, 2011). ROS plays a role in activating the nucleotide-binding oligomerization domain (NOD)-like receptor protein 3 inflammasome inducing IL-1β secretion (Yang *et al.*, 2019) and assists with immune response to invading pathogens (Tschopp, 2011; Bonini and Malik, 2014) linking ROS with inflammation. In a balanced redox state ROS are important for maintaining cellular homeostasis and cellular survival (Liu *et al.*, 2017), destroy invading pathogens and protect the cell from infection (Halliwell, 2006), modulate intracellular calcium and act as second messengers phosphorylating and dephosphorylating proteins.

ROS is produced in the process providing energy for the high metabolic demand of the brain (de Araújo Boleti *et al.*, 2020). ATP (adenosine triphosphate) production via oxidative phosphorylation at the inner mitochondrial membrane results in superoxide as a byproduct of electron leakage (Hroudová and Fišar, 2013). ATP is needed for energy to maintain cellular processes. Neurons have a high ATP demand due to their metabolic rate and the need to maintain membrane potential (Gaignard *et al.*, 2018; de Araújo Boleti *et al.*, 2020) leaving them vulnerable to oxidative damage which is further exacerbated by low levels of antioxidant defences in these cells (Dringen, 2000; Berg, Youdim and Riederer, 2004; Liu *et al.*, 2017). Oxidative stress is implicated in neurodegenerative (Niedzielska *et al.*, 2016) and psychiatric disorders (Ng *et al.*, 2008) which is unsurprising regarding the brain's high metabolic demand and lipid-rich environment rendering the CNS susceptible to damage incurred by oxidative stress. Oxidative stress causes lipid peroxidation and damage to cell membranes, as well as damage to proteins and deoxyribonucleic acid (DNA) (Bitanihirwe and Woo, 2011). Neurotransmission can be disrupted by ROS-induced cellular

membrane damage (Yao and Keshavan, 2011). Redox-sensitive signalling proteins in neurons can be rendered dysfunctional when redox homeostasis is imbalanced (Apel and Hirt, 2004). Lipid peroxidation measured, using TBARS assay, has been recorded to be elevated in treatment-naïve FEP patients with schizophrenia (Zhang *et al.*, 2010). This effect was reduced in patients receiving antipsychotic treatment indicating that lipid peroxidation may be involved in the pathology of the disease and is alleviated by antipsychotics.

Mitochondria regulate the oxidative stress levels of the cell through ROS production, from nicotinamide adenine dinucleotide phosphate hydrogen oxidase (Nox) and xanthine oxidase (XO) (Liu *et al.*, 2017) and antioxidant mechanisms such as superoxide dismutases (SODs) and GSH pool (Gaignard *et al.*, 2018). Mitochondrial dysfunction has been associated with schizophrenia pathology (Zhang *et al.*, 2010) as well as decreased mitochondrial density in the prefrontal cortex and the caudate nucleus (Uranova *et al.*, 2001) with reduced ATP recorded in the frontal lobe, temporal lobe and basal ganglia of these patients (Fujimoto *et al.*, 1992; Kegeles, Humaran and Mann, 1998; Maurer, Zierz and Möller, 2001). The electron transport chain found on the inner mitochondrial membrane is altered in patients with schizophrenia with complex I and complex III activity recorded to be significantly reduced in post mortem basal ganglia and temporal cortex of patients compared to controls (Maurer, Zierz and Möller, 2001). Elevated levels of ROS or dysfunctional antioxidant mechanisms leads to oxidative stress (Berg, Youdim and Riederer, 2004) which can result in damage to mitochondria leading to mitochondrial dysfunction initiating activation of cell death processes such as necrosis or apoptosis (Scherz-Shouval and Elazar, 2007).

In a balanced redox status, ROS production is balanced out by antioxidant mechanisms (Liu *et al.*, 2017). Antioxidant mechanisms counteract ROS and RNS and prevent oxidative stress from occurring and causing damage to lipids, proteins and DNA. One mechanism involves glutathione peroxidase (GPx) and glutathione reductase. GPx converts ROS into non-reactive forms while oxidising GSH into glutathione disulphide (GSSG). Glutathione reductase (GR) recycles GSSG to GSH (Bitanihirwe and Woo, 2011). GPx activity is recorded to be decreased in patients with schizophrenia reducing conversion of $O_2^{\bullet-}$ into nitrite (nitrite levels were observed to be decreased in patients) resulting in greater conversion of superoxide radicals into hydroxyl radicals. Increased production of hydroxyl radicals is further exacerbated by decreased GPx activity with decreased conversion of H_2O_2 into water and oxygen shunting H_2O_2 towards OH radical production. Elevated levels of hydroxyl levels causes lipid peroxidation which is affirmed by recorded elevated levels of TBARS (Flatow, Buckley and Miller, 2013). GSH has been reported to be reduced in the caudate nucleus (Yao, Leonard and Reddy, 2006) and the prefrontal cortex (Gawryluk *et al.*, 2011) of post-mortem samples from patients with schizophrenia. Do *et al.*, (2000) reported reduced GSH levels in cerebral spinal fluid (CSF) as well as reduced GSH levels in the prefrontal cortex, using magnetic resonance spectroscopy, in patients with schizophrenia. GSH modulates glutamatergic signalling (Oja *et al.*, 2000) and the reduced GSH levels in patients with schizophrenia may be implicated in

dysfunctional long-term potentiation (Steullet *et al.*, 2006) affecting learning and memory (Martin, Grimwood and Morris, 2000). Treatment with N-acetyl cysteine has shown efficacy in alleviating schizophrenia symptoms likely due to its effects of upregulating GSH levels in the brain (Berk *et al.*, 2008) supporting the postulated key role of oxidative stress in schizophrenia pathology and the therapeutic potential of antipsychotics that have antioxidant effects.

Superoxide dismutase interacts with glutathione peroxidase to inactivate superoxide radicals (Dringen, Pawlowski and Hirrlinger, 2005). SOD inhibits Nox by regulating Rac1 (Li *et al.*, 2011; Zuo *et al.*, 2015). SOD therefore reduces Nox-produced superoxide (Bitanihirwe and Woo, 2011). SOD was recorded to be elevated in chronic patients with schizophrenia receiving treatment (Zhang *et al.*, 2003) but not in the treatment-naïve patients with this disorder (Raffa *et al.*, 2009). Neuroleptic drugs potentially upregulate SOD activity which may be linked to the efficacy of this class of drugs. SOD converts superoxide radicals to hydrogen peroxide (Liu *et al.*, 2017) and is decreased in patients with schizophrenia (Flatow, Buckley and Miller, 2013). The decrease in SOD would result in elevated $O_2^{\bullet-}$ levels. Superoxide activates nuclear factor κβ (NFκβ) translocation as seen in Figure 2.5.

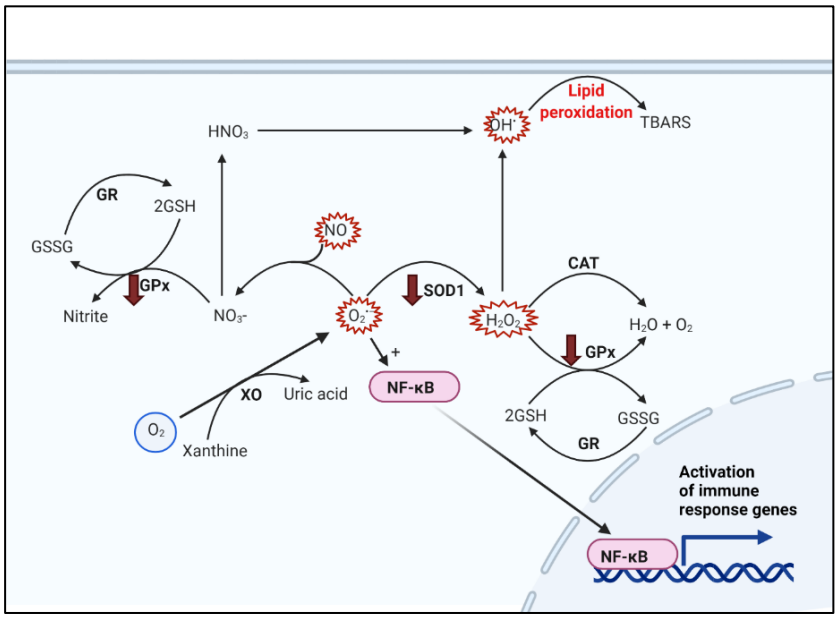

Figure 2.5: Decreased SOD and GPx in schizophrenia patients leads to oxidative stress and inflammation. *SOD converts superoxide to hydrogen peroxide downregulating NF-κβ signalling. NF-κβ activates transcription of immune response genes shifting towards a pro-inflammatory state. Decreased levels of SOD in schizophrenia patients results in elevated superoxide radicals which activates a proinflammatory shift. Decreased GPx activity in patients with schizophrenia shunts superoxide away from conversion into nitrite towards hydroxyl radical production. CAT: catalase, GPx: glutathione peroxidase, GR: glutathione reductase, GSH: glutathione, GSSG, oxidised glutathione, HNO_3: nitric acid, H_2O_2: Hydrogen peroxide, NF-κβ: nuclear factor κβ, NO: nitric oxide, NO_3^-: nitrate, $O_2^{\bullet-}$: superoxide, $OH^{\bullet}$: hydroxyl radical, SOD1: superoxide dismutase 1. (Created with Biorender.com).*

NFκβ, activator protein-1 and protein 53 (p53) are modulated by redox status of the cell (Sun and Oberley, 1996). ROS, such as $O_2^{\bullet-}$, degrades inhibitor of kappa beta (Iκβ) which is an inhibitor of NFκB activity. Increased ROS levels and therefore increased degradation of Iκβ increases the transcriptional activity of NFκβ (Hayden and Ghosh, 2004) which upregulates production of pro-

inflammatory cytokines (Monkkonen and Debnath, 2018) leading to inflammation. Antipsychotic treatment with antioxidant capacity would alleviate the downstream effects of reduced SOD in patients with schizophrenia potentially improving prognosis.

Another antioxidant defence mechanism against ROS and RNS is the regeneration of antioxidant molecules (such as lipoic acid, ascorbic acid and ubiquinone) catalysed by thioredoxin and thioredoxin reductase (Bitanihirwe and Woo, 2011). Endogenous antioxidant molecules including albumin, uric acid and bilirubin have been observed to be significantly lower in patients with schizophrenia independent of smoking status (Reddy, Keshavan and Yao, 2003). Exogenous antioxidants such as niacin, carotenoids, α-tocopherol (vitamin E) and flavonoids combat ROS and RNS (Nordberg and Arnér, 2001) and could potentially compensate for the reduced levels of endogenous antioxidant molecules, in patients with schizophrenia, as an adjunctive treatment for antipsychotics found to have little to no effect on redox status.

Oxidative stress has various downstream effects that could play a major role in schizophrenia symptomology such as supressed NMDA receptor activity which attenuates its modulation on serotonergic signalling (see Figure 2.2) leading to hyperdopaminergic signalling in patients with schizophrenia (Bitanihirwe and Woo, 2011). NMDA receptor suppression decreases Nitric oxide synthase (NOS) activity reducing production of NO and reduced plasma NO metabolites have been observed in patients with schizophrenia and has been associated to severity of negative symptoms (Nakano *et al.*, 2010) indicating oxidative stress as a therapeutic target to impact on severity of the clinical outcome. Nitric oxide has both antioxidant as well as pro-oxidant effects (Bitanihirwe and Woo, 2011). NO is implicated in synaptic plasticity regulation (Hölscher and Rose, 1992), neurodevelopment (Gibbs, 2003) and neurotransmitter release (Lonart, Wang and Johnson, 1992). Proceeding NMDA receptor activation, NO acts as a second messenger modulating dopaminergic and serotonergic signalling (Brenman and Bredt, 1997). NOS activity is elevated in treatment-naïve schizophrenia patients compared to controls and patients treated with antipsychotics (Das *et al.*, 1995). An increase in NO has been recorded in patients with schizophrenia (Yao, Leonard and Reddy, 2004) with a significantly greater elevation in NO levels observed in medicated patients (Zhang *et al.*, 2010). Antipsychotics possessing antioxidant capacity have therapeutic potential to not only manage the clinical symptoms of the disease at dopaminergic and serotonergic signalling dysfunction through antagonism of dopamine and serotonin receptors but also to address pathology upstream of these dysfunctions by managing oxidative stress which shows promise of a better clinical outcome.

2.5. Antipsychotic treatment and potential impact on redox status

Turning attention now to schizophrenia treatment, current treatment is mainly antipsychotics and aimed at managing clinical symptoms of the disorder. The median dose of the prescribed range for each antipsychotic usually corresponds to about 60% to 80% of striatal D_2 dopamine receptors being

occupied leading to optimal drug efficacy (Uchida *et al.*, 2011). The prescribed range of Flupentixol dihydrochloride is 3 mg to 12 mg per day.

Antipsychotic treatment results in a high prevalence of metabolic side effects such as weight gain, insulin resistance, elevated lipid plasma levels increasing risk of developing metabolic syndrome and cardiovascular disease (Marder and Cannon, 2019). Antipsychotics bind to histamine-1 receptors as an antagonist, resulting in sedation and weight gain leading to increased risk for hyperlipidaemia, hypertension and hyperglycaemia (Kroeze *et al.*, 2003). The mechanism by which histamine-1 receptor antagonism results in weight gain is not fully understood but it is suggested that the mechanism is leptin dependent (Masaki *et al.*, 2001).

First generation antipsychotics (FGAs) are the first antipsychotics developed for treating psychosis including drugs such as haloperidol, fluphenazine, trifluoperazine, thiothixene, perphenazine, thioridazine, chlorpromazine, clozapine and flupentixol (Corson *et al.*, 1999; Grohmann *et al.*, 2014; Solmi *et al.*, 2017). FGAs are also known as typical antipsychotics and are dopamine antagonists that bind to dopamine D_2 receptors in the central nervous system (Seeman *et al.*, 1975; Smieskova *et al.*, 2009). The side effects of typical antipsychotics include prolactin elevation due to decreased dopamine signalling in the tuberoinfundibular pathway (Wieck and Haddad, 2002; Bargiota *et al.*, 2013). Cardio-metabolic syndrome and extrapyramidal side effects are also prevalent during FGA treatment (Scigliano and Ronchetti, 2013). Extrapyramidal symptoms include acute dystonia, Parkinsonism, akathisia (or motor restlessness) and tardive dyskinesia and arise from decreased dopamine signalling in the nigrostriatal pathway. FGAS are typically effective in reducing positive symptoms of schizophrenia but have little effect on the patient's negative symptoms (Leucht *et al.*, 2009) flupentixol, however, has shown efficacy in reducing negative symptoms as well as positive symptoms and although it is classified as an FGA it shows similarities with atypical, second generation antipsychotics (SGAs) (Stargardt *et al.*, 2011). FGAs have been recorded to induce oxidative damage in an *in vivo* rat model study which was not an effect observed by SGAs (Martins *et al.*, 2008). With flupentixol being an FGA with SGA similarities it would be beneficial to elucidate whether it has antioxidant or pro-oxidant effects.

Second generation antipsychotics were developed after FGAs and include drugs such as clozapine, risperidone, quetiapine, ziprasidone and olanzapine and are effective in reducing psychosis as well as alleviating negative symptoms of schizophrenia (Corson *et al.*, 1999; Leucht *et al.*, 2009; Smieskova *et al.*, 2009). SGAs have shown to improve cognitive impairment except for Clozapine which only shows improvement in motor functions (Bilder *et al.*, 2002; Keefe *et al.*, 2004). SGAs have a lower affinity for dopamine receptors than FGAs but also bind to serotonergic 5-HT_{2A} receptors (Smieskova *et al.*, 2009). Atypical antipsychotics have fewer extrapyramidal side effects but more metabolic side effects in relation to typical antipsychotics (Wieck and Haddad, 2002; Bargiota *et al.*, 2013). Clozapine is usually only prescribed if drug resistance to other SGAs is

experienced by the patient (Hasan *et al.*, 2012). Atypical antipsychotics have shown to reduce oxidative stress through reduced activation of microglia (Bian *et al.*, 2008; Obuchowicz *et al.*, 2017).

Fluanxol® comes in tablet form, flupentixol dihydrochloride, to be taken orally and in injectable form, flupentixol decanoate and is an atypical antipsychotic part of the thioxanthene neuroleptics class of drugs (Kaatz *et al.*, 2003; Mostafa *et al.*, 2018). Fluanxol® is commonly prescribed as a treatment for schizophrenia in South Africa (Mostafa *et al.*, 2018; Joubert *et al.*, 2021). The product monograph of Fluanxol® by Lundbeck Canada Inc. (2017) states that the mechanisms of action of the drug are unknown. Although the drug shows efficacy in reducing psychosis, it has not been fully elucidated as to what physiological mechanisms and pathways it uses to achieve reduced psychosis. The effects of Fluanxol® on oxidative stress and inflammation will shed light on whether the drug is effective in reducing progression of the disease through alleviating oxidative stress and inflammation or whether the treatment simply masks the symptoms whilst potentially aggravating disease progression through redox mechanisms. Although the mechanisms of action have not been fully elucidated for Fluanxol®, some studies have indicated mechanisms that could result in its efficacy. Such mechanisms may include potent antagonistic binding to dopamine receptors D_1 and D_2 as well as binding to serotonin 5-HT_{2A} receptor (Mishara and Goldberg, 2004; Reimold *et al.*, 2007). Efficacy of antipsychotics is usually assessed by investigating dopamine antagonism (Howes and Kapur, 2009) and are not always assessed for their effects on oxidative stress or inflammation. Little is known about the effects and possible mechanisms of action of Fluanxol® in schizophrenia patients especially in the context of inflammation and oxidative stress as shown by Table 2.1 which summarises the sparse number of studies of the effect of Fluanxol® on redox status and inflammation.

Table 2.1: Studies assessing effects of Fluanxol® on redox or inflammatory status

Study design	Oxidative Stress	Inflammation	Reference
15 post-mortem brains of schizophrenia patients treated with flupentixol (5 of which were treatment free for 4 weeks prior to death) and 10 control post-mortem brains.	↓Superoxide (O_2^-) ↓Lipid peroxidation		(Whatley *et al.*, 1998)
Human lymphocytes isolated from whole blood of male schizophrenia patients treated with flupentixol and controls.	↓mitochondrial NADH ubiquinone reductase activity		(Whatley *et al.*, 1998)

	↓ NADH-cytochrome b5 reductase expression ↓Superoxide (O_2^-)		
Frontal cortex sections of rats treated with 1 mg/kg flupentixol daily for 3 weeks.	↓mitochondrial NADH ubiquinone reductase activity ↓ NADH-cytochrome b5 reductase expression ↓Superoxide (O_2^-)		(Whatley *et al.*, 1998)
Primary mixed glia cultures from 1-day-old Wistar rat brains were stimulated with 1µg/ml LPS and treated with 0.2, 2, 10 and 20µM Fluanxol®. Supernatants were assessed at 6 and 24 hours after treatment for TNF-α and NO.	↓NO production by microglia	↓TNF-α production by microglia	(Kowalski, Labuzek and Herman, 2003)
Primary mixed glia cultures from 1-day-old Wistar rat brains were stimulated with 1µg/ml LPS and treated with 0.2, 2, 10 and 20µM Fluanxol®. Supernatants were assessed at 24 and 72 hours after treatment for IL-1β and IL-2 .		↓IL-1β production by microglia ↓IL-2 production by microglia	(Kowalski, Labuzek and Herman, 2004)
22 patients with schizophrenia treated with FGAs (flupentixol=17 and haloperidol=5) mean flupentixol dosage of 3.5 mg/day compared to 70 patients with schizophrenia treated with SGAs.	Lower levels of MDA in patients treated with SGAs compared to FGAs (including flupentixol).		(Kropp *et al.*, 2005)
32 treatment-naïve patients with schizophrenia compared to healthy	↑Antioxidant capacity	↓Neopterin levels in CSF	(Chittiprol *et al.*, 2010)

control volunteers. Only 2 of the 32 patients were treated with 20 mg of flupentixol decanoate injection once every two weeks.		
Mouse microglial BV2 cell culture treated with doses of flupentixol ranging from 1 to 30µM concentrations.	↓Proton currents in microglial cells ↓ROS production from Nox	(Kim and J. H. Song, 2016)

CSF: cerebral spinal fluid, IL-1β: interleukin-1β, IL-2: interleukin-2, MDA: malondialdehyde, NADH: nicotinamide adenine dinucleotide (NAD) + hydrogen (H), NO: nitric oxide, Nox: NADPH oxidase, ROS: reactive oxygen species, SGAs: second generation antipsychotics, TNF-α: tumour necrosis factor alpha.

It is evident that there is quite an extensive gap in the literature regarding investigation of redox status effects of antipsychotic treatment, Fluanxol®, as shown by the sparse number of studies listed in Table 2.1. Although there are only a few studies, it is however, evident that redox may indeed play an imperative role in schizophrenia pathology and treatment outcome, this interpretation is supported by the findings, which consistently report positive outcomes in terms of redox after flupentixol dihydrochloride treatment. A limitation of the available studies is that only a few isolated parameters are assessed in context of redox. Furthermore, some studies have a very small sample size, such as 2 patients in Chittiprol *et al.* (2010), rendering a lack of a comprehensive understanding of this particular antipsychotic and its effect on redox. Given the interaction of free radical production and the counteracting upregulating of antioxidant defences, measuring either in isolation cannot reflect the full picture at tissue level. This thesis aims to contribute to the gap in knowledge on the effects of Fluanxol® on redox status.

2.6. Methodological considerations

In light of the suggested key role oxidative stress plays in the aetiology, risk of relapse and severity of symptoms of schizophrenia; it is imperative to investigate the effects of schizophrenia treatment on redox status. Flupentixol dihydrochloride is administered in tablet form and orally ingested. It is absorbed in the gut into circulation and reaches its target site in the brain once crossing the BBB at 40% bioavailability according to kinetic studies (Abdelbary *et al.*, 2014; Bailey and Taylor, 2019). After calculating cell culture appropriate doses for clinically relevant prescribed doses, bioavailability should be taken into account when treating gut epithelial cellular models compared to neural cellular models. CaCo2 human gut epithelial carcinoma cells were selected to simulate the absorption site in the gut and Be(2)-M17 human neuroblastoma cells were stimulated with retinoic acid to differentiate into neural cells to simulate target site in the brain. Such an approach is especially important in the context of this thesis where at least two regulatory systems (as opposed to localised organ systems) are implicated. The biological half-life of flupentixol dihydrochloride is 35 hours,

according to the product monograph by Lundbeck Canada Inc. (2017) and pharmacokinetic studies (Abdelbary *et al.*, 2014; Bailey and Taylor, 2019), therefore treatment time points should be kept within this time frame and was selected to be 24 hours to mimic once a day treatment regime.. Cellular models are useful for probing a mechanism of action of a drug and will indicate its effects on redox status using oxidative stress and antioxidant capacity assays.

Known importance of the gut in brain function (Oriach *et al.*, 2016; Hasan Mohajeri *et al.*, 2018; Sudo, 2019) warranted investigation in the gut. The gut is even referred to as the second brain (Young, 2012; Ridaura and Belkaid, 2015; Ochoa-Repáraz and Kasper, 2016). The gut microbiome plays a role in psychiatric pathologies and drug response through the interactions with the brain (Kanji *et al.*, 2018). The gut-brain axis involves a complex relationship between the gut microbiota, the enteric nervous system and the central nervous system. The antipsychotics prescribed to patients with schizophrenia may alter redox status in gut epithelia or alter the microbiota resulting in some of the side effects of these consumed pharmaceuticals. Although an extensive review of the gut as role player in schizophrenia is beyond the scope of this thesis, it should not be ignored in research investigating effects of regulatory systems – such as inflammation and the interconnected redox system.

However, cellular models lack the complexity to represent the disease state and psychosis. Animal models pose useful in this regard and *in vivo* probing in zebrafish models of psychosis (Afrikanova *et al.*, 2013) allows for investigation at whole organism complexity of interactions between different cell and tissue types and the gut microbiome. *Danio rerio* (zebrafish) has been selected as a model for studying human pathologies due to benefits such as high throughput due to frequent spawning of many eggs and the quick maturation of the fish. The model is highly cost effective compared to other vertebrate models and visualisation of the internal systems is easily accessible (Kim *et al.*, 2014; Baran *et al.*, 2018). In the last two decades zebrafish have been used for drug discovery and toxicity screening. The first drug screen in zebrafish was conducted in 2004 (Goldsmith, 2004) and since has shown to be a useful model for drug discovery as some effects of therapeutic compounds are not observed *in vitro* but only *in vivo* as some compounds require endogenous activation and their effects are only evident in the presence of complex molecular pathway interactions that are seen in *in vivo* models (Kokel *et al.*, 2010). The conserved proteins between these species allow inferences to be made about the drug effects in humans when utilising a zebrafish model regarding drugs that target neurotransmitter modulation such as those used to treat neuropsychiatric diseases (Rico *et al.*, 2011).

The specific pharmacokinetics of flupentixol in zebrafish regarding absorption and metabolism have not been elucidated impeding translation of clinical doses from humans to zebrafish. A model for psychosis was used to consider optimal doses displaying antipsychotic effect. The pentylenetetrazole (PTZ)-induced model of psychosis has been used in the context of epilepsy to investigate the efficacy of anti-epileptic drugs such as diazepam (Valium®) (Afrikanova *et al.*, 2013;

Moradi-Afrapoli *et al.*, 2017). PTZ is a $GABA_A$ receptor antagonist decreasing GABAergic signalling (Huang *et al.*, 2001) and diazepam reverses the seizure-like movement effects of PTZ through its potent $GABA_A$ receptor agonism (Campo-Soria, Chang and Weiss, 2006). Other models using zebrafish administered ketamine or PCP to induce aberrant behaviour representative of psychosis (Zakhary *et al.*, 2011; Kyzar *et al.*, 2012). Ketamine and PCP are NMDA antagonists and induce erratic movement in zebrafish. NMDA hypofunction in schizophrenia is upstream of GABAergic hyper signalling from the pyramidal V interneurons. Probing antipsychotic effect at this point in the pathway indicates a potential $GABA_A$ receptor agonistic effect of Fluanxol® or downstream effects on serotonin and dopamine antagonism. As the clinically relevant dose in zebrafish is still to be elucidated, investigations of which doses of flupentixol that induce behaviour similar to that of untreated, control, zebrafish and diazepam-treated zebrafish would indicate effective antipsychotic doses in this animal model and are to be used to visualise and assess oxidative stress *in vivo* using fluorescent ROS-probe, chloromethyl-2,7-dichlorodihydro-fluorescein diacetate (CM-H_2DCFDA) (Mendieta-Serrano *et al.*, 2019). Zebrafish larvae models serve as great research tools as they provide the opportunity for live imaging of internal mechanisms and systems that are not accessible in other animal models such as rodents or primates. Oxidative stress is able to be quantified in zebrafish larvae with fluorescent microscopy and image analysis techniques.

2.7 Summary

Schizophrenia is a complex disease involving the interaction of multiple pathways in its pathology. Inflammation and oxidative stress are hypothesised to be a driving force in schizophrenia progression with genetic association of elevated NF-κβ transcription upregulating inflammation and microglia activation. ROS produced from microglial activation induces oxidative stress enhanced by impaired antioxidant mechanisms in patients with schizophrenia. Oxidative stress decreases NMDA receptor activation which leads to dysfunctional neurotransmitter signalling manifesting the symptoms of schizophrenia as well as further activation of microglia fuelling oxidative stress. Oxidative stress and its modulatory effects on microglial activation and transition to M1 phenotype with a pro-inflammatory shift associated with symptom relapse indicate oxidative stress as a key determinant factor in long-term disease outcome. Redox status imbalance in schizophrenia is attenuated by treatments with antioxidant capacity and remission from symptoms is associated with prominently M2 phenotype of microglia and increased IL-10 levels. Some typical antipsychotics have shown to have pro-oxidant effects whereas some atypical antipsychotics have shown to have antioxidant effects. Despite the evident role that redox plays in clinical outcome of schizophrenia very little is yet elucidated on the effects of the antipsychotic prescribed in South Africa, Fluanxol®, on inflammation and oxidative stress in the patient. Literature reveals a gap in knowledge in understanding what effect Fluanxol® has on inflammation and oxidative stress with very few studies having assessed isolated parameters involved in redox status. It is therefore imperative that these effects are investigated and the mechanisms of action of Fluanxol® further elucidated.

2.8 Hypothesis statement

Flupentixol dihydrochloride will not display toxicity at the doses usually prescribed by clinicians. The prescribed drug will potentially decrease lipid peroxidation (reducing oxidative damage), decrease ROS production (shifting redox status away from a pro-oxidant state), as well as increase antioxidant capacity. Fluanxol® will induce toxicity, indicated by cell viability loss, at an overdose concentration verifying the prescribed range as appropriate. Flupentixol dihydrochloride will prevent erratic movement induced by $GABA_A$ receptor antagonism, in zebrafish, in a dose dependent manner.

2.9 Aims and objectives

The aim of this thesis is to investigate the effect of the anti-psychotic Flupentixol dihydrochloride (Fluanxol®) on redox status *in vitro* and *in vivo*. We have formulated specific objectives by which to achieve this aim, namely:

- Assessing the effect of Flupentixol dihydrochloride *in vitro* on BE(2)-M17 human neuronal cells (representing the neurological target site) and CaCo2 gut epithelial cells (representing the site of intestinal absorption), in terms of cell viability and redox status.
- Determining maximal therapeutic dose in an *in vivo* zebrafish model of experimentally induced psychosis-like behaviour, simultaneously probing GABAergic activity as potential additional mechanism of action of Fluanxol®.
- Assessing the impact of the maximally effective treatment dose on *in vivo* ROS production, using immunohistochemistry, and live whole organism imaging using fluorescent brightfield microscopy.

Chapter 3:

Methods

3.1. Introduction

Inflammation is a hypothesised driver of schizophrenia development, onset, and progression. As mentioned above in Chapter 2 of my thesis, inflammation and oxidative stress are intricately linked. Flupentixol dihydrochloride (Fluanxol®) is prescribed to patients with Schizophrenia but very little is understood about its effects on the inflammatory response or the redox status of the individual. Therefore, it is essential to investigate these effects of the drug on various sites it comes into contact with.

Fluanxol® is typically prescribed within the range of 3 mg/day to 12 mg/day and can either be administered intravenously or orally. For this thesis the focus was on oral administration. Fluanxol® tablets were used for experimental treatments. Ingestion orally would expose the gut epithelium to the drug at around 100% of the dose assuming that absorption in the oral mucosa is negligible due to minimal contact time of swallowing the pill. To simulate site of absorption of the drug, CaCo2 human gut epithelial cells were chosen to probe redox response to Fluanxol®. CaCo2 cells are typically used as a model for gut epithelial physiology. In the clinical setting, the tablet is then absorbed through the gut epithelium into the blood stream where flupentixol dihydrochloride is transported to the blood-brain barrier (BBB) to enter its target site in the central nervous system. BE(2)-M17 human neuroblastoma cells were differentiated into neuronal cells with retinoic acid (Andres *et al.*, 2013) to simulate the drug's target site in the brain. BE(2)-M17 cells are commonly used as a model for neural physiology and are an appropriate choice for investigating redox mechanisms without the confounding effects of serotonin release such as from enterochromaffin cells (Alcaino *et al.*, 2018). It is indicated that the bioavailability of orally ingested Fluanxol® is 40% in the brain (Bailey and Taylor, 2019). For the purpose of this thesis, I thus opted for conducting experiments in cellular models representative of both the gut and neuronal compartments, taking into account the different bioavailability at the different sites. Schizophrenia pathology is not sufficiently simulated in cellular models, an inflammatory challenge in the form of LPS, however, was used to represent the pro-inflammatory status observed in patients (Debnath and Berk, 2014; Luo *et al.*, 2019). .

In terms of other specific methodological choices, WST-1 (4-[3-(4-iodophenyl)-2-(4-nitrophenyl)-2H-5-tetrazolio]-1,3-benzene disulphonate) was used in a colorimetric assay to assess cellular viability. Cellular viability measures validated the integrity of our cell lines and was selected to indicate the presence or absence of toxicity of the drug within prescribed doses and at overdose concentration. WST-1 is converted to formazan dye by mitochondrial succinate dehydrogenases (Toimela and

Tähti, 2004). Formazan is measured to represent mitochondrial activity which is a representation of cellular viability; as the amount of formazan produced correlates with number of cells that are metabolically active (Narayanan *et al.*, 2005). Consideration of the effect of the compound assessed (Fluanxol® or LPS) on the enzymatic reaction is imperative as certain compounds, such as manganese-containing compounds, can inhibit the WST-1 reaction in the absence of loss of cell viability (Scarcello *et al.*, 2020) whereas other compounds my induce elevated mitochondrial dehydrogenase activity in the absence of proliferation (Lin *et al.*, 2004). Therefore, trypan blue was also used in conjunction to assess cell viability.

Redox status can be assessed through various methods that investigate antioxidant capacity, ROS production or downstream effects of oxidative stress. Trolox Equivalent Antioxidant Capacity (TEAC) assay was used to assess antioxidant capacity in CaCo2 cells and BE(2)-M17 cells. This assay measures presence of antioxidants. Conversion of 2,2′-azinobis(3-ethylbenzothiazoline-6-sulfonic acid) (ABTS) radical to reduced ABTS quantifies the antioxidant levels with a standard known concentration of an antioxidant, vitamin E analog, Trolox (Zhong and Shahidi, 2015). ROS production was assessed using a hydrogen peroxide assay kit from Elabscience. The hydrogen peroxide assay kit is a colorimetric assay that measures ROS concentration as ROS interacts with horse radish peroxidase to produce a colour and is compared with known H_2O_2 concentration standards. Thiobarbituric acid reactive substances (TBARS) assay uses malondialdehyde (MDA) as a standard to measure lipid peroxidation as TBARS including MDA are by-products of lipid peroxidation caused by oxidative damage (Flatow, Buckley and Miller, 2013). TBARS react with added thiobarbituric acid to produce a red colour that can be quantified using a plate reader.

Cell culture models are useful for probing the effects of the drug on redox status with reduced confounding effects but are limited by not being able to effectively mimic the disease state or account for integrated reactions between physiological systems in an organism *in vivo*. Zebrafish models are therefore beneficial to investigate *in vivo* effects of Fluanxol® on ROS production, to screen for toxicity as well as to observe the effects of the drug in the context of a psychosis model.

Zebrafish share genetic similarity with humans and the functions of many proteins are well conserved (Howe *et al.*, 2013). The physiology of the nervous system and immune system of *Danio rerio* and *Homo sapiens* share similarities rendering zebrafish as an appropriate model for investigating the pathology of psychotic diseases and their immunological aetiology (Kalueff, Stewart and Gerlai, 2014). Three days post fertilisation (dpf) the BBB begins to develop in zebrafish (Jeong *et al.*, 2008; Xie *et al.*, 2010) which allows for appropriate bioavailability and drug effect investigation in the context of the central nervous system.

Schizophrenia has dopamine dysfunction as a hallmark of the disease as well as serotonergic dysfunction. Dopamine can be detected in zebrafish larvae from 5 dpf (Sallinen *et al.*, 2009). The dopaminergic, serotonergic and histaminergic neuronal populations are well conserved in humans

when compared to zebrafish and rodents. There are strong similarities between the rodent and zebrafish neuronal networks (Vaz, Outeiro and Ferreira, 2018). Dopamine receptors are present in zebrafish and studies have shown a decrease in motor activity in zebrafish larvae (7 dpf) with dopamine antagonists such as clozapine, haloperidol, and chlorpromazine (Farrell *et al.*, 2011; Wasel and Freeman, 2020) or haloperidol in larvae from 5 hours post fertilisation to 5 dpf (Oliveri and Levin, 2019). Other studies have shown an increase in zebrafish larvae motor activity when exposed to dopamine agonists such as apomorphine, SFK-38393 and quinpirole at 6 dpf (Irons *et al.*, 2013a) and apomorphine at 10 dpf (Ek *et al.*, 2016). These similarly observed drug effects in zebrafish when compared to mammals suggests that *Danio rerio* could be a useful model for studying dopamine-related pathologies, but realistically only in longer-duration models employing larvae older than 5 dpf. However, these neurotransmitter pathways are also linked by GABAergic interneurons as shown in Chapter 2 of this thesis. GABAergic signalling is implicated in the PTZ psychosis model in zebrafish (Afrikanova *et al.*, 2013) – a model utilising zebrafish larvae at 4 to 7 dpf and which is commonly used as screening tool in drug discovery. Here, we opted to use the latter model to determine dose of peak antipsychotic efficacy in zebrafish, at which to investigate potential effects of this dose on redox.

Below, I provide a more detailed description of cellular and zebrafish models utilised to further elucidate effects of Fluanxol®.

3.2. Cell Culture and WST-1 Assays

3.2.1 Materials

The Dulbecco's modified eagle's medium (DMEM) (41966029), Dulbecco's modified eagle medium: nutrient mixture F-12 (DMEM/F12) (31330038), Hank's balanced salt solution (HBSS) (14185-045), foetal bovine serum (FBS) (10082147) and penicillin-streptomycin (PenStrep) (15640055) were purchased from Gibco Laboratories (MA, USA). Phosphate buffered saline (PBS) (70011044) and 0.25% Trypsin ethylenediaminetetraacetic acid (trypsin-EDTA) (25200056) were acquired from Thermo Fisher Scientific (MA, USA). Dimethyl sulfoxide (DMSO) (1.02952), trypan blue (T8154), water soluble tetrazolium salt 1 (WST-1) reagent (11644807001) and lipopolysaccharides (LPS) (L4516) were purchased from Sigma Aldrich (Merck) (MO, USA). Retinoic acid (ab120728) was purchased from Abcam (Cambridge, UK). 1 mg Fluanxol® tablets were purchased from Stelkor Kampus Apteek and is sourced from Lundbeck (NSW, Australia). Cell culture plastics were purchased from NEST (JS, China).

3.2.2 WST-1 experiments with CaCo2 gut-epithelial adenocarcinoma cells

Gut epithelial cells were cultured in DMEM with 10% FBS and 1% PenStrep. Cells were passaged at a confluency of about 70% from a T25 culture flask to a T75 culture flask. At about 70% confluency in the T75 flask, cells were then plated into a 48-well plate at a seeding density of $30x10^3$ cells per well. Seeding density was selected based on a pilot study designed to assess what density would reach confluency at 48 hours after plating. When cells plated at $30x10^3$ cells/well, reached about

70% confluency in each well, they were treated with Fluanxol® at different clinically relevant concentrations (3 mg/day to 12 mg/day) and an overdose concentration (30 mg/day) at 100% bioavailability, to investigate Fluanxol® dose response, or with varying concentrations of LPS (0 µg/ml, 1 µg/ml, 2 µg/ml, 5 µg/ml, 10 µg/ml and 20 µg/ml) as seen in Figure 3.1. LPS concentrations

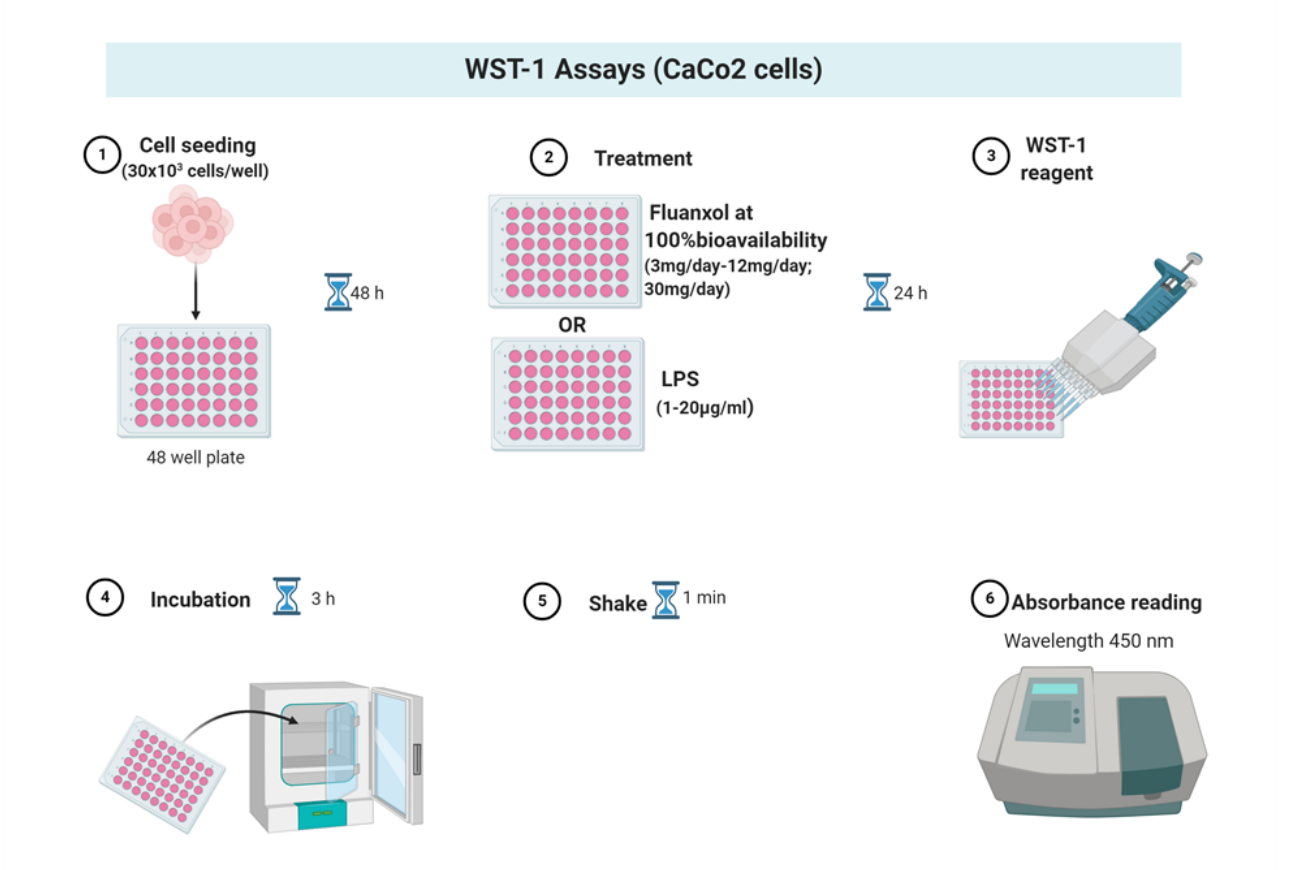

Figure 3.1: WST-1 Method in CaCo2 gut epithelial carcinoma cells. *WST-1 assays were performed to assess toxicity of Fluanxol® at various concentrations and to assess LPS dose response to investigate optimal dose for oxidative stress stimulus without significant loss in viability.*

were made up through serial dilutions from a 2 mg/ml stock solution made up in HBSS. The Fluanxol® concentrations were calculated from the orally ingested dose (mg/day) in a 15-litre human to an appropriate concentration (ng/ml) for cell culture (see table 3.1).

Fluanxol® treatment preparation involved weighing a Fluanxol® tablet and grinding it into powder using a mortar and pestle. Pharmaceutical weight of the drug (1 mg per tablet) was then divided by the total weight of the tablet to calculate mg flupentixol dihydrochloride per mg of ground tablet. Stock solution of Fluanxol® was made up fresh on the day of treatment by weighing Fluanxol® powder and dissolving in PBS to a concentration of 10 µg/ml. Stock solution was then heated to 37°C and vortexed for 20 minutes to dissolve the Fluanxol® tablet in PBS before it was filter sterilized and used to make up treatment concentrations displayed in Table 3.1. 24 hours after treating cells with Fluanxol® or with LPS, 10 µl of WST-1 was added to each well and incubated for 3 hours after which plates were shaken for 1 minute in a shaking incubator and read at 450 nm using a BioTek EL800

microplate reader (BioTek Instruments). WST-1 experiments were run in triplicate and experiments were repeated 3 times.

Table 3.1: Fluanxol® concentrations administered to CaCo2 cells and BE(2)-M17 cells to obtain clinically relevant doses prescribed to patients

Clinically Relevant Fluanxol® Concentration (mg/day)	3	4	5	6	7	8	9	10	11	12	30
Fluanxol® Concentration for CaCo2 Cells at 100% Bioavailability (ng/ml)	200	266.7	333.3	400	466.7	533.3	600	666.7	733.3	800	2000
Fluanxol® Concentration for BE(2)-M17 Cells at 40% Bioavailability (ng/ml)	80	106.7	133.3	160	186.7	213.3	240	266.7	293.3	320	800

3.2.3 WST-1 experiments with BE(2)-M17 neuroblastoma cells

Neuroblastomas were cultured in DMEM/F12 media with 10% FBS and 1% PenStrep. Cells were passaged at a confluency of about 70% from a T25 culture flask to a T75 culture flask. At about 70% confluency in the T75 flask cells were then plated into a 48-well plate at a seeding density of $10x10^3$ cells per well (Figure 3.2). Seeding density was decided based on a pilot study designed to assess what density would reach confluency at 48 hours after plating. 9 hours after plating the cells at $10x10^3$ cell/well, cells were treated with 10 µM retinoic acid to differentiate the cells into neuron-like cells and then again 48 hours later (Andres *et al.*, 2013). As seen in Figure 3.2, 48 hours after the second treatment of 10 µM retinoic acid, cells were about 70% confluent in each well and were either treated with varying concentrations of LPS (0 µg/ml, 0.1 µg/ml, 0.2 µg/ml, 0.5 µg/ml, 1 µg/ml and 2 µg/ml; made up from a 2 mg/ml stock solution) or with Fluanxol® at different clinically relevant concentrations (3 mg/day to 12 mg/day) and an overdose concentration (30 mg/day) at 40% bioavailability. The Fluanxol® concentrations were calculated from mg/day in a 15-litre human to concentration per ml for cell culture (see table 3.1). The 40% bioavailability, elucidated by product monograph by Lundbeck Canada Inc. (2017) and pharmacokinetic studies (Abdelbary *et al.*, 2014; Bailey and Taylor, 2019), was taken into account when calculating the concentrations for treatment of the neuroblastoma cells. Flupentixol is partially metabolised by the liver and when it is absorbed in the gut (Jørgensen, 1980). 24 hours after treating cells with Fluanxol®, 10 µl of WST-1 was added to

each well and incubated for 3 hours after which plates were shaken for 1 minute in a shaking incubator and read at 450 nm using a BioTek EL800 microplate reader (BioTek Instruments).

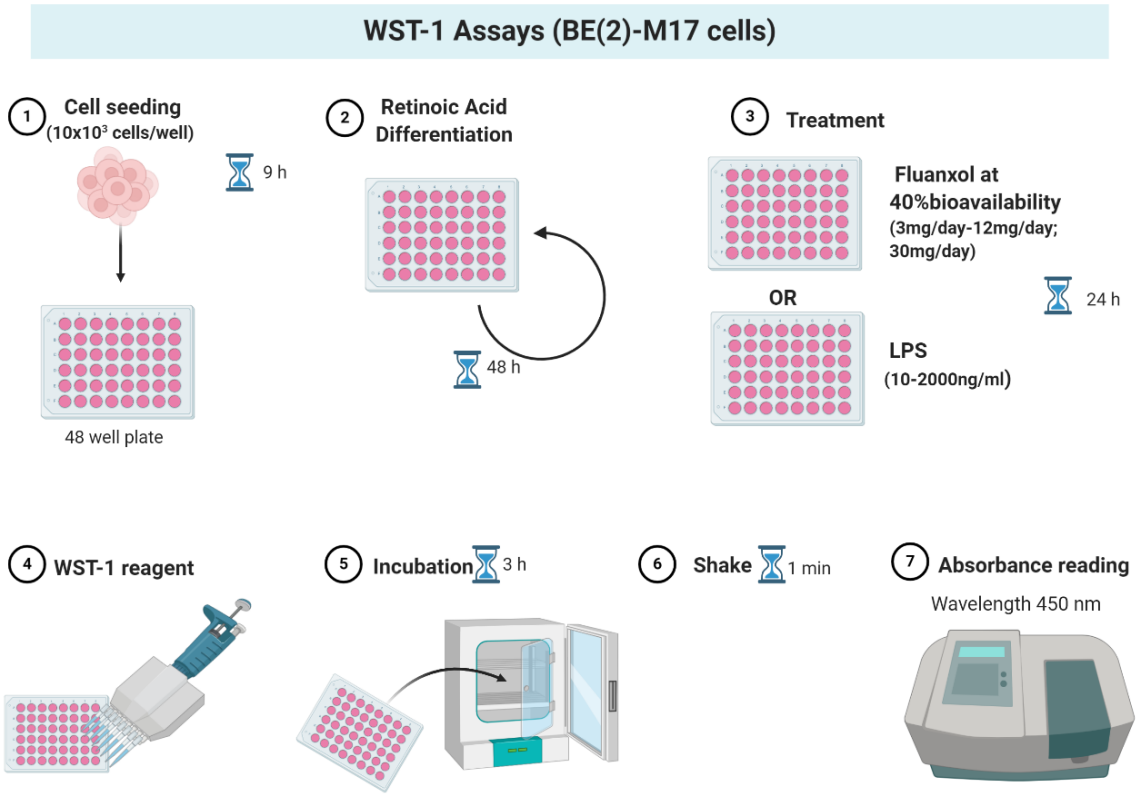

Figure 3.2: WST-1 Method in BE(2)-M17 neuroblastoma cells. *WST-1 assays were performed to assess toxicity of Fluanxol® at various concentrations and to assess LPS dose response to investigate optimal dose for oxidative stress stimulus without significant loss in viability. BE(2)-M17 cells required differentiation with retinoic acid before receiving treatment.*

3.3. Redox Assays

3.3.1 Materials

Malondialdehyde tetrabutylammonium salt (MDA) (63287), Trolox (6-Hydrox-2,5,7,8-tetramethylchroman-2-carboxylic acid) (238831), Butylated hydroxytoluene (BHT) (B1378), 2-thiobarbituric acid (TBA) (T5500), ABTS diammonium salt (A1888) and sodium chloride (NaCl) (S7653), were purchased from Sigma-Aldrich. Ortho-phosphoric acid (OPA) (536092) was purchased from Emsure (Merck). Sodium hydroxide (NaOH) pellets (1.93102.0500) was purchased from Emparta. H202 kit from Elabscience (Houston, TX). Potassium-peroxodisulphate (105091) was purchased from Merck. Falcon tubes (15ml and 50ml) and 96-well plates were purchased from NEST (JS, China). Phosphate buffered saline (PBS) (70011044) was acquired from Thermo Fisher Scientific (MA, USA). 1 mg Fluanxol® tablets were purchased from Stelkor Kampus Apteek and is sourced from Lundbeck (NSW, Australia)

3.3.2 Cell culture for redox assays

Cells were cultured up in the same manner as with the WST-1 experiments but instead of plating into a 48-well plate when the cells were confluent in a T75 flask, they were split into 9 T75 flasks for the BE(2)-M17 cells (Figure 3.4) and further passaged to a T175 for the CaCo2 cells (Figure 3.3) and then split into 9 T75 flasks (8 flasks for treatment groups and 1 flask for the next experimental repeat). On the third experimental repeat cells were only split into 8 T75 flasks. Difference in splitting into treatment T75 flasks from a T75 for the BE(2)-M17s when compared to a T175 for the CaCo2 cells was due to the subcultivation ratio of 1:4 to 1:6 recommended for CaCo2 cells in the ATCC product sheet.

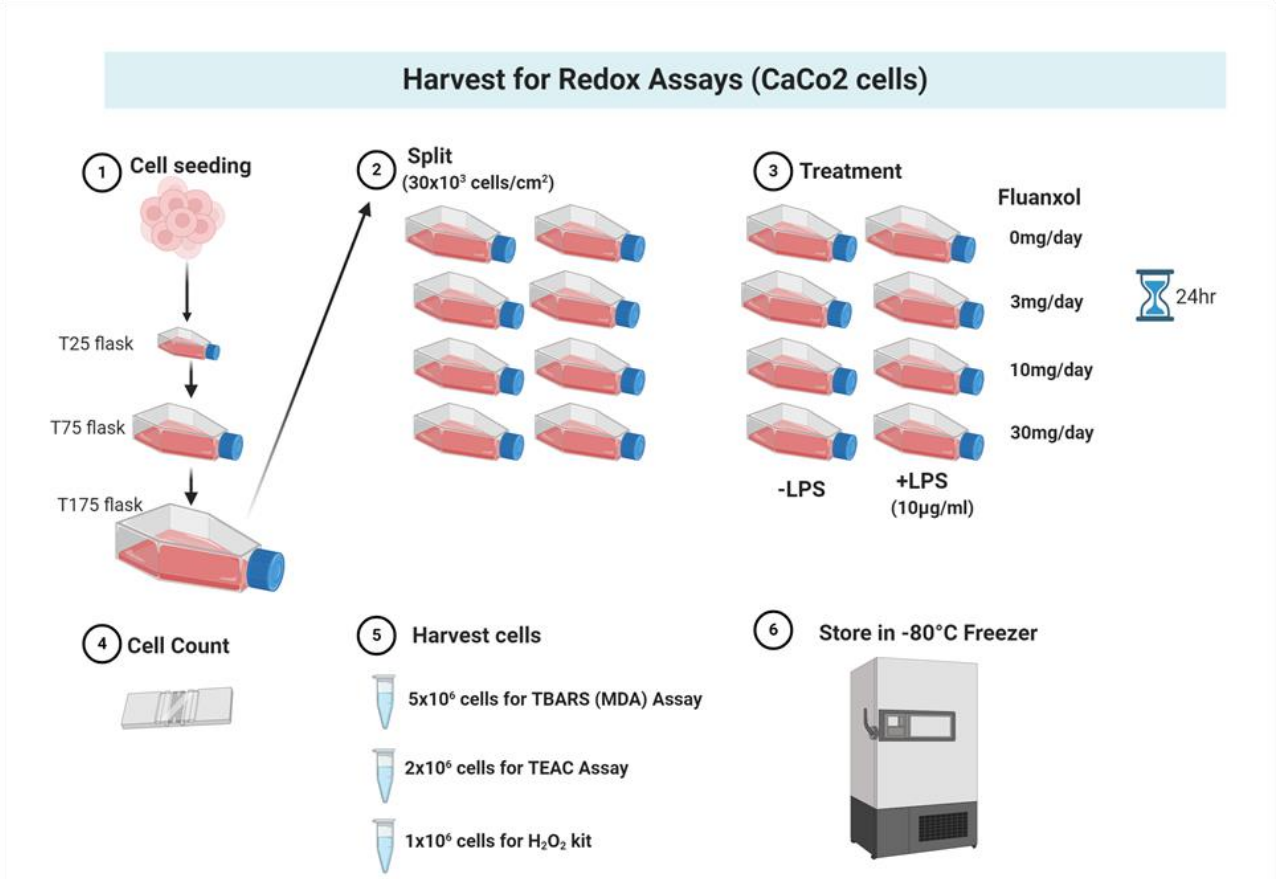

Figure 3.3: Culturing Method and cell harvest for redox assays using CaCo2 gut epithelial carcinoma cells. *CaCo2 cells were cultured up and split into treatment flasks. At 70% confluency cells were treated with various doses of Fluanxol® in the presence or absence of 10 µg/ml LPS. 24 hours after treatment cells were counted and harvested for TEAC, H_2O_2 kit and TBARS assay and stored in a -80°C freezer until the assays were run.*

Cells were grown until they reached confluency. BE(2)-M17 neuroblastoma cells were treated with 10 µM retinoic acid 9 hours after they were split into treatment T75 flasks (30% confluency) and then every 2 days until confluency was reached. When confluency was reached cells were treated with Fluanxol® concentrations equivalent to clinical doses of 0 mg/day, 3 mg/day, 10 mg/day and 30 mg/day. Two T75 flasks were treated with each Fluanxol® concentration. One of each treatment group pair was treated with 100 ng/ml LPS for the neuroblastoma cells and 10 µg/ml LPS for the gut epithelial cells (Lin *et al.*, 2015). These LPS concentrations were chosen based on literature and results obtained from the LPS dose response WST-1 experiments. 24 hours after treatment with Fluanxol® and LPS, supernatant was removed, cells were lifted with trypsin-EDTA, neutralised with culture media, spun down and resuspended. Cells were then counted using an Invitrogen countess chamber and trypan blue to assess cell viability and cell concentration. Appropriate volumes based on the cell density of each group were allocated into separate tubes to harvest the required number of cells for each redox assay. Cells were spun down in a centrifuge and resuspended in room temperature PBS. Cells were spun down again and resuspended in cold PBS, placed on ice and stored in a -80°C freezer until redox assays were run.

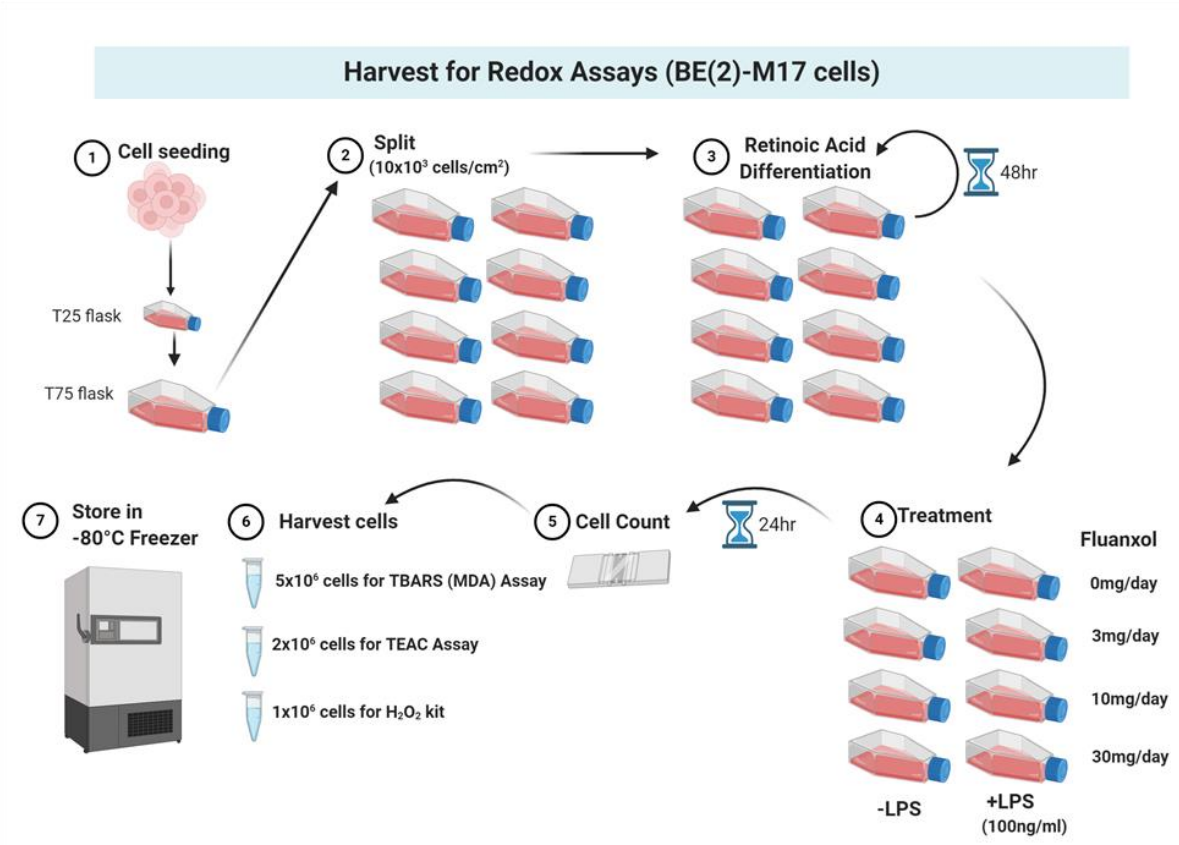

Figure 3.4: Culturing Method and cell harvest for redox assays using BE(2)-M17 neuroblastoma cells. *BE(2)-M17 cells were cultured up, split into treatment flasks and differentiated into neuron-like morphology using retinoic acid. At 70% confluency cells were treated with various doses of Fluanxol® in the presence or absence of 100 ng/ml LPS. 24 hours after treatment cells were counted and harvested for TEAC, H_2O_2 kit and TBARS assay and stored in a -80°C freezer until the assays were run*

3.3.3 TBARS (MDA)

5x10^6 cells were harvested in 200 µl cold PBS for the Thiobarbituric Acid Reactive Substances (TBARS) assay (see Appendix A for protocol used; adapted from Ross *et al.* (2020)). Samples were immediately placed on ice and stored in a -80°C freezer until the assay was performed. Samples were thawed and sonicated on ice for three pulses, 5 seconds in length, with an amplitude of 5 and with 20 second intervals between pulses. Samples were then centrifuged for 15 minutes at 12000 rpm as seen in Figure 3.5.

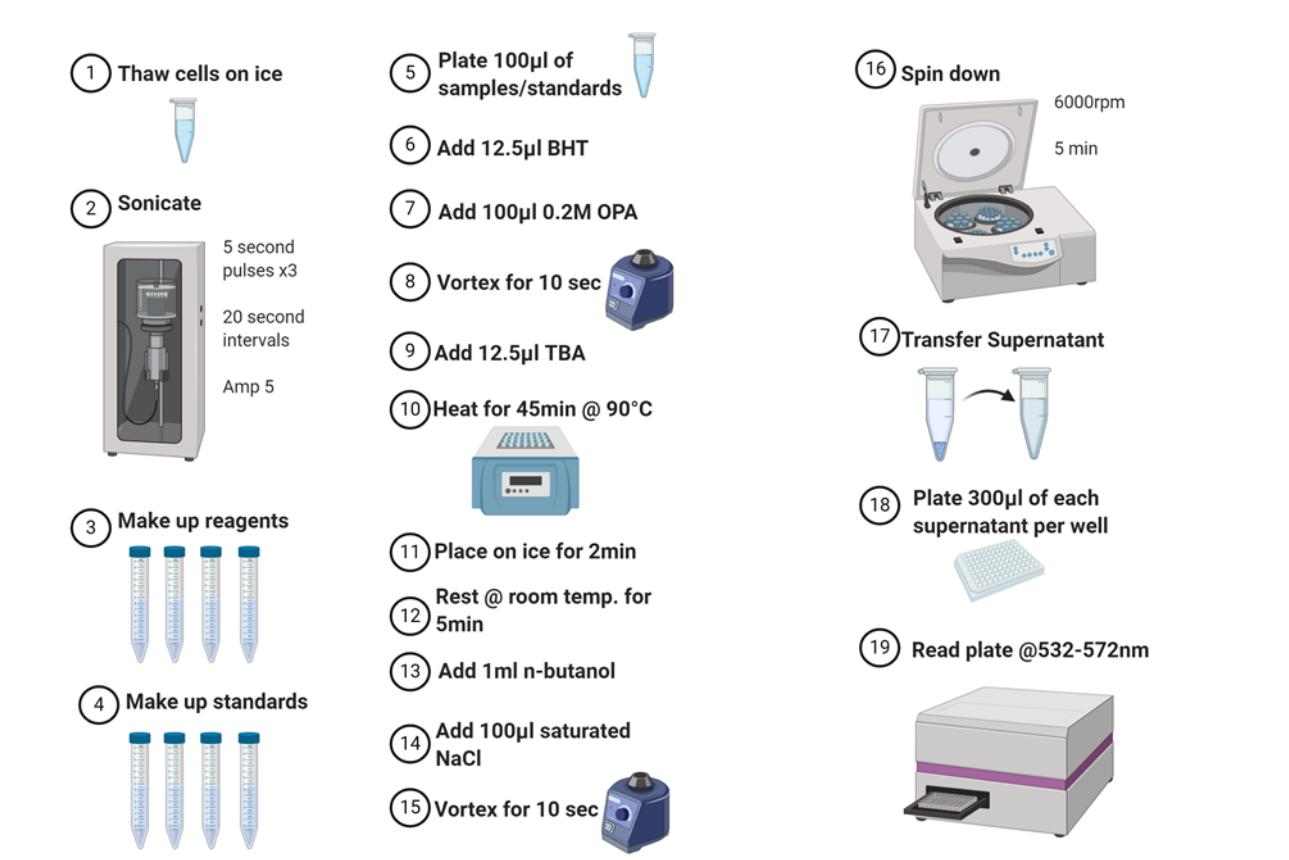

Figure 3.5: TBARS(MDA) assay. *Lipid peroxidation was assessed in CaCo2 and BE(2)-M17 cell lysates by measuring malondialdehyde, a by-product of lipid peroxidation. Amp: amplitude, BHT: butylated hydroxytoluene, NaCl: sodium chloride, OPA: ortho-phosphoric acid, TBA: 2-thiobarbituric acid.*

Standards were prepared according to Table 3.2. 100 µl of samples and standards were transferred to correctly labelled 2 ml Eppendorf tubes. To each sample and standard 12.5 µl of 4 mM BHT and 100 µl of 0.2 M OPA was added and then each tube was vortexed for 10 seconds. 12.5 µl of TBA was then added to each tube and placed on a heating block at 90°C for 45 minutes. Samples and standards were placed on ice for 2 minutes followed by being kept at room temperature for 5 minutes. Each tube had 1 mL n-butanol and 100 µl saturated NaCl added to it and then were vortexed for 10 seconds. Samples and standards were centrifuged at 6000 rpm for 5 mins at 4°C. From each sample and standard, 300 µl of supernatant was aliquoted into a 96 well plate, in triplicate. The plate was read at 532-572nm using a SPECTROstar Nano® absorbance plate reader (BMG Labtech, Ortenberg, Germany).

Table 3.2: Standard preparation for TBARS assay.

	MDA (ul of stock)	dH_2O (ul)	Concentration (mM)
Std A	1000	0	2
Std B	500	500	1
Std C	250	750	0.5
Std D	125	875	0.25
Std E	62.5	937.5	0.125
Std F	31.25	968.75	0.0625
Std G	15.625	984.375	0.03125
Std H	7.8125	992.1875	0.015625
Blank	0	1000	0

MDA: malondialdehyde, dH_2O: distilled water.

3.3.4 H_2O_2 Assay

$1x10^6$ cells were harvested in 200 µl cold PBS for the hydrogen peroxide analysis. Samples were immediately placed on ice and stored in a -80°C freezer until the assay was performed. Samples were thawed and sonicated on ice for three pulses, 5 seconds in length, with an amplitude of 5 and with 20 second intervals between pulses. Samples were then spun down at 5000 rpm for 10 min as seen in Figure 3.6.

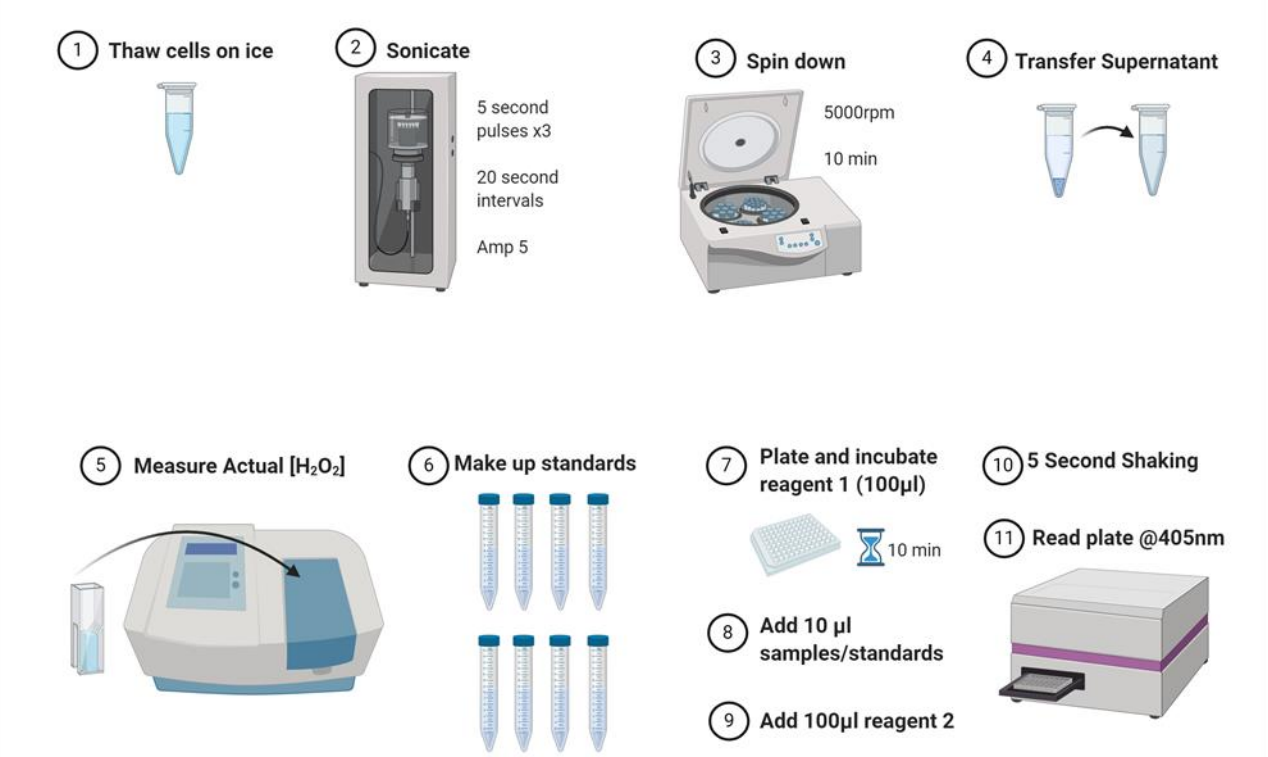

Figure 3.6: Hydrogen peroxide assay. *ROS production was assessed by measuring hydrogen peroxide levels in CaCo2 and BE(2)-M17 cell lysates.*

Supernatants were transferred to new eppendorf tubes. Whilst samples were thawing, the actual concentration of the hydrogen peroxide, from the H_2O_2 assay kit from Elabscience (USA), was calculated by diluting it 100 times in distilled water and measuring the absorbance reading, using a glass cuvette, in a spectrophotometer at 240 nm. Actual concentration was calculated using formula:

$$Actual\ concentration = 22.94 \times A_{240} \times 100 \div 1000$$

Standards were made up by a serial dilution with the actual concentration of H_2O_2 taken into account. 100 µl of reagent 1 from the kit was plated into each well and incubated at 37°C for 10 minutes. 10 µl of either samples or standards were plated into a well of a 96-well (Appendix B). 100 µl of reagent 2 was added to each well and the plate was shaken for 5 seconds and then read at 405 nm using a SPECTROstar Nano® absorbance plate reader (BMG Labtech, Ortenberg, Germany).

3.3.4 TEAC Assay

$1x10^6$ cells were harvested in 100 µl cold PBS for the Trolox Equivalent Antioxidant Capacity (TEAC) assay. Samples were immediately placed on ice and stored in a -80°C freezer until the assay was performed. 2,2'-Azino-bis(3-ethylbenzothiazoline-6-sulfonic acid) diammonium salt ($ABTS^{\bullet-}$) stock solution was prepared by adding 88 µl of 140 mM potassium persulphate with 5 ml of 7 mM ABTS. The $ABTS^{\bullet-}$ stock solution was then covered in foil and left to develop for 16 hours in the dark. Samples were thawed and sonicated on ice for three 5 second pulses with 20 second intervals with an amplitude of 5. Samples were then centrifuged for 15 minutes at 12000 rpm as seen in Figure 3.7. During sample preparation, Trolox (a vitamin E analog) standards were prepared from a 1 mM stock solution, diluted in ethanol to concentrations of 0, 50, 100, 150, 250 and 500 µM. $ABTS^{\bullet-}$ was diluted in ethanol to obtain an absorbance reading of 0.7 ± 0.02. 25 µl of each standard and sample was loaded in triplicate into wells of a 96-well plate (see Appendix C for protocol used; adapted from

Ross *et al*. (2020)). 300 µl of diluted $ABTS^{\bullet-}$ was then added to each well and the plate was left to stand in the absence of light, at room temperature for 30 minutes, and then read at 734 nm at 25°C.

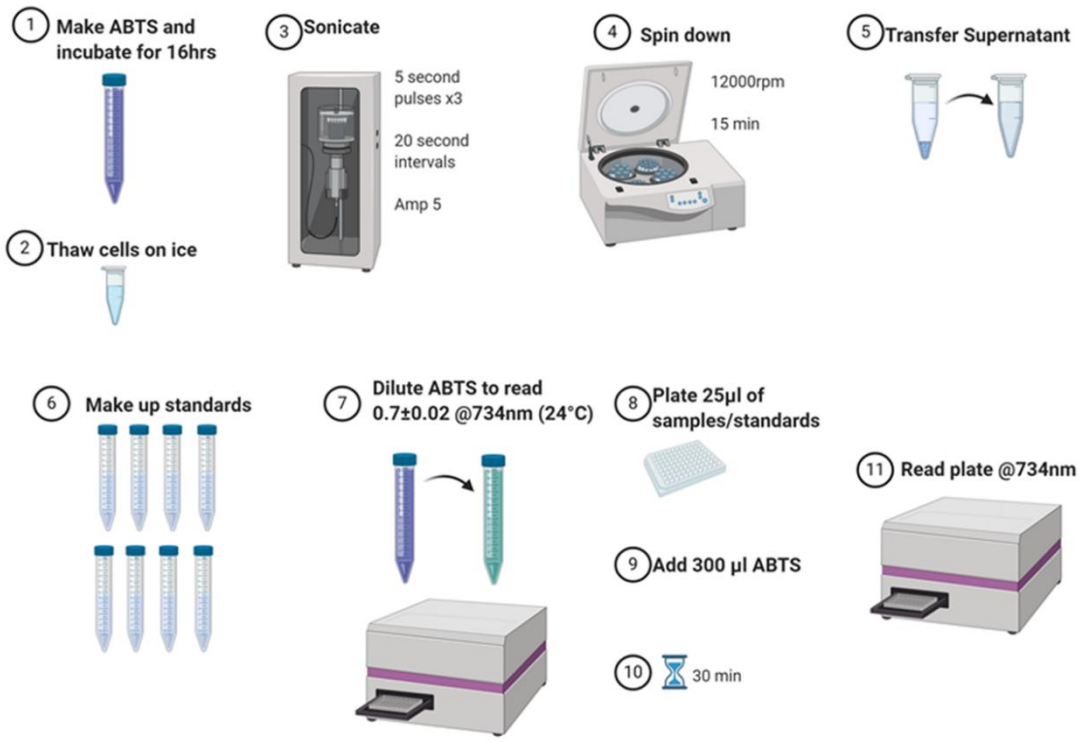

Figure 3.7: TEAC assay. *Antioxidant capacity was assessed comparing the radical scavenging capacity in CaCo2 and BE(2)-M17 cell lysates when compared to a known antioxidant (Trolox). $ABTS^{\bullet-}$: 2,2'-Azino-bis(3-ethylbenzothiazoline-6-sulfonic acid) diammonium salt.*

3.4. Zebrafish *in vivo* models

3.4.1 Materials

Danio rerio eggs were obtained from the zebrafish unit at Stellenbosch University, Tygerberg Campus. Pentylenetetrazole (PTZ) (P6500), lipopolysaccharides (LPS) (L4516), low melting-point agarose (A9414), methyl cellulose (M0387), methylene blue, tricaine (ethyl 3-aminobenzoate methanesulfonate salt) (A5040), and E3 salts; sodium chloride (NaCl) (S7653), magnesium sulphate ($MgSO_4$) (208094), potassium chloride (KCl) (P9541) and calcium chloride (CaCl) (C5670) were purchased from Sigma Aldrich (Merck) (MO, USA). 1 mg Fluanxol® tablets were purchased from Stelkor Kampus Apteek and is sourced from Lundbeck (NSW, Australia). Diazepam, also known as Valium, (F1149) was purchased from Roche. Hank's balanced salt solution (HBSS) (14185-045) was purchased from Gibco Laboratories (MA, USA). 96-well plates were purchased from Nest. Petri dishes were purchased from Cellstar. Lab-tek chambered cover glasses (155411) were purchased through central analytical facilities (CAF) who sourced them from Thermo Fisher Scientific (NY, USA). 5-(and 6-)chloromethyl-2',7'-dichlorodihydrofluorescein diacetate (CM-H_2DCFDA) (C6827) was purchased from Thermo Fisher Scientific (NY, USA).

3.4.2 Zebrafish maintenance and egg harvesting

Danio rerio were maintained at 28.5°C under a 14:10 light-dark cycle. Adults were bred with a ratio of 1 female: 2 males. Breeding tanks were set up the day before breeding to allow adults to acclimatise overnight. Once fish had spawned, eggs were collected and divided into groups of 50 eggs per petri dish. Embryos were kept in an incubator set at 28.5°C in petri dishes containing E3 embryo medium (5 mM NaCl, 0.17 mM KCl, 0.33 mM CaCl2, 0.33 mM $MgSO_4$, 0.01% methylene blue) (Westerfield, 1993). E3 medium was renewed every 24 hours by removing half the volume along with debris and topping up with fresh, warm, E3 medium. Once larvae had reached 4 dpf they were plated into 96-wells for various experiments to assess toxicity, antipsychotic action, and effect on redox of Flupentixol dihydrochloride *in vivo* as shown in Figure 3.8. All zebrafish were anaesthetised using tricaine solution after the completion of experiments within 5 dpf. Tricaine stock solution (0.1% w/v) was made by adding 200 mg ethyl 3-aminobenzoate methanesulfonate salt to 48.95 ml of distilled water and 1.05 ml of 1 M Tris (pH 9.0) and adjusted to a PH of 7.0. Then, 4 ml of tricaine stock solution was diluted to 100 ml using E3 media for working solution anaesthetic.

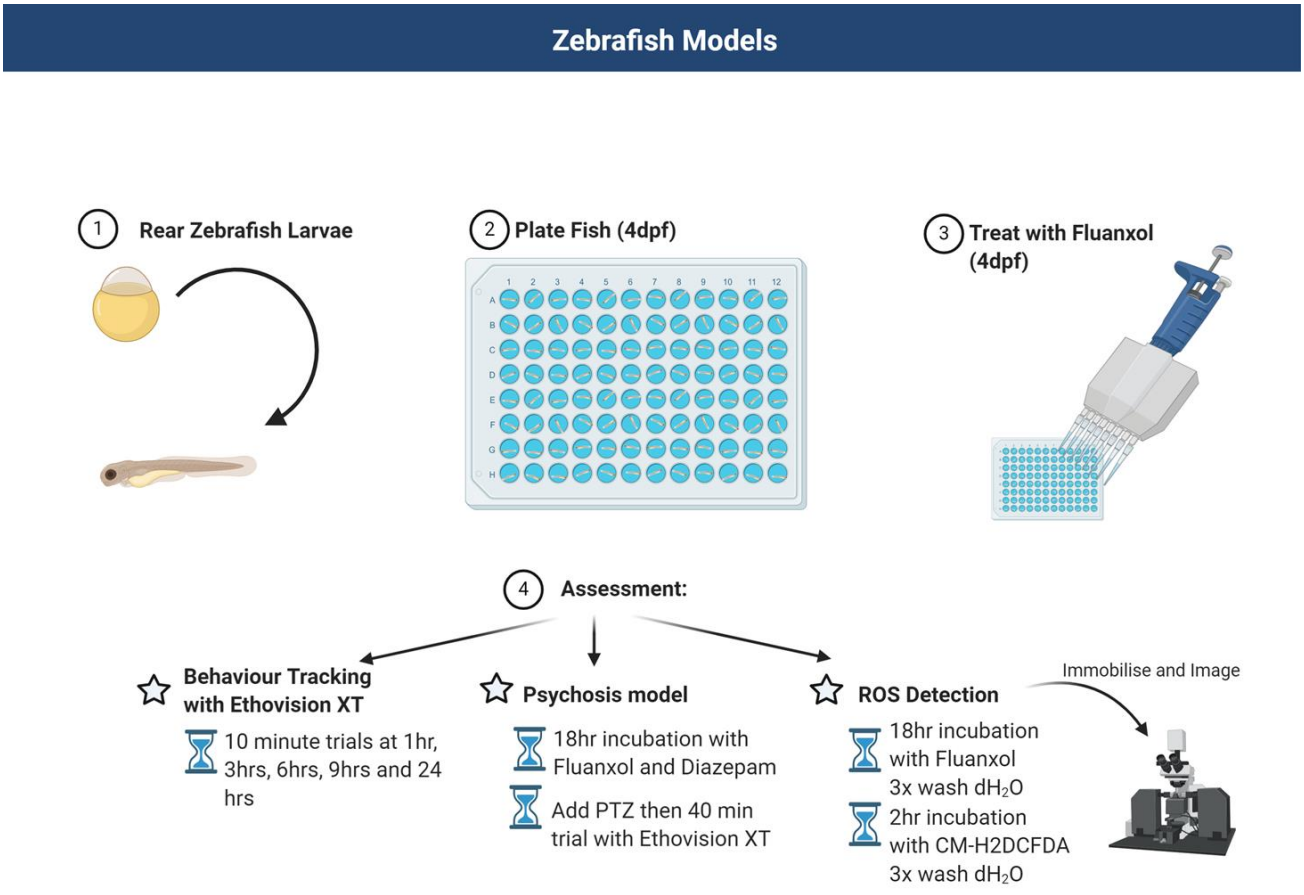

Figure 3.8: Zebrafish models to assess toxicity, antipsychotic action and effect on redox. *After Fluanxol treatment larvae movement was tracked to investigate toxicity over a broad range of doses. Antipsychotic action of Fluanxol was investigated in a model for psychosis. Redox effects of the drug were assessed by investigating ROS levels using a fluorescent marker; CM-H_2DCFDA. PTZ: pentylenetetrazole.*

3.4.3 Toxicity screening

Zebrafish larvae were treated at 4 dpf with various doses of Fluanxol® across a broad range up to 13.14 M flupentixol dihydrochloride (6,67 µg/ml) in a pilot study using touch response to assess toxicity (Kokel *et al.*, 2010) with 8 zebrafish per treatment group. Larvae were touched gently using a pipette tip, careful not to induce damage, and monitored for rapid response as per normal, slow response, posture deformations or death according to ethics committee-approved protocol. Touch response assessment was performed at time intervals at time of treatment followed by 1 hour, 3 hours, 6 hours, 9 hours and 24 hours after treatment. The qualitative assessment was then followed up by a quantitative assessment where zebrafish larvae were treated with increasing doses of Fluanxol® and monitored using Ethovision software connected to a Daniovison chamber from Noldus. Behavioural monitoring was then quantified across treatment groups to assess toxicity of the drug by measuring zebrafish larvae movement. Larvae were allowed 10 minutes to acclimatise to the Daniovision chamber followed by 20 minutes of recorded locomotor activity. Trials were set up and run at baseline and time points of 3 hours, 9 hours and 18 hours post treatment.

3.4.4 Psychosis model

Antipsychotic action of flupentixol dihydrochloride was assessed *in vivo* using an accepted zebrafish psychosis model. The model involves inducing psychosis-like behaviour using pentylenetetrazole (PTZ), which is a $GABA_A$ receptor antagonist (Afrikanova *et al.*, 2013). GABA receptor antagonism by PTZ results in erratic movement and an increase in locomotor activity in zebrafish, an effect that is reversed by potent GABA receptor agonist, diazepam, also known as Valium® (Mussulini *et al.*, 2013). Increased activity and erratic movement observed in zebrafish larvae after PTZ treatment indicates GABAergic signalling agonism simulating hyperGABAergic signalling present in psychosis. Attenuation of the erratic elevated locomotor behaviour indicates therapeutic benefit in restoring GABA signal transmission towards basal levels if the therapeutic target has been ruled out as sedatory in the absence of PTZ (Afrikanova *et al.*, 2013). Zebrafish larvae were plated individually into wells on a 96-well plate at 4 dpf and allowed to acclimatise while treatments were made up. All treatments were made up fresh on the day. Zebrafish larvae were treated with doses of Fluanxol® (0 µM, 0.3 µM, 0.6 µM, 1.2 µM, 2.5 µM, 5 µM, 10 µM, 25 µM and 50 µM) and 4 µM Diazepam. Each of the 10 treatment groups (n=8 per group) were then treated with 10 mM PTZ for an acute assessment of Fluanxol® antipsychotic effects. Behavioural studies with PTZ induced hyperlocomotion in zebrafish larvae used between 10 and 12 zebrafish per treatment group (Berghmans *et al.*, 2007; Afrikanova *et al.*, 2013; Gupta, Khobragade and Shingatgeri, 2014). In our study, as previously stated, we used 8 fish per treatment group to reduce number of larvae required while maintaining sufficient statistical power. A control group (n=8) was plated in E3 media alone. After addition of PTZ with a multichannel the plate was placed in the Daniovision observation chamber and a 35-minute trial was run, through Ethovision XT15 software, recording movement over time. An 18 hour incubation was also assessed (Afrikanova *et al.*, 2013) as Fluanxol® has a half-life of 35 hours and may take more time to be effective than in the acute setting. Zebrafish larvae were treated with the

same doses of Fluanxol® (0 µM, 0.3 µM, 0.6 µM, 1.2 µM, 2.5 µM, 5 µM, 10 µM, 25 µM and 50 µM) and 4 µM Diazepam and left to incubate at 28.5°C overnight. 18 hours after treatment, 10 mM PTZ was added and a 35-minute trial was run, through Ethovision XT15 software, recording movement over time.

3.4.5 Oxidative stress detection

A fluorescent marker, CM-H_2DCFDA, was used to assess ROS levels *in vivo* with a protocol adapted from (Kim *et al.*, 2014). Zebrafish larvae were plated at 4 dpf into a 96-well and treated with 0 µM, 1.2 µM, 25 µM and 50 µM in the presence and absence of 10 µg/ml LPS. These doses were selected based on the results of previous experiments in the PTZ model and an incubation time of 18 hours was opted for. 18 hours after treatment, larvae were washed with distilled water three times using self-engineered baskets to prevent damage to larvae from pipetting, minimise time larvae are exposed to air and reduce overall time taken to perform wash and stain steps. Larvae were incubated in 1 µg/ml CM-H_2DCFDA for 2 hours and washed again three times in distilled water (Kim *et al.*, 2014; Sökmen *et al.*, 2020). Mounting media was optimised in a pilot study and it was determined that 1% low melting-point agarose was easier to work with due to its low viscosity while mounting that then sets, when compared to 3% methyl cellulose which is quite viscous and more difficult to mount with but more cost effective. 1.5 g of methyl cellulose was made up in 25 ml of E3 medium at 30°C and stirred, 25 ml of cold (0-4°C) E3 medium was then added and the solution was stirred vigorously until fully dissolved. The solution was refrigerated overnight to remove all the bubbles. Zebrafish were mounted into 8-chamber slides and imaged using Zeiss AxioObserver 7 inverted microscope. Images were processed using ZEN 2.6 (blue edition) software and analysed using ImageJ.

3.5 Statistical analysis

Statistical analysis was performed in GraphPad Prism Version 7.04. Normality was assessed using the D'Agostino-Pearson omnibus normality test. Depending on the results of the normality test, if data was normally distributed an ANOVA parametric test was used and if data was not normally distributed Kruskal Wallis nonparametric test was used. Multiple comparisons tests were used when parametric and nonparametric tests indicated a significant difference between groups and were selected for their appropriate conservativeness to avoid type I error from α inflation (Lee and Lee, 2018). One-way ANOVAs were performed with a Bonferroni post hoc test in WST-1 assay data if the data was normally distributed. WST-1 data that did not pass the normality test were analysed using Kruskal Wallis test with Dunn's multiple comparisons test. Two-way ANOVAs were performed for the redox assay data to test statistical significance between change in Fluanxol® treatment doses with or without LPS treatment. Statistical significance was noted at a p-value less than 0.05. Zebrafish toxicity screen data, PTZ model data and imaging data were analysed with a two-way repeated measures Two-way ANOVA and a Bonferroni multiple comparisons test was performed when the ANOVA analysis indicated statistical significance.

3.6 Ethical considerations

Zebrafish larvae were analysed before 5dpf and therefore all experiments performed as such in this thesis are exempt from requiring ethical clearance as according to SANS guidelines. This study was cleared according to these guidelines (11820).

Chapter 4:

Results

4.1 WST-1 assays

4.1.1 Fluanxol® dose response in CaCo2 gut-epithelial adenocarcinoma cells

As depicted in Figure 4.1, mitochondrial succinate dehydrogenase activity showed no change within the prescribed doses - (3 mg/day to 12 mg/day) equivalent doses of Fluanxol® at 100% concentration representing 100% bioavailability (200 ng/ml to 800 ng/ml Fluanxol® concentration) - when compared to the control group in gut epithelial carcinoma CaCo2 cells. In the 30 mg/day overdose equivalent (2000 ng/ml Fluanxol® concentration) a significant reduction ($p<0.0001$) in mitochondrial dehydrogenase activity was observed in these cells indicating a loss of cell viability at this dose.

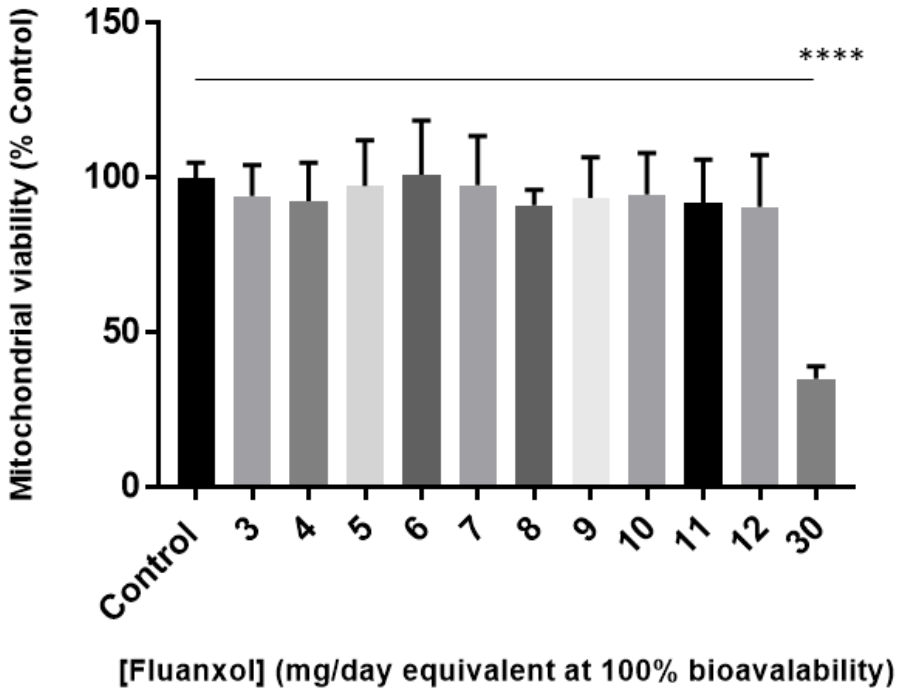

Figure 4.1: Fluanxol® dose response in CaCo2 cells. *Gut epithelial carcinoma cells incubated for 3 hours with WST-1 reagent after 24 hour incubation with clinically relevant prescribed doses (3 mg/day to 12 mg/day) and an overdose 30 mg/day Fluanxol® concentration treated at 100% concentrations adjusted for a 48-well plate cell monolayer (200 ng/ml to 800 ng/ml and 2000 ng/ml Fluanxol® concentration respectively). Data displayed as mean ± SD and given as a percentage of the control to indicate change in mitochondrial dehydrogenase activity across increasing treatment doses (Kruskal Wallis test, Dunn's post hoc; significance with *p<0.05, ****p<0.0001; n = 3).*

4.1.2 Fluanxol® dose response in BE(2)-M17 neuroblastoma cells

Mitochondrial dehydrogenase activity showed no change within the prescribed doses - (3mg/day to 12mg/day) equivalent doses of Fluanxol® at 40% concentration representing 40% bioavailability (80 ng/ml to 320 ng/ml Fluanxol® concentration) – when compared to the control group in BE(2)-M17 neuroblastoma cells; except for at the 11mg/day equivalent dose (293.3 ng/ml Fluanxol® concentration) which showed a slight decrease in mitochondrial dehydrogenase activity ($p<0.05$) (Figure 4.2). In the 30 mg/day overdose equivalent (800 ng/ml Fluanxol® concentration) a significant reduction ($p<0.0001$) in mitochondrial dehydrogenase activity was observed in these cells, indicating a loss of cell viability at this overdose concentration.

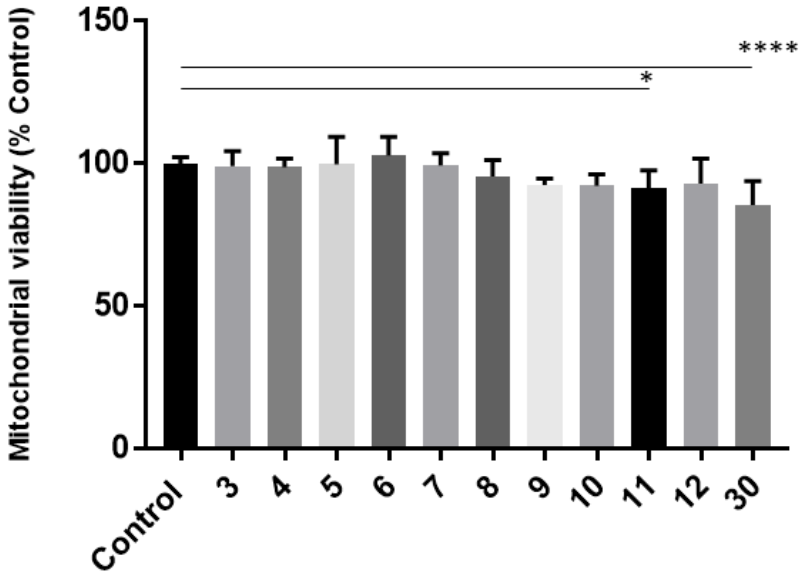

Figure 4.2: Fluanxol® dose response in BE(2)-M17 cells. *Neuroblastoma cells incubated for 3 hours with WST-1 reagent after 24 hour incubation with clinically relevant prescribed doses (3mg/day to 12mg/day) and an overdose 30mg/day Fluanxol® concentration treated at 40% concentrations adjusted for a 48-well plate cell monolayer (80ng/ml to 320ng/ml and 800ng/ml Fluanxol® concentration respectively). Data displayed as mean ± SD and given as a percentage of the control to indicate change in mitochondrial dehydrogenase activity across increasing treatment doses (one-way ANOVA, Bonferroni post hoc; significance with *p<0.05, ****p<0.0001; n = 3).*

4.1.3 LPS dose response in CaCo2 gut-epithelial adenocarcinoma cells

LPS treatment induced a significant increase in mitochondrial dehydrogenase activity at a dose of 2 µg/ml when compared to control group of CaCo2 cells (Figure 4.3). A dose response was observed with increasing mitochondrial dehydrogenase activity with increasing doses up to 20 µg/ml. 10 µg/ml is an LPS concentration that resulted in very significant increase in mitochondrial dehydrogenase

activity at a sub lethal dose. This dose has been used previously to stimulate CaCo2 cells with LPS (Lin *et al.,* 2015) and was therefore was the chosen concentration for further redox experiments.

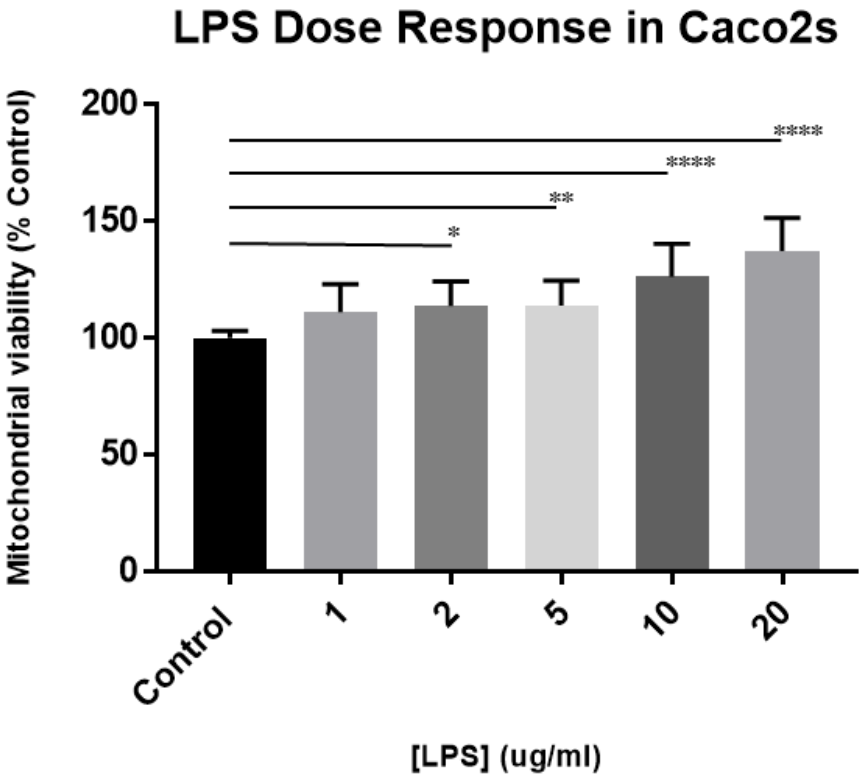

Figure 4.3: LPS dose response in CaCo2 cells. *Gut epithelial carcinoma cells incubated for 3 hours with WST-1 reagent after 24-hour incubation with ranging doses of LPS (1 µg/ml to 20 µg/ml concentrations) in a 48-well plate. Data displayed as mean ± SD and given as a percentage of the control to indicate change in mitochondrial dehydrogenase activity across increasing treatment doses (Kruskal-Wallis test, Dunn's post hoc; significance with *p<0.05, **p<0.01, ****p<0.0001; n = 3).*

4.1.4 LPS dose response in BE(2)-M17 neuroblastoma cells

LPS treatment induced a significant increase in mitochondrial dehydrogenase activity at a dose of 10 ng/ml and 100 ng/ml concentration when compared to control group of BE(2)-M17 cells (Figure 4.4). LPS concentration of 100 ng/ml induced a significant increase ($p<0.01$) in mitochondrial dehydrogenase activity at a sub lethal dose and has been used previously to stimulate BE(2)-M17

cells with LPS (Minter *et al.*, 2015). No significant change was observed at treated LPS concentrations of 500 ng/ml and higher.

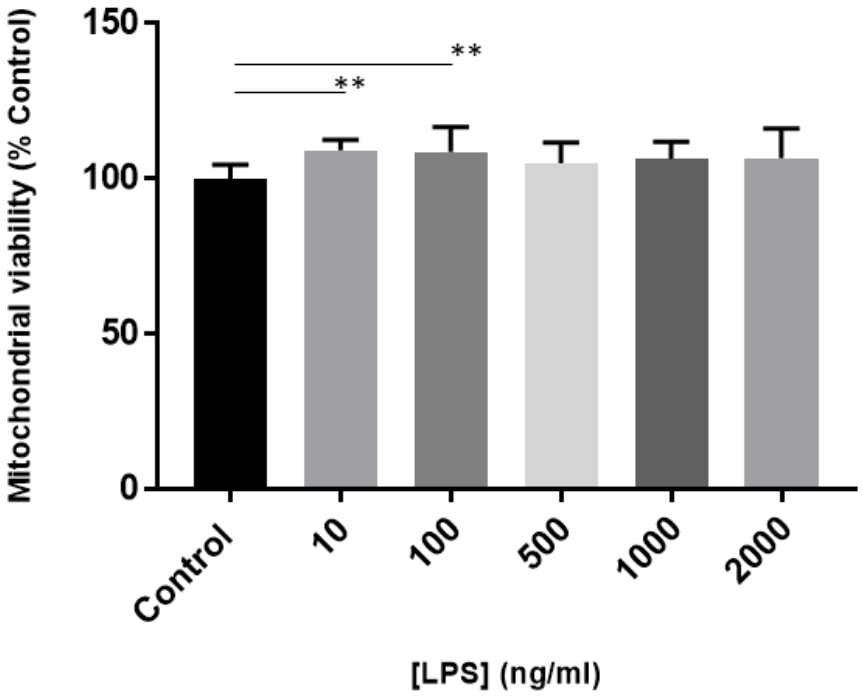

***Figure 4.4*: LPS dose response in BE(2)-M17 cells.** Gut epithelial carcinoma cells incubated for 3 hours with WST-1 reagent after 24-hour incubation with ranging doses of LPS (10 ng/ml to 2000 ng/ml concentrations) in a 48-well plate. Data displayed as mean ± SD and given as a percentage of the control to indicate change in mitochondrial dehydrogenase activity across increasing treatment doses (one-way ANOVA, Bonferroni post hoc; significance with **p<0.01; n = 3).

4.2 Cell viability assessed with trypan blue

Trypan blue stains cells that are no longer viable. Viable cells are impermeable to trypan blue dye. The percentage of live cells from the total number of cells was used to determine cell viability. Unfortunately, due to equipment malfunction the data was unreliable and erring on the side of caution was not interpreted.

4.3 Redox Assays

4.3.1 Lipid peroxidation

Thiobarbituric Acid Reactive Substances (TBARS) malondialdehyde (MDA) assay measures lipid peroxidation by reacting with by-product of lipid peroxidation; MDA. No change was observed in either the CaCo2 gut epithelial or the BE(2)-M17 cell line across treatment doses of Fluanxol® with or without LPS stimulation (Figure 4.5). The CaCo2 cell levels of lipid peroxidation fell below the limit of detection for this assay (1.1 µM) (Aguilar Diaz De Leon and Borges, 2020). The MDA levels were observed to be generally higher in the neuroblastoma cells (in the range of 1.5 to 2 µM).

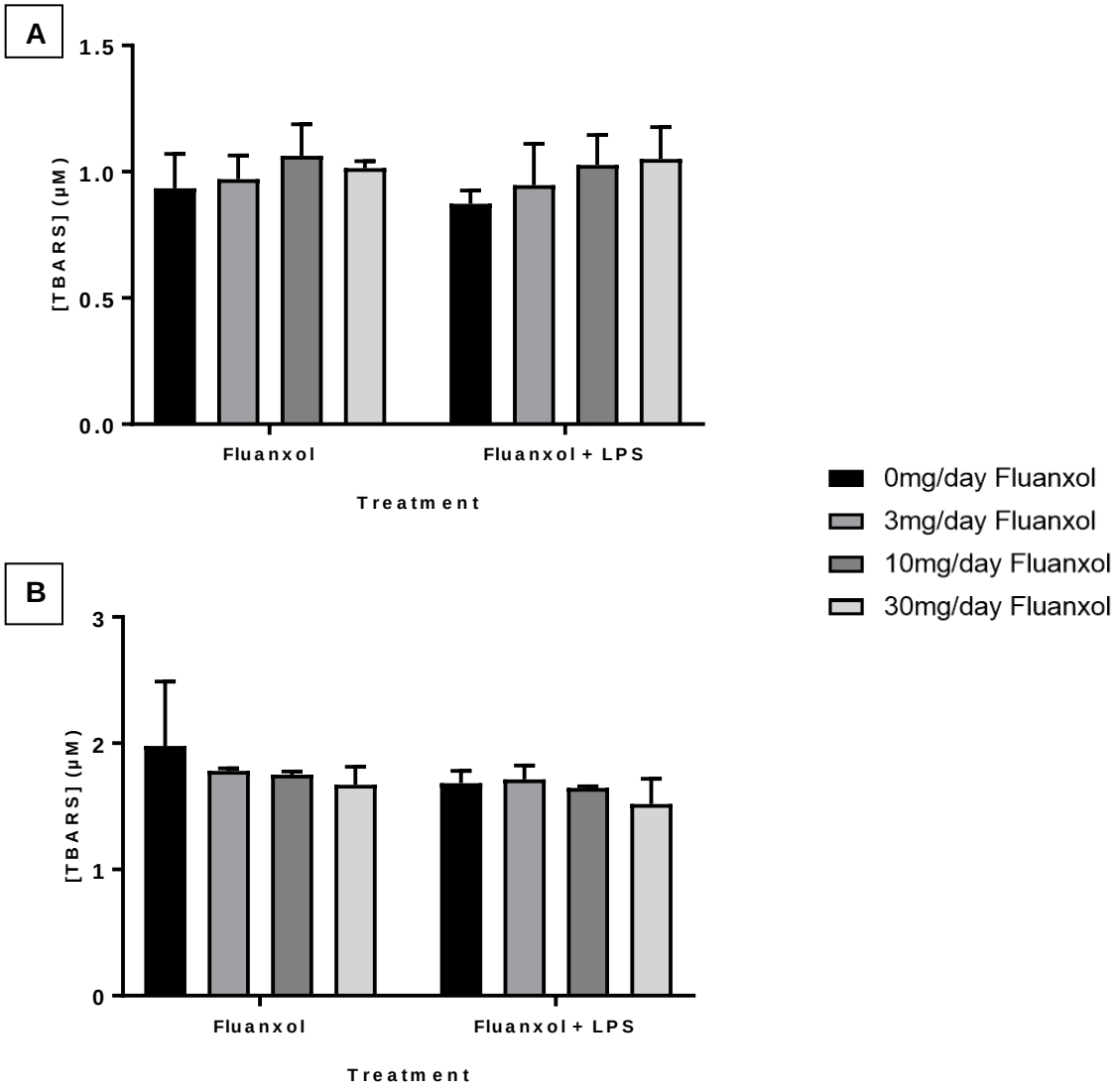

***Figure 4.5*: Lipid peroxidation in CaCo2 and BE(2)-M17 cells.** Gut epithelial carcinoma cells (A) and BE(2)-M17 cells (B) were cultured and treated with Fluanxol® with or without LPS stimulation for 24 hours. Cells were harvested at $5x10^6$ cells and assessed in terms of oxidative damage with TBARS (MDA) assay indicating MDA concentration in µM. Data displayed as mean ± SD (two-way ANOVA, n = 3).

4.2.2 H_2O_2 assay

The hydrogen peroxide assay kit from Elabscience measures levels of H_2O_2 in samples, an indicator of oxidative stress. No significant difference was observed between treatment groups of Fluanxol® in the presence or absence of LPS in either CaCo2 gut-epithelial cells or BE(2)-M17 neuroblastoma

cells (Figure 4.6). H_2O_2 levels were observed to relatively higher in gut-epithelial cells (range from 5.51 mmol/l ± 0.95 to 8.32 mmol/l ±0.17) than in neuroblastoma cells (range from 2.49 mmol/l ±0.75 to 3.89 mmol/l ±1.30). All data was above the assay's limit of detection (1.5 mmol/l).

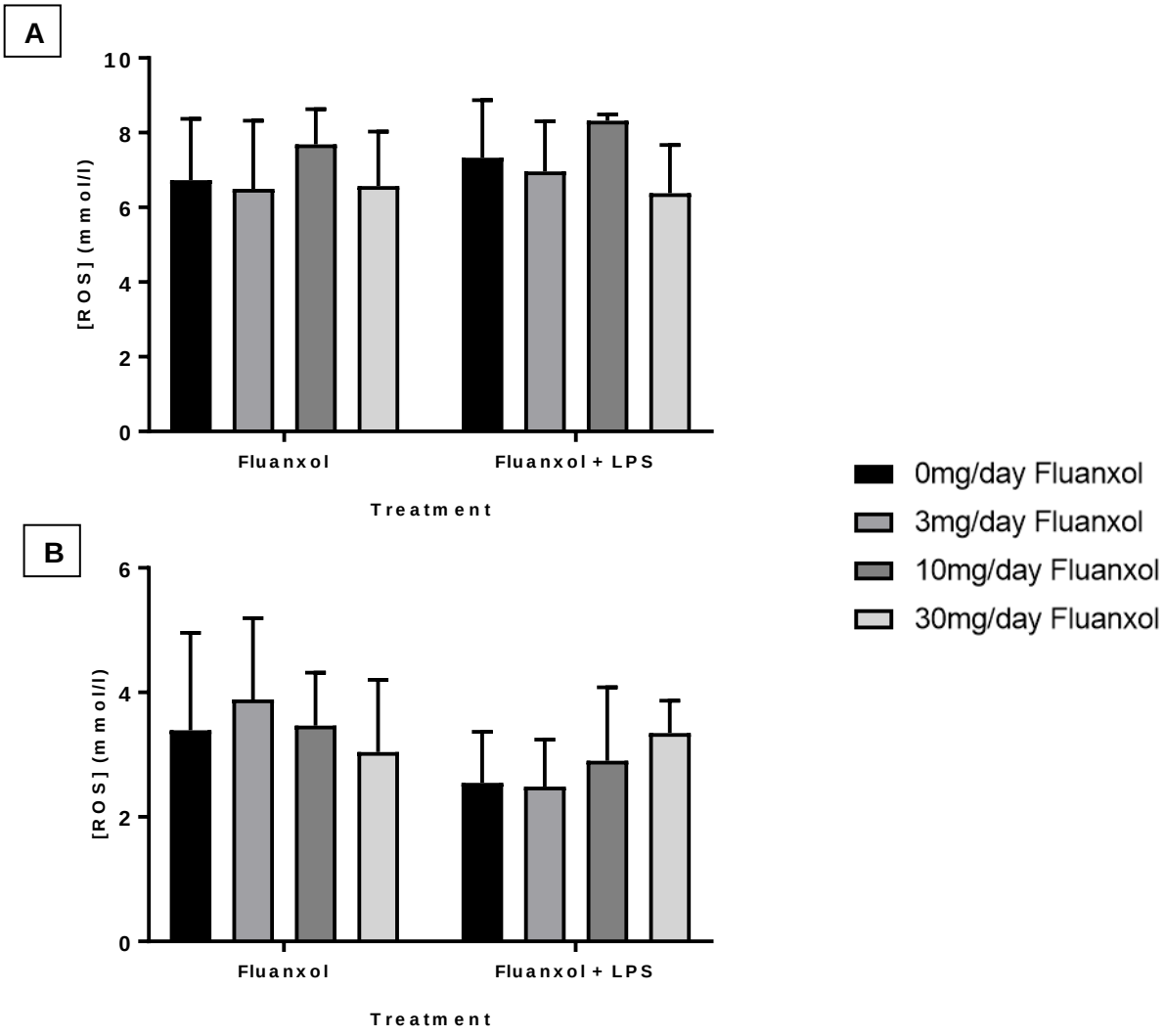

Figure 4.6: Hydrogen peroxide levels (ROS) in CaCo2 and BE(2)-M17 cells. *Gut epithelial carcinoma cells (A) and BE(2)-M17 cells (B) were cultured and treated with Fluanxol® with or without LPS stimulation for 24 hours. Cells were harvested at 1x10^6 cells and assessed in terms of ROS levels and oxidative stress by measuring H_2O_2 concentrations in cell lysate. Data displayed as mean ± SD (two-way ANOVA, n = 3).*

4.2.3 TEAC

Trolox Equivalent Antioxidant Capacity assay measures antioxidant capacity by comparing sample readings to a known concentration of antioxidant Trolox (a vitamin E analog). No change was observed in either the CaCo2 gut epithelial or the BE(2)-M17 cell line across treatment doses of Fluanxol® with or without LPS stimulation (Figure 4.7). Antioxidant capacity was lower in the neuroblastoma cells (ranging from 189.68 µM ±20.42 to 220.6 µM Trolox equivalent antioxidant capacity) when compared to gut epithelial cells (ranging from 229.45 µM ±42.93 to 257.65 µM ±34.89 Trolox equivalent antioxidant capacity).

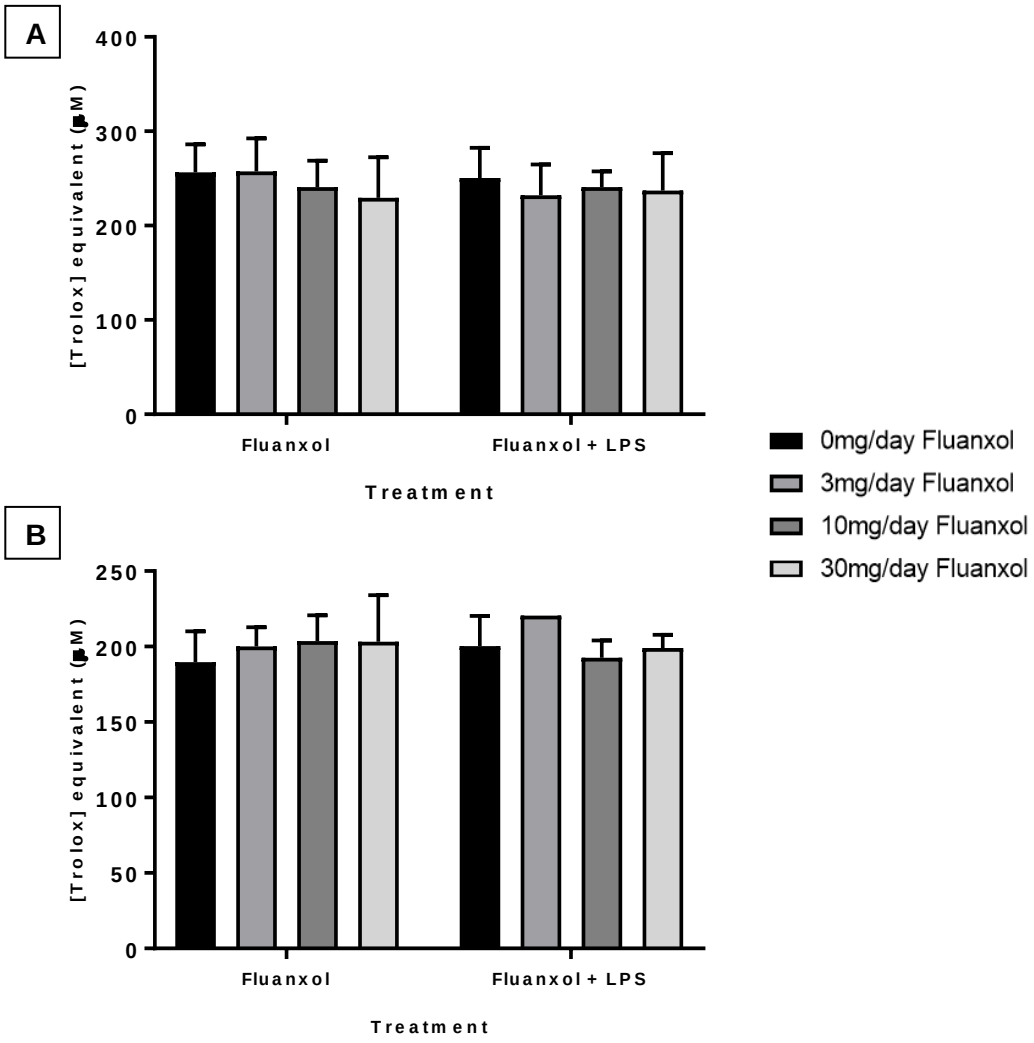

Figure 4.7: TEAC assay in CaCo2 and BE(2)-M17 cells. *Gut epithelial carcinoma cells (A) and BE(2)-M17 cells (B) were cultured and treated with Fluanxol® with or without LPS stimulation for 24 hours. Cells were harvested at 1x10^6 cells and assessed in terms of antioxidant capacity by comparing sample values to known concentrations of Trolox (μM). Data displayed as mean ± SD (Kruskal Wallis test (A), two-way ANOVA (B), n = 3).*

4.3 Zebrafish models

4.3.1 Toxicity Screen *in vivo*

Zebrafish larvae treated with various doses of Fluanxol® (0.3 µM to 49.27 µM) displayed no indications of toxicity as assessed by locomotor activity. There was not a consistent difference observed between untreated control zebrafish larvae and larvae treated with Fluanxol® in terms of mean distance moved in mm at baseline (Figure 4.8 A), 3 hours (Figure 4.8 B), 9 hours (Figure 4.8 C) and 18 hours (Figure 4.8 D) after treatment as well as velocity in mm/sec at baseline (Figure 4.9 A), 3 hours (Figure 4.9 B), 9 hours (Figure 4.9 C) and 18 hours (Figure 4.9 D) after treatment with various doses of Fluanxol®. Significant differences between groups were infrequent and inconsistent

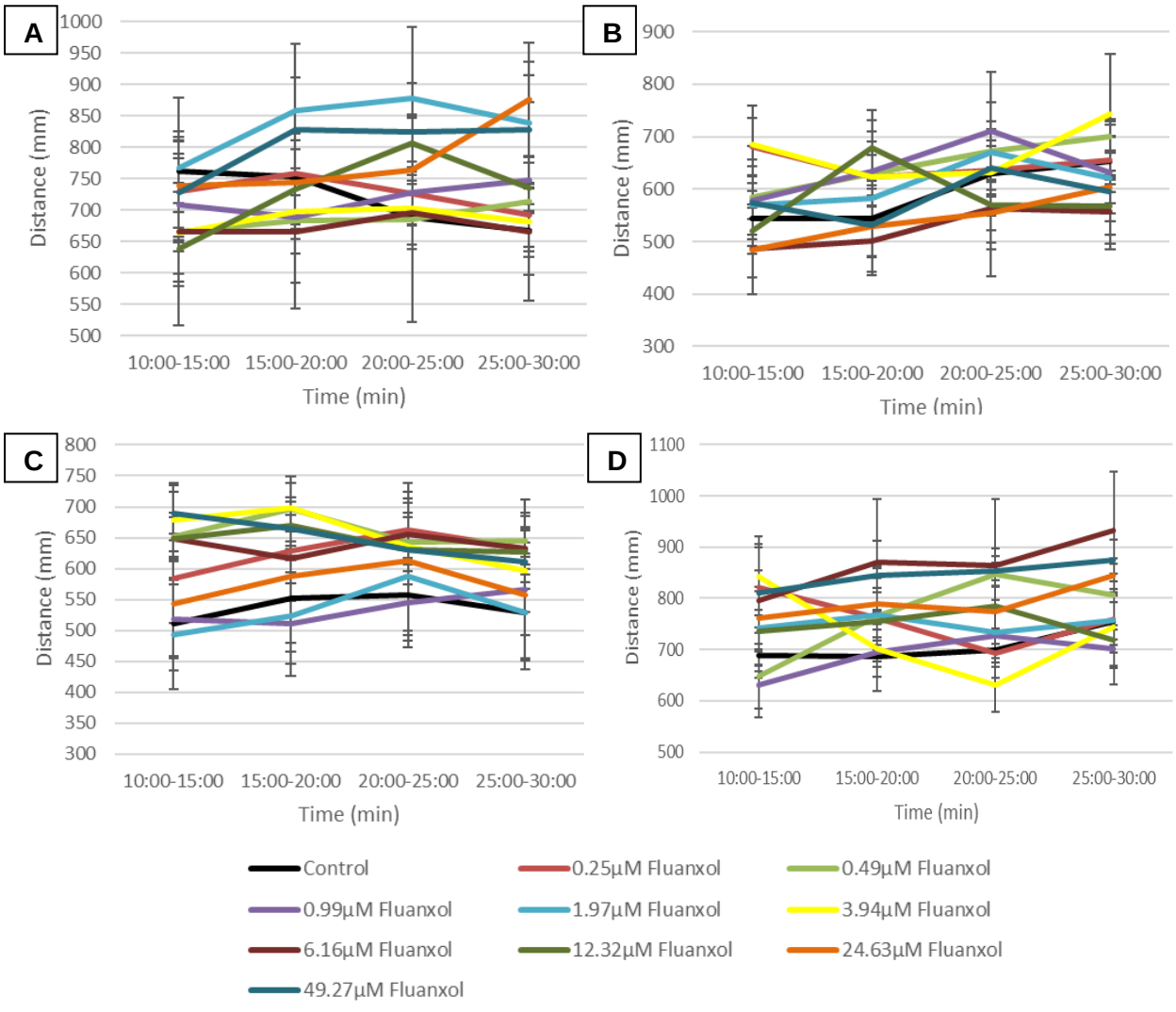

Figure 4. 8: Mean total distance moved of zebrafish larvae after treatment of Fluanxol. *Mean total distance moved was measured using behaviour tracking at baseline (A), 3 hours post treatment (B), 9 hours post treatment (C) and 18 hours post treatment (D). Trials were recorded 10 minutes after 4 dpf zebrafish were placed into the Daniovision chamber to allow for acclimatisation. Zebrafish were treated with a range of Fluanxol doses (0.25 µM, 0.49 µM, 0.99 µM, 1.97 µM, 3.94 µM, 6.16 µM, 12.32 µM, 24.63 µM and 49.27 µM). Data displayed as mean ± SE (two-way ANOVA, Bonferroni post hoc, significance with p<0.05 not shown on graph for clearer visibility of data (Appendix D); n=8).*

across the trials at different time points. Statistical significance was not indicated on the graphs in Figure 4.8 and Figure 4.9 for clearer visibility of data (Appendix D.1 to D.8).

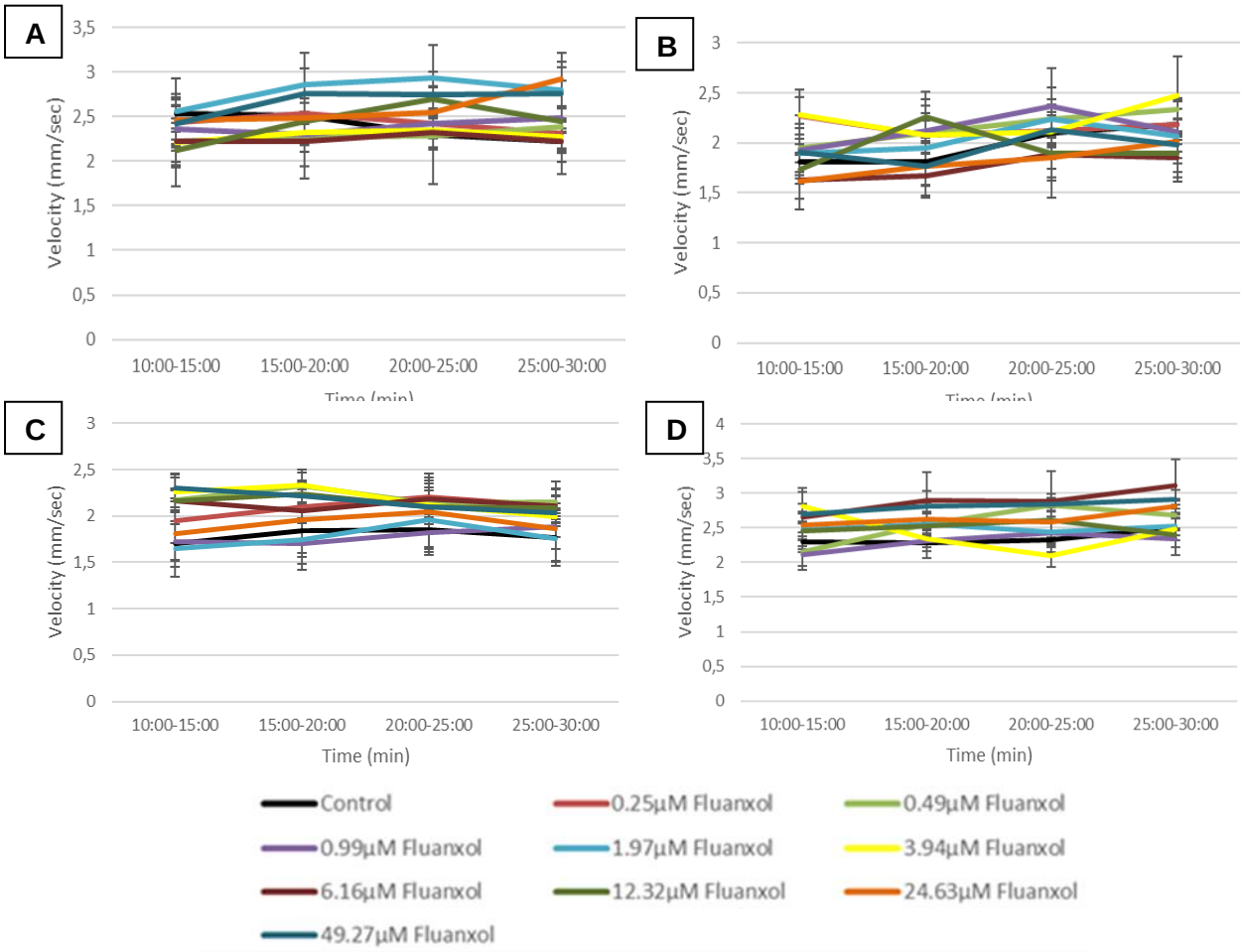

Figure 4.9: Mean velocity of zebrafish larvae after treatment of Fluanxol. *Mean velocity was measured using behaviour tracking at baseline (A), 3 hours post treatment (B), 9 hours post treatment (C) and 18 hours post treatment (D). Trials were recorded 10 minutes after 4 dpf zebrafish were placed into the Daniovision chamber to allow for acclimatisation. Zebrafish were treated with a range of Fluanxol doses (0.25 µM, 0.49 µM, 0.99 µM, 1.97 µM, 3.94 µM, 6.16 µM, 12.32 µM, 24.63 µM and 49.27 µM). Data displayed as mean ± SE (two-way ANOVA, Bonferroni post hoc, significance with p<0.05 not shown on graph for clearer visibility of data (Appendix D); n=8).*

After behaviour monitoring with Ethovision XT15 software, zebrafish larvae were assessed under a microscope for abnormalities such as a change in posture, mortality and response to touch. All zebrafish were normal at baseline, with no abnormalities or slow response to touch (Table 4.1). Within 1-hour post treatment all the zebrafish larvae treated with the higher doses of Fluanxol® 24.63 µM and 49.27 µM were slow responders. At 3 hours post-treatment, half of the treatment groups had 50% or more zebrafish with altered touch response, including 0.99 µM, 6.16 µM, 12.32 µM, 24.63 µM and 49.27 µM Fluanxol®. The first appearance of posture deformity occurred at 3 hours post-treatment within the 12.32 µM Fluanxol® which resulted in mortality of one subject in this treatment group by 6 hours post-treatment. At 6 hours post-treatment, most of the treatment groups had 50% or more zebrafish with altered touch response; 0.25 µM, 0.49 µM and 3.94 µM Fluanxol®. At 9 hours

post-treatment one subject of the 24.63µM Fluanxol® group experienced mortality. At 24 hours post-treatment, all the treatment groups had 50% or more zebrafish with altered touch response, excluding control group.

Table 4.1: Zebrafish mortality, deformities and touch response after treatment of Fluanxol®. Touch response and morphological changes was assessed under a light microscope. Zebrafish were treated with a range of Fluanxol® doses (0.25 µM, 0.49 µM, 0.99 µM, 1.97 µM, 3.94 µM, 6.16 µM, 12.32 µM, 24.63 µM and 49.27 µM) and assessed at baseline, 1 hour, 3 hours, 6 hours, 9 hours and 24 hours after treatment. Normal response to touch, slow response to touch, posture abnormalities or death were recorded and are displayed in the table as number of subjects of the treatment group (n=8).

Treatment Group	Baseline				1 Hour				3 Hours			
	Normal	Slow	Posture	Dead	Normal	Slow	Posture	Dead	Normal	Slow	Posture	Dead
Control	8	0	0	0	8	0	0	0	8	0	0	0
0.25µM	8	0	0	0	8	0	0	0	7	1	0	0
0.49µM	8	0	0	0	6	2	0	0	6	2	0	0
0.99µM	8	0	0	0	8	0	0	0	4	4	0	0
1.97µM	8	0	0	0	7	1	0	0	5	3	0	0
3.94µM	8	0	0	0	4	4	0	0	5	3	0	0
6.16µM	8	0	0	0	2	6	0	0	3	5	0	0
12.32µM	8	0	0	0	3	5	0	0	2	5	1	0
24.63µM	8	0	0	0	0	8	0	0	0	8	0	0
49.27µM	8	0	0	0	0	8	0	0	0	8	0	0
Treatment Group	6 Hours				9 Hours				24 Hours			
	Normal	Slow	Posture	Dead	Normal	Slow	Posture	Dead	Normal	Slow	Posture	Dead
Control	8	0	0	0	8	0	0	0	5	3	0	0
0.25µM	5	3	0	0	6	2	0	0	4	4	0	0
0.49µM	6	2	0	0	5	3	0	0	4	4	0	0
0.99µM	4	4	0	0	6	2	0	0	1	6	0	1
1.97µM	4	4	0	0	6	2	0	0	1	6	0	1
3.94µM	5	3	0	0	3	5	0	0	0	8	0	0
6.16µM	2	6	0	0	2	6	0	0	0	8	0	0
12.32µM	1	6	0	1	0	7	0	1	0	7	0	1
24.63µM	0	8	0	0	0	7	0	1	0	6	1	1
49.27µM	0	8	0	0	0	8	0	0	0	7	0	1

4.3.2 PTZ-induced Psychosis model

Pentylenetetrazole (PTZ) induces seizure-like movement in zebrafish through $GABA_A$ receptor antagonism. Diazepam, used as a positive treatment control, counteracts the effects of PTZ through GABA receptor agonism. The group of 4 dpf larvae treated with PTZ alone were significantly more motile than the control group ($p<0.001$) for distance measures and velocity measures from 15 minutes into the trials for acute treatment (Appendix D.9 and D.10) and 18-hour Fluanxol® incubation (Appendix D.11 and D.12). Validity of the psychosis model was supported by evident elevated total distance moved and velocity of zebrafish larvae when treated with PTZ alone when compared to control group and this effect was reversed by treatment with Diazepam (Figures 4.10 and 4.11).

After acute treatment with increasing doses of Fluanxol®, locomotor activity recorded in the control group was significantly different from all the groups of zebrafish larvae treated with Fluanxol®, except for 10µM Fluanxol®, 25µM Fluanxol® and 50µM Fluanxol® doses from 15 minutes into the trial ($p>0.9999$) but these effects were not long lasting and zebrafish in these respective treatment groups increased locomotor activity and were significantly elevated compared to the control group 25 minutes into the trial ($p<0.05$). After an 18-hour incubation with Fluanxol® doses, 25µM Fluanxol®

and 50µM Fluanxol® treatment consistently reduced zebrafish larvae locomotor activity similar to that of the control group (p>0.9999) indicating a reversed effect of PTZ-induced psychotic movement.

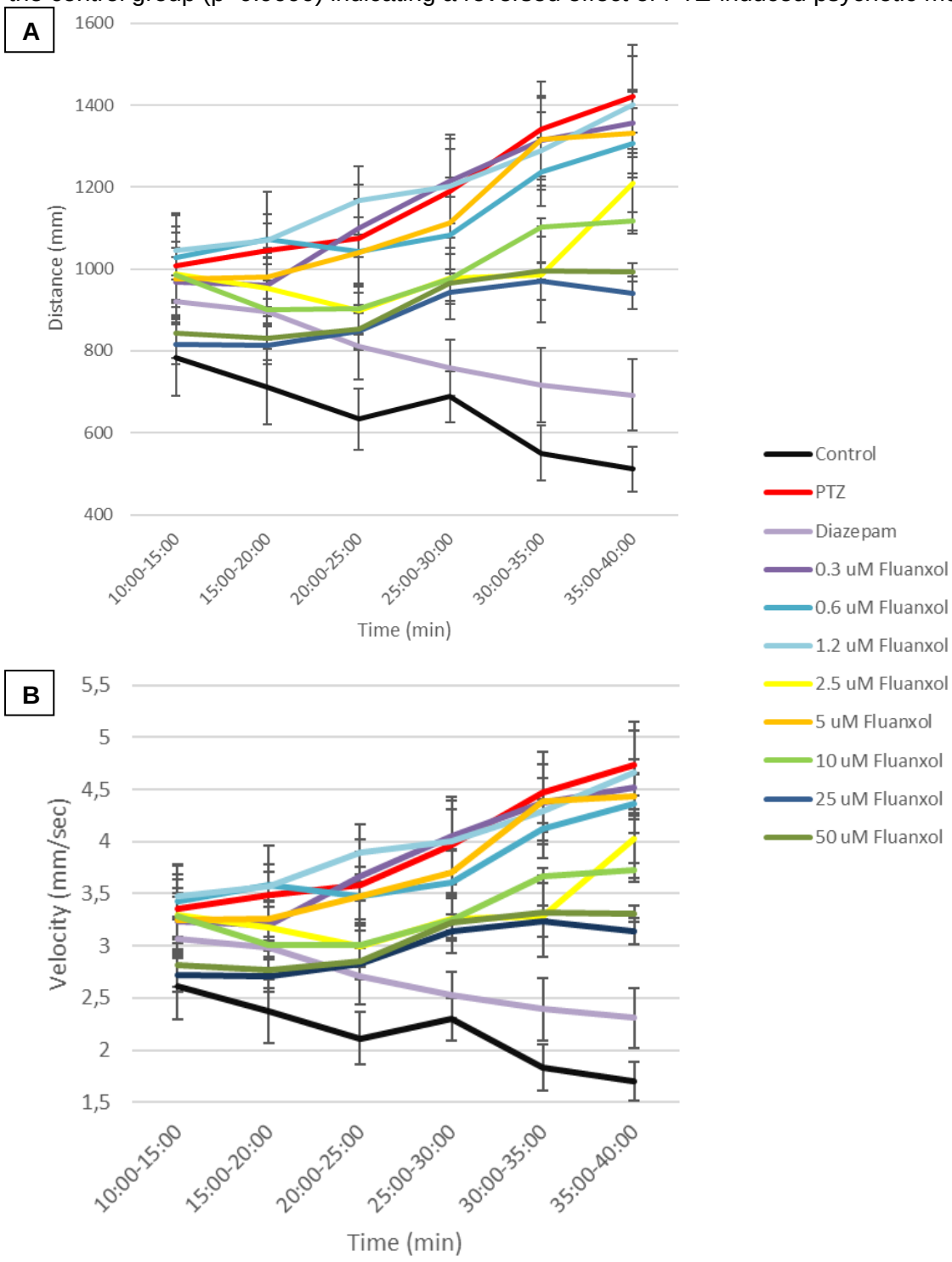

Figure 4.10: Psychosis model with acute treatment of Fluanxol. *Distance moved (A) and velocity (B) were recorded 10 minutes after addition of 10 mM PTZ to 4 dpf larvae (n=8 per group) to an untreated control group and zebrafish treated with 4 µM Diazepam or Fluanxol doses (0.3 µM, 0.6 µM, 1.2 µM, 2.5 µM, 5 µM, 10 µM, 25 µM, 50 µM). Data displayed as mean ± SE (two-way ANOVA, Bonferroni post hoc, significance with p<0.05 not shown on graph for clearer visibility of data (Appendix D); n=8).*

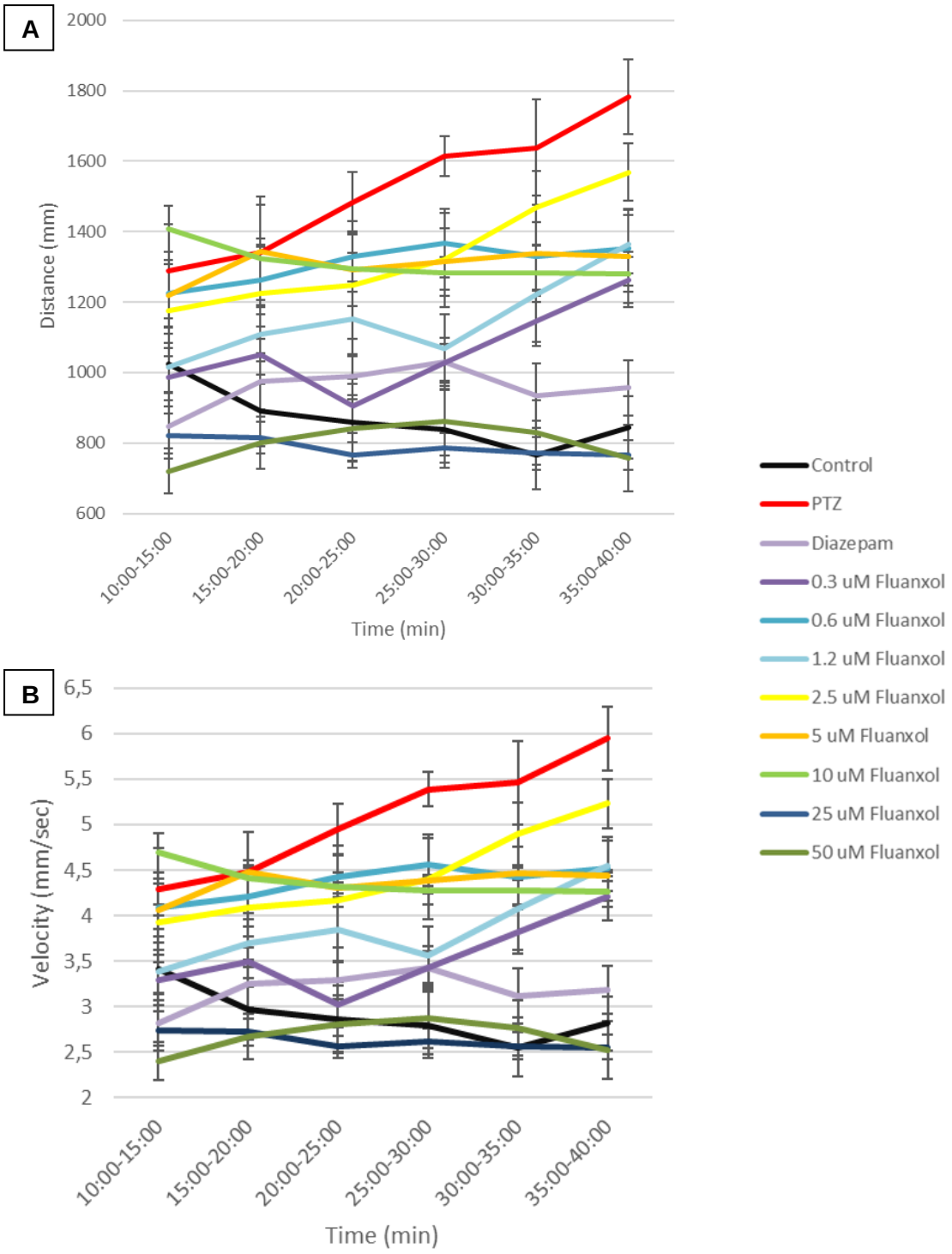

Figure 4.11: 18-hour incubation of Fluanxol® treatment. *Distance moved (A) and velocity (B) were recorded 10 minutes after addition of 10 mM PTZ to zebrafish larvae (n=8 per group) to an untreated control group and zebrafish treated with 4 µM Diazepam or Fluanxol doses (0.3 µM, 0.6 µM, 1.2 µM, 2.5 µM, 5µM, 10µM, 25µM, 50µM) 18 hours prior to PTZ exposure. Data displayed as mean ± SE (two-way ANOVA, Bonferroni post hoc, significance with p<0.05 not shown on graph for clearer visibility of data (Appendix D); n=8).*

4.3.3 ROS Detection *in vivo*

Zebrafish larvae (4 dpf) were incubated in E3 media only, 1.2 µM, 25 µM and 50 µM Fluanxol® with or without 10 µg/ml LPS and stained with CM-H_2DCFDA to assess relative ROS levels *in vivo.* ROS levels (Figure 4.12) appear reduced in zebrafish treated with increasing doses of Fluanxol®. This effect seemed to be exacerbated in the presence of LPS, with the most prominent reduction in ROS levels visible in the zebrafish treated with 50 µM Fluanxol® and 10 µg/ml LPS. Fluorescence was only observed in the digestive system of zebrafish larvae.

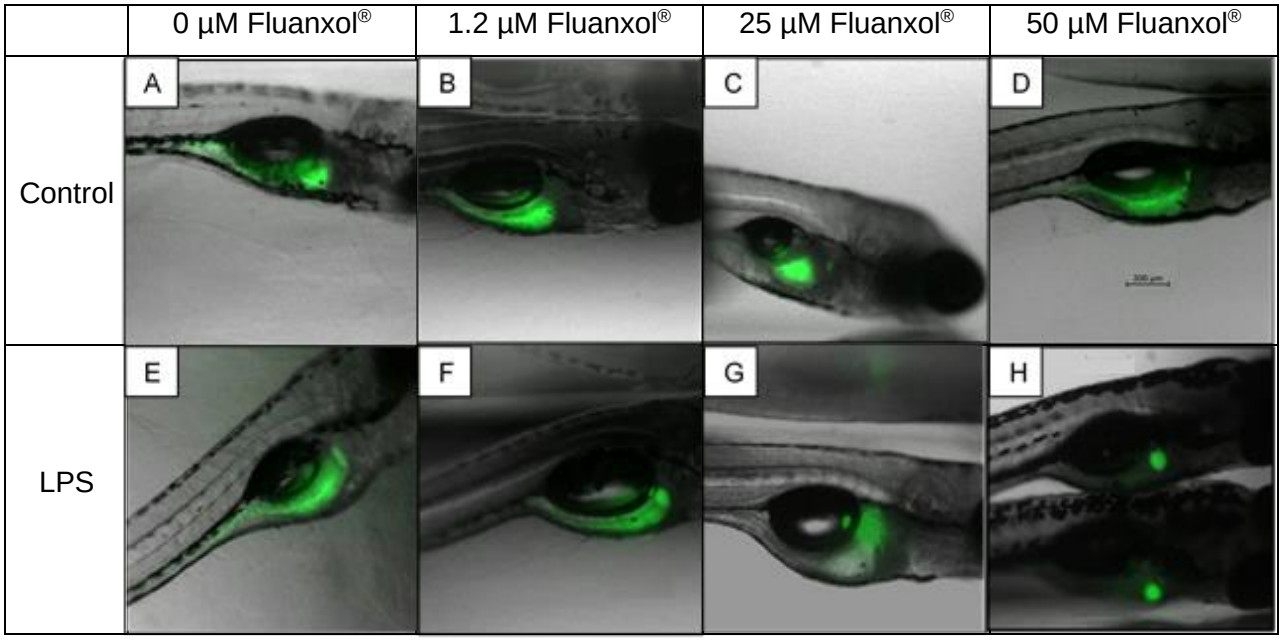

Figure 4.12: ROS detection in vivo. *Zebrafish larvae stained with 1 µg/ml CM-H_2DCFDA for two hours. Zebrafish were treated at 4 dpf with E3 media for the control group (A), 1.2 µM Fluanxol® (B), 25 µM Fluanxol® (C), 50 µM Fluanxol® (D), 10 µg/ml LPS (E), 1.2 µM Fluanxol® and 10 µg/ml LPS (F), 25 µM Fluanxol® and 10 µg/ml LPS (G), 50 µM Fluanxol® and 10 µg/ml LPS (H) and incubated for 18 hours before imaging. CM-H_2DCFDA: 5-(and 6-)chloromethyl-2',7'-dichlorodihydrofluorescein diacetate; dpf: days post-fertilisation; LPS: lipopolysaccharide; ROS: reactive oxygen species.*

Fluorescent images were processed and quantified using ZEN (blue edition) software and ImageJ. Mean fluorescent intensity (Figure 4.13) confirmed qualitative observations and was significantly decreased in zebrafish treated with 25 µM Fluanxol® and 50 µM Fluanxol® ($p<0.01$). LPS treated zebrafish had lower levels of ROS (expressed as mean fluorescent intensity) than LPS-negative controls ($p<0.05$) (Figure 4.13). In addition, there was a significant decrease in fluorescent area in zebrafish treated with both 50 µM Fluanxol® ($p<0.05$) and LPS when compared to both LPS-positive and LPS-negative control groups (Figure 4.14).

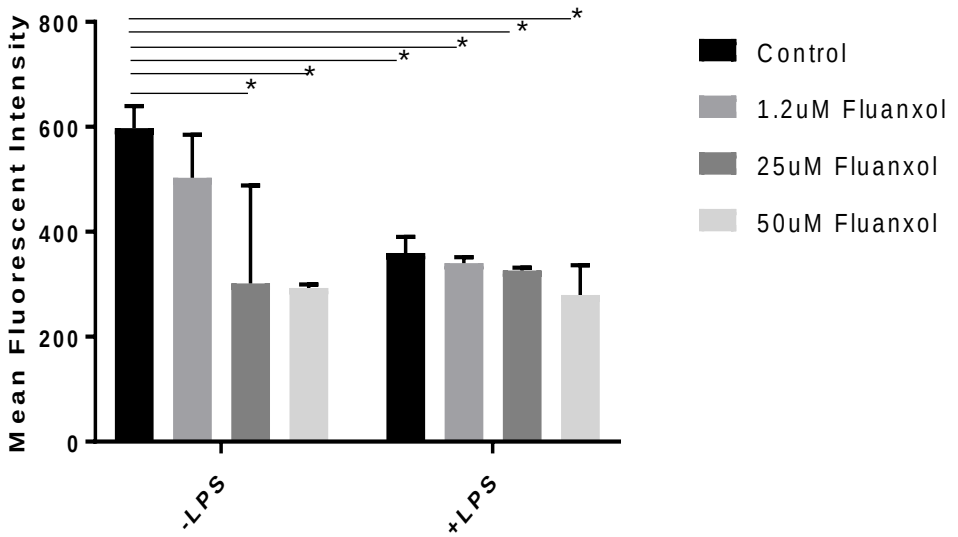

Figure 4.13: Mean fluorescent intensity indicating ROS in vivo. *Zebrafish larvae stained with 1 µg/ml CM-H₂DCFDA for two hours. Zebrafish were treated at 4 dpf with E3 media for the control group, 1.2 µM, 25 µM and 50 µM Fluanxol®, 10 µg/ml LPS, 1.2 µM Fluanxol® and 10 µg/ml LPS, 25 µM Fluanxol® and 10 µg/ml LPS, and 50 µM Fluanxol® and 10 µg/ml LPS. Zebrafish were exposed to treatment for 18 hours before imaging, Fluorescent intensity is given in arbitrary units. Data displayed as mean ± SD (two-way ANOVA, Bonferroni post hoc, significance with p<0.05. *=p<0.05; **p<0.01;* n=3). CM-H₂DCFDA: 5-(and 6-)chloromethyl-2',7'-dichlorodihydrofluorescein diacetate; dpf: days post fertilisation; LPS: lipopolysaccharide; ROS: reactive oxygen species.

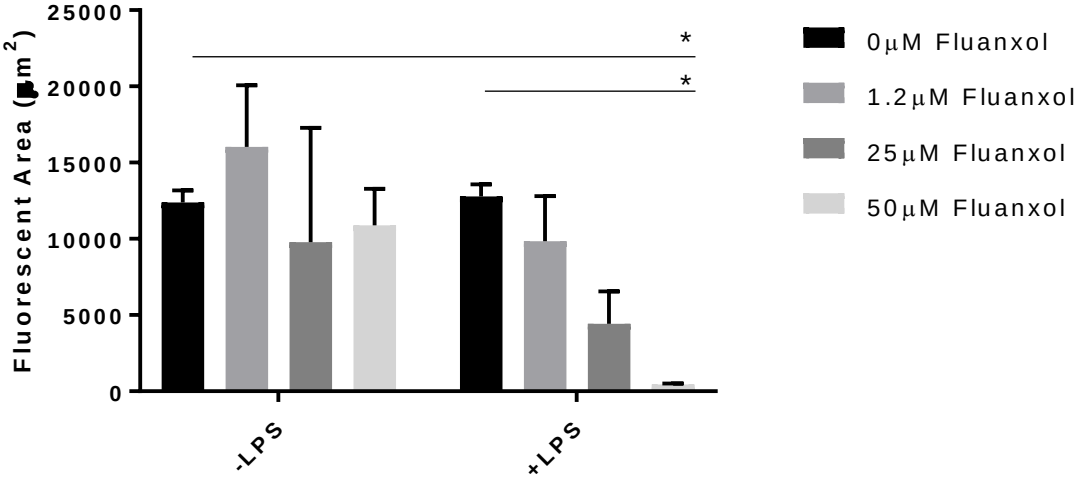

Figure 4.14: Fluorescent area of ROS detection in vivo. *Zebrafish larvae stained with 1 µg/ml CM-H₂DCFDA for two hours. Zebrafish were treated at 4 dpf with E3 media for the control group, 1.2 µM, 25 µM and 50 µM Fluanxol®, 10 µg/ml LPS, 1.2 µM Fluanxol® and 10 µg/ml LPS, 25 µM Fluanxol® and 10 µg/ml LPS, and 50 µM Fluanxol® and 10 µg/ml LPS. Zebrafish were exposed to treatment for 18 hours before imaging, Fluorescent area is reported as µm². Data displayed as mean ± SD (two-way ANOVA, Bonferroni post hoc, significance with p<0.05. *=p<0.05; **p<0.01; n=3).CM-H₂DCFDA: 5-(and 6-)chloromethyl-2',7'-dichlorodihydrofluorescein diacetate; dpf: days post fertilisation; LPS: lipopolysaccharide; ROS: reactive oxygen species.*

Chapter 5:

Discussion

The data presented here adds significantly to the literature pertaining to Fluanxol®, firstly by providing additional scientific support for its safety and secondly, by illustrating an additional mechanism of action of the drug – that of an antioxidant. In addition, current data also adds to the broader research methodology literature, by illustrating the importance of drug-related investigations in different tissue compartments – or simulations of different cellular environments – and in a way that takes into consideration bioavailability of the drug, which is often not done in tissue culture models.

5.1. *In vitro* findings

Fluanxol® is typically prescribed in the range of 3 mg/day to 12 mg/day. In our study we did not detect toxicity within these ranges at the site of absorption in the gut or at the target site in the brain, with the exception of a slight decrease in cell viability at the *in vitro* dose equivalent to an *in vivo* dose of 11 mg/day, represented by respective cellular models. With regard to treatment of the BE(2)-M17 neuroblastoma cells representing the target site, bioavailability was taken into account and concentrations altered to be 40% that of which the CaCo2 gut epithelial cells were treated. Had this not been considered, toxicity would have been reported at lower doses, falling within the prescribed range, and lead to inaccurate inferences on the drug's toxicity. Our results indicate that the prescribed range as indicated on the drug product monograph by Lundbeck Canada Inc. (2017) is appropriate with toxicity mainly observed in the context of overdose concentrations indicating that it is important in the clinical setting for patients to stick within their prescribed ranges as overdose can lead to detrimental effects as seen by a loss of mitochondrial dehydrogenase activity which is representative of cell viability. To our knowledge, this is the first study to report on cellular tolerance of Fluanxol® in cellular environments analogous to the sites of drug absorption and therapeutic modulation.

When oxidative stress parameters are assessed in isolation the full picture is difficult to discern as an increase in oxidants does not necessarily indicate oxidative stress; only when there is an imbalance in oxidants and the endogenous countering antioxidants, the redox status will shift in a pro-oxidative direction and result in oxidative damage. Therefore, in this study we not only assessed one parameter but three including oxidant production, antioxidant capacity and oxidative damage. No effects on ROS production, antioxidant capacity and oxidative damage were observed with increasing doses of Fluanxol® with or without LPS stimulation. Similar basal levels of TBARS were reported in CaCo2 cells (Dükel *et al.*, 2019; Reis *et al.*, 2020), validating the successful execution of this assay in our study. Similar basal levels in neuroblastoma cells was observed in a study

performed by Domenicotti *et al.* (2003) but could not be compared further to other studies as most other studies report their TBARS data in percentage of controls or in concentration per mg of protein without reporting quantified protein levels (Bayati and Yazdanparast, 2011; Da Frota *et al.*, 2011; Querobino, Ribeiro and Alberto-Silva, 2018). Antioxidant capacity using TEAC assay has mainly been used to assess the antioxidant capacity of compounds (Bakuradze *et al.*, 2010; Xie *et al.*, 2014; Gómez *et al.*, 2019) and studies that assessed antioxidant capacity in cell culture were unable to be compared to due to lack of units reported (Li *et al.*, 2020) or presenting data as percentage of controls (Cecchi *et al.*, 2008). It was hypothesised based on the sparse number of previous studies which indicated antioxidant effects of the antipsychotic of interest, that Fluanxol® would reduce ROS levels (Whatley *et al.*, 1998; Kowalski, Labuzek and Herman, 2003; Kim and J. H. Song, 2016) and increase antioxidant capacity (Chittiprol *et al.*, 2010). This was not, however, observed in our results and it is suspected that the lack of a treatment effect in our study, may be due to compensatory, endogenous upregulation of antioxidant mechanisms that could balance (or normalise) redox status by the 24-hour timepoint. Kowalski, Labuzek and Herman, (2003) observed a decrease in NO at 24-hours after treatment with flupentixol and stimulation with LPS but this was in microglial cells which are immunomodulatory cells and would respond differently in terms of redox status than other cell types. Differences in redox parameters were noted between the cell lines used in this study, such as higher levels of ROS production from gut epithelial cells compared to neuroblastoma cells but also higher antioxidant capacity in gut epithelial cells compared to neuroblastoma cells. Antioxidant capacity, measured by TEAC assay, and oxidant production, measured by H_2O_2 assay kit, were balanced in these cell models resulting in little to no oxidative damage, measured by TBARS assay.

5.2. *In vitro* limitations and future recommendations

Cell lines used in this study are established models representative of gut epithelial and neural cell physiology. However, they still have limitations in that they have cancerous morphology and may therefore respond differently to treatment than primary gut and neural cells. The CaCo2 gut epithelial carcinoma cells and the BE(2)-M17 neuroblastoma cells, as most cellular models, are also limited in terms of their capacity to accurately simulate the specific disease state that is the topic here. Compensatory redox mechanisms in these cells may therefore differ somewhat from the impaired antioxidant mechanisms observed in patients with schizophrenia. Nevertheless, despite these limitations, we are confident that our approach of assessing a panel of redox indicators returned sound support for an interpretation of drug safety in terms of redox.

In this study, we were somewhat limited by the cell lines to our disposal. However, looking forward, follow-up investigations could benefit from consideration of other cell lines in addition to those reported on here. For example, olfactory neurosphere-derived cells – cells originally sampled from schizophrenia patients (Matigian *et al.*, 2010) – would be “pre-conditioned” cells perhaps better representative of schizophrenia pathology at a cellular level. If possible, for the use of this, or similar human-derived cells, in future studies to investigate the mechanisms of action of Fluanxol® may

better reflect effects of the drug on redox status in the context of the disease state it is prescribed to treat. Another useful model by which to achieve this would be to use schizophrenia patient-induced pluripotent stem cells, or to differentiate them into neurons (Czepiel *et al.*, 2011; Emdad *et al.*, 2012) or other disease-relevant cell types. Such models may be especially important when probing cellular mechanisms specifically targeted by the drug treatment. However, realistically, for the purpose of this study, the cell models used were appropriate for probing the effects of Fluanxol® on redox mechanisms where the drug will be absorbed in the gut represented by gut epithelial-like cells and target site in the CNS represented by neural-like cells in the absence of pathology-related impairments that could possibly confound the understanding of the direct effects of the drug.

A final consideration is that the time point chosen for our assessments, although commonly used in cellular protocols of this nature, may not have been optimal. Assessments over a range of time points, and specifically including earlier ones, might have revealed primary effects of the drug before these were countered by endogenous cellular mechanisms. However, the fact that no undesired effects were observed after 24 hours, suggest that no long-term detrimental outcome in terms of redox should be anticipated. Nevertheless, due to these limitations, we further investigated mechanisms of action of Fluanxol® *in vivo* to include complex intercellular interactions and the complexities of a whole organism which the *in vitro* cellular monolayer models lack.

5.3. *In vivo* findings

Zebrafish models are still quite novel compared to long-standing rodent models but are increasing in popularity for the study of various pathologies including psychiatric disorders (Rihel and Schier, 2012). Toxicity screening of pharmaceuticals has been performed using touch response and movement tracking (Afrikanova *et al.*, 2013). In our study, zebrafish larvae were observed to increase in frequency of a delayed touch response with increasing doses of Fluanxol® over time. These were, however, investigator observations only and our quantified data from behaviour tracking of zebrafish larvae did not indicate a decrease in locomotor activity across treatment groups. On the contrary, at 18 hours of treatment incubation, larvae treated with 6.16 µM and 49.27 µM Fluanxol® had a consistently elevated locomotor activity throughout the trial recording when compared to untreated zebrafish larvae. The elevated (but not seizure-like) basal locomotor activity suggests effective doses of Fluanxol®, as seen with dopamine receptor antagonism in zebrafish in dark conditions (Irons *et al.*, 2013b; Oliveri and Levin, 2019). Oxidative stress, immunotoxicity and neurotoxicity are associated with reduced locomotor activity when compared to controls in zebrafish (Zhong *et al.*, 2014; X. Wang *et al.*, 2019; Niu *et al.*, 2021). Oxidative stress-induced locomotor deficiency has been shown to be attenuated by antioxidants, such as vitamin E (Vaz, Outeiro and Ferreira, 2018), indicating that redox status has modulatory effects on zebrafish locomotor activity and therefore this model is an appropriate starting point to probe toxicity as well as potential redox effects of Fluanxol® *in vivo*. The behavioural tracking of larvae movement, after treatment with various doses of Fluanxol®, therefore indicated that Fluanxol® does not exert toxic effects at these doses. No other

studies, to the best of our knowledge, have reported flupentixol dihydrochloride toxicity or assessed its effect on redox status in a zebrafish model.

To infer clinically prescribed doses in humans to equivalent doses in an animal model, understanding of the drug's absorption, metabolism and excretion and whether these factors are well conserved, in the animal model being used, is imperative. Cytochrome P450 (CYP) enzymes are frequently involved in drug metabolism, and although metabolism of flupentixol dihydrochloride is stated to be via sulphoxidation, N-dealkylation and glucuronic acid conjugation (as stated in the Lundbeck product monograph) the specific enzymes involved have yet to be elucidated (Davies *et al.*, 2004). Based on the chemical structure of flupentixol dihydrochloride it is suspected the CYP2D6 or CYP3A4 are potential candidates (Davies *et al.*, 2004) although CYP2D6 was later found to not be involved in flupentixol metabolism (Waade, Solhaug and Høiseth, 2020). CYP families 1 to 4, including CYP3A4, are not so well conserved in zebrafish as the CYP families 5 to 51 (Goldstone *et al.*, 2010). It is therefore suspected that the equivalent dose in zebrafish will differ to the clinical dose in humans beyond size considerations. At the time of experimental design, no literature to the best of our knowledge was available to discern clinically relevant doses in zebrafish, therefore, we employed a psychosis model to determine effective dose of the antipsychotic of interest. PTZ induces seizure-like movement through its antagonistic effects on $GABA_A$ receptors (Afrikanova *et al.*, 2013). Diazepam (Valium®) reverses the effects of PTZ through $GABA_A$ receptor agonism and was therefore used as a positive control in this model. The PTZ model has been used in zebrafish as an established model for psychosis (Moradi-Afrapoli *et al.*, 2017). In this model, effective (therapeutic) doses of Fluanxol® were not observed acutely after administration, but after 18 hours of incubation, treatment with 25 µM and 50 µM Fluanxol® displayed antipsychotic effect. Coupled with the toxicity screening behaviour tracking results, it is suggested that flupentixol dihydrochloride potentially exerts agonistic effects on the $GABA_A$ receptor. This is likely, as the effects of reduced locomotor activity, observed at higher doses of Fluanxol® when compared to the PTZ-only treated group, are not due to overall sedation as these doses did not decrease locomotor activity in the toxicity screening experiments. These effective doses were therefore selected, as well as a lower, ineffective dose, 1.2 µM Fluanxol®, to draw a comparison between therapeutic doses and influence of the drug on redox *in vivo*.

Assessment of ROS levels *in vivo* using live organism fluorescent imaging suggested that Fluanxol® has a dose-dependent antioxidant effect. Fluorescent intensity was also reduced in the LPS only treated group when compared to untreated control zebrafish larvae. In line with our interpretation of upregulated endogenous antioxidant counter mechanisms coming into play *in vitro*, here the decrease in ROS levels with LPS treatment is again suspected to be due to compensatory antioxidant mechanisms such as SOD, which are known to be upregulated by mild LPS stimulation (Markus *et al.*, 2018; Han *et al.*, 2020) and therefore quenching the increased ROS production (Dringen, Pawlowski and Hirrlinger, 2005; Bitanihirwe and Woo, 2011; Liu *et al.*, 2017).

In terms of methodology, in addition to fluorescent intensity, the fluorescent area size per standardised sample area was also assessed, and it was also observed to be reduced in the 50 µM flupentixol treatment in the presence of LPS, further supporting our interpretation of fluorescent intensity data. Of interest, in the larval images, fluorescence was observed to be localised in the gastrointestinal tract of zebrafish larvae. The decrease in ROS detection with increasing doses of Fluanxol®, indicated reduced ROS levels firstly in the gut, the first site of detoxification and where response to drugs is observed in zebrafish larvae (Poon *et al.*, 2017), before the liver and gall bladder.

5.4. *In vivo* limitations and future recommendations

The touch response assessment is susceptible to bias as the assessment is subjective. It is therefore proposed that future studies are set up a way to double blind the treatment groups when being analysed for their response to touch, as well as pairing this assessment with behaviour tracking as we did in this study. Further reduction in bias can be achieved by repeating the assessment and averaging the response assigned to each zebrafish larva. At the time of study design, no literature was available on the potential calculation of equivalent doses from human dosing to that employed in zebrafish. However, subsequently, a study published indeed proposed an equation to calculate human equivalent dose in zebrafish larvae (Usai *et al.*, 2020). Usai and colleagues (2020) investigated equivalent dose in the context of chemotherapy and calculated equivalent plasma concentration (EPC) in humans to be equal to mg of drug administration divided by volume of blood (5400ml). The maximum tolerated dose (MTD) was then investigated and used to determine dilution factor required, from human EPC to administered concentration for zebrafish larvae in water. It was then proposed that to calculate the equivalent dose to treat zebrafish (C_{fish}) in mg/ml the equation $C_{fish} = \frac{M}{V}/ED$ should be used, where M is the mg of treatment administered to humans, V is the volume of blood taken to be 5400ml and ED is the dilution factor calculated by Usai *et al.* (2020) to equal 5. According to this equation, our lowest dose used in the toxicity screen and PTZ assay is near equivalent dose for 4 mg/day prescription in humans. Our higher doses, 25 µM and 50 µM flupentixol dihydrochloride, that indicated effect in the PTZ model and ROS detection with fluorescent probe, CM-H_2DCFDA, are equivalent to 342,5 and 685 mg/day equivalent doses in humans. Equivalent doses of 342,5 mg/day and 685 mg/day would be expected to induce toxic effects as suggested by our *in vitro* data indicating toxicity at an overdose concentration equivalent to 30mg/day. It is possible that our effective doses of 25 µM and 50 µM Fluanxol® are not equivalent to 342,5 mg/day and 685 mg/day, respectively, as the equation proposed by Usai *et al.* (2020) was based on the effects of chemotherapeutic drug doses and potentially may not be translatable to other pharmaceuticals, such as antipsychotics, as these drugs may be metabolised by different cytochrome P450 enzymes (Rodriguez-Antona and Ingelman-Sundberg, 2006; Waade, Solhaug and Høiseth, 2020) which would affect the efficacy and toxicity that determined maximum tolerated dose and therefore the proposed dilution factor to calculate equivalent dose. The study by Usai *et al.*

(2020) is valuable in terms of chemotherapeutic equivalent doses and their approach to attain this is recommended to be investigated in the context of antipsychotic drugs using the equivalent plasma concentrations in humans, which differs from their EPC calculation as 5mg flupentixol dihydrochloride stabilises at a plasma concentration of about 1.7 ng/ml (as stated in the product monograph by Lundbeck, 2020) and would potentially require a different equation factoring in bioavailability. Investigating the maximum tolerated dose in zebrafish, as well as effective doses, and comparing this to plasma concentrations in patients treated with Fluanxol® will shed insight into appropriate equivalent doses. Without further insight, selecting doses based on effects observed in the PTZ model was therefore appropriate in this study.

Although the PTZ assay in zebrafish is commonly referred to as a model for psychosis, it is also frequently used in the context of epilepsy and investigation of efficacy of anticonvulsant drugs. The strength of the model lies in the capacity to probe a very specific signalling mechanism *in vivo*, but it is important to remember that it is not specifically a model of schizophrenia pathology and that the complexity of schizophrenia cannot be simulated accurately in a simple model such as the PTZ model. Despite its limitations, this model has shown insight into the mechanisms of action of flupentixol dihydrochloride to potentially include $GABA_A$ receptor agonism. In future studies, an NMDA antagonist model of schizophrenia in zebrafish could be employed to investigate effective doses and verify what we observed in the PTZ model. NMDA receptor antagonist models increase locomotor activity, such as in the PTZ model, in larval zebrafish and the effects of NMDA antagonist, dizocilpine maleate, are attenuated by antipsychotic pharmaceuticals (Chen *et al.*, 2010; Seibt *et al.*, 2010).

Staining and mounting zebrafish larvae was optimised in this study for ROS detection with CM-H_2DCFDA. However, further optimisation is advised. Mounting in the 8 chamber slides resulted in zebrafish localising on different planes, so that the process of uniformly orienting larvae for microscopy was a labour-intensive process. Perhaps one way in which robust uniformity in orientation and depth in medium could be achieved, would be by mounting zebrafish on a coverslip.

Chapter 6:

Conclusions

The clinical outcome of schizophrenia patients appears to be modulated by redox status. Further elucidation is required; however, studies point to some antipsychotics exerting antioxidant effects. Shifting the redox status in patients with schizophrenia away from a pro-oxidant state may improve symptoms, prolong remission and prevent relapse and/or risk for co-morbid conditions. The mechanisms of action of antipsychotic, Fluanxol®, however are not fully elucidated, especially in the context of redox status.

From current data it is evident that Fluanxol® exhibited *in vitro* mitochondrial toxicity only at a dose equivalent to human overdose concentration, but that little to no toxicity is present within the prescribed doses. In line with this *in vitro* data, various doses of Fluanxol® indicated no toxicity *in vivo* with behaviour tracking of zebrafish larvae movement. Doses of Fluanxol® showing maximal antipsychotic effect in a zebrafish larval model, also reduced ROS levels, suggesting its therapeutic effect to include a positive outcome in terms of redox status. Finally, the observed antipsychotic effect of Fluanxol® in the PTZ model in zebrafish additionally suggest GABAergic modulation as a potential additional mechanism of action of this drug.

Further elucidation of the equivalent dose of antipsychotic treatment in zebrafish from clinically relevant doses is still required. An NMDA antagonist model may provide further insight to effective doses in zebrafish. An investigation *in vivo* of effects of Fluanxol® on antioxidant mechanisms such as GSH and SOD activity as well as oxidative damage by assessing TBARS production would be insightful in future studies. Lastly, investigating the effects of Fluanxol® in patient samples would provide insight to the effects of the antipsychotic in terms of redox effects in the context of the disease state in future research.

Chapter 7:

References

Abdelbary, A. *et al.* (2014) 'Pharmaceutical and pharmacokinetic evaluation of a novel fast dissolving film formulation of flupentixol dihydrochloride', *Ageing International*. Springer New York LLC, 15(6), pp. 1603–1610. doi: 10.1208/s12249-014-0186-8.

Adams, R. C. M. C. and Smith, C. (2020) 'In utero exposure to maternal chronic inflammation transfers a pro-inflammatory profile to generation F2 via sex-specific mechanisms', *Frontiers in Immunology*. Frontiers Media S.A., 11. doi: 10.3389/fimmu.2020.00048.

Adell, A. (2020) 'Brain NMDA Receptors in Schizophrenia and Depression', *Biomolecules*. MDPI AG, 10(6), p. 947. doi: 10.3390/biom10060947.

Afrikanova, T. *et al.* (2013) 'Validation of the zebrafish pentylenetetrazol seizure model: locomotor versus electrographic responses to antiepileptic drugs', *PLoS ONE*, 8(1), pp. 1–9. doi: 10.1371/journal.pone.0054166.

Aghajanian, G. K. and Marek, G. J. (2000) 'Serotonin model of schizophrenia: Emerging role of glutamate mechanisms', in *Brain Research Reviews*. Brain Res Brain Res Rev, pp. 302–312. doi: 10.1016/S0165-0173(99)00046-6.

Aguilar Diaz De Leon, J. and Borges, C. R. (2020) 'Evaluation of oxidative stress in biological samples using the thiobarbituric acid reactive substances assay', *Journal of Visualized Experiments*. Journal of Visualized Experiments, 2020(159). doi: 10.3791/61122.

Akhondzadeh, S. *et al.* (2007) 'Celecoxib as adjunctive therapy in schizophrenia: A double-blind, randomized and placebo-controlled trial', *Schizophrenia Research*. Elsevier, 90(3), pp. 179–185. doi: 10.1016/j.schres.2006.11.016.

Alcaino, C. *et al.* (2018) 'A population of gut epithelial enterochromaffin cells is mechanosensitive and requires Piezo2 to convert force into serotonin release', *Proceedings of the National Academy of Sciences of the United States of America*. National Academy of Sciences, 115(32), pp. E7632–E7641. doi: 10.1073/pnas.1804938115.

Alex, K. D. and Pehek, E. A. (2007) 'Pharmacologic mechanisms of serotonergic regulation of dopamine neurotransmission', *Pharmacology and Therapeutics*. NIH Public Access, 113(2), pp. 296–320. doi: 10.1016/j.pharmthera.2006.08.004.

Amargós-Bosch, M. *et al.* (2006) 'Clozapine and olanzapine, but not haloperidol, suppress serotonin efflux in the medial prefrontal cortex elicited by phencyclidine and ketamine', *International Journal of Neuropsychopharmacology*. Int J Neuropsychopharmacol, 9(5), pp. 565–573. doi: 10.1017/S1461145705005900.

Andres, D. *et al.* (2013) 'Morphological and functional differentiation in BE(2)-M17 human neuroblastoma cells by treatment with trans-retinoic acid', *BMC Neuroscience*, 14(1), p. 49. doi: 10.1186/1471-2202-14-49.

Apel, K. and Hirt, H. (2004) 'Reactive oxygen species: Metabolism, oxidative stress, and signal transduction', *Annual Review of Plant Biology*. Annual Reviews, 55(1), pp. 373–399. doi: 10.1146/annurev.arplant.55.031903.141701.

de Araújo Boleti, A. P. *et al.* (2020) 'Neuroinflammation: An overview of neurodegenerative and metabolic diseases and of biotechnological studies', *Neurochemistry International*. Elsevier Ltd, 136, p. 104714. doi: 10.1016/j.neuint.2020.104714.

Ashok, A. H. *et al.* (2017) 'Association of stimulant use with dopaminergic alterations in users of cocaine, amphetamine, or methamphetamine a systematic review and meta-analysis', *JAMA Psychiatry*. American Medical Association, 74(5), pp. 511–519. doi: 10.1001/jamapsychiatry.2017.0135.

El Assar, M., Angulo, J. and Rodríguez-Mañas, L. (2013) 'Oxidative stress and vascular inflammation in aging', *Free Radical Biology and Medicine*. Pergamon, 65, pp. 380–401. doi: 10.1016/j.freeradbiomed.2013.07.003.

Avital, A. *et al.* (2003) 'Impaired interleukin-1 signaling is associated with deficits in hippocampal memory processes and neural plasticity', *Hippocampus*. Hippocampus, 13(7), pp. 826–834. doi: 10.1002/hipo.10135.

Bailey, L. and Taylor, D. (2019) 'Estimating the optimal dose of flupentixol decanoate in the maintenance treatment of schizophrenia—a systematic review of the literature', *Psychopharmacology*. Psychopharmacology, 236(11), pp. 3081–3092. doi: 10.1007/s00213-019-05311-2.

Bakuradze, T. *et al.* (2010) 'Antioxidant effectiveness of coffee extracts and selected constituents in cell-free systems and human colon cell lines', *Molecular Nutrition & Food Research*. John Wiley & Sons, Ltd, 54(12), pp. 1734–1743. doi: 10.1002/mnfr.201000147.

Bantick, R. A. *et al.* (2004) 'A positron emission tomography study of the 5-HT1A receptor in schizophrenia and during clozapine treatment', *Journal of Psychopharmacology*. J Psychopharmacol, 18(3), pp. 346–354. doi: 10.1177/026988110401800304.

Baran, A. *et al.* (2018) 'Determination of developmental toxicity of zebrafish exposed to propyl gallate dosed lower than ADI (Acceptable Daily Intake)', *Regulatory Toxicology and Pharmacology*. Academic Press Inc., 94, pp. 16–21. doi: 10.1016/j.yrtph.2017.12.027.

Bargiota, S. I. *et al.* (2013) 'The effects of antipsychotics on prolactin levels and women's menstruation', *Schizophrenia Research and Treatment*. Hindawi Limited, 2013, pp. 1–10. doi: 10.1155/2013/502697.

Barnes, P. J. and Adcock, I. M. (2009) 'Glucocorticoid resistance in inflammatory diseases', *The Lancet*. Elsevier B.V., 373(9678), pp. 1905–1917. doi: 10.1016/S0140-6736(09)60326-3.

Baxter, P. S. *et al.* (2015) 'Synaptic NMDA receptor activity is coupled to the transcriptional control of the glutathione system', *Nature Communications*. Nature Publishing Group, 6(1), pp. 1–13. doi: 10.1038/ncomms7761.

Bayati, S. and Yazdanparast, R. (2011) 'Antioxidant and free radical scavenging potential of yakuchinone B derivatives in reduction of lipofuscin formation using H2O2-treated neuroblastoma cells', *Iranian Biomedical Journal*. Pasteur Institute of Iran, 15(4), pp. 134–142. doi: 10.6091/IBJ.1010.2012.

Becher, B., Spath, S. and Goverman, J. (2017) 'Cytokine networks in neuroinflammation', *Nature Reviews Immunology*. Nature Publishing Group, 17(1), pp. 49–59. doi: 10.1038/nri.2016.123.

Berg, D., Youdim, M. B. H. and Riederer, P. (2004) 'Redox imbalance', *Cell and Tissue Research*. Springer, 318(1), pp. 201–213. doi: 10.1007/s00441-004-0976-5.

Berger, M. *et al.* (2018) 'Allostatic load is associated with psychotic symptoms and decreases with antipsychotic treatment in patients with schizophrenia and first-episode psychosis', *Psychoneuroendocrinology*. Elsevier Ltd, 90, pp. 35–42. doi: 10.1016/j.psyneuen.2018.02.001.

Berghmans, S. *et al.* (2007) 'Zebrafish offer the potential for a primary screen to identify a wide variety of potential anticonvulsants', *Epilepsy Research*. Elsevier, 75(1), pp. 18–28. doi: 10.1016/j.eplepsyres.2007.03.015.

Berk, M. *et al.* (2008) 'N-acetyl cysteine as a glutathione precursor for schizophrenia-A double-blind, randomized, placebo-controlled trial', *Biological Psychiatry*. Elsevier USA, 64(5), pp. 361–368. doi: 10.1016/j.biopsych.2008.03.004.

Bernier, P. J. *et al.* (2002) 'Newly generated neurons in the amygdala and adjoining cortex of adult primates', *Proceedings of the National Academy of Sciences of the United States of America*. National Academy of Sciences, 99(17), pp. 11464–11469. doi: 10.1073/pnas.172403999.

Bian, Q. *et al.* (2008) 'The effect of atypical antipsychotics, perospirone, ziprasidone and quetiapine on microglial activation induced by interferon-γ', *Progress in Neuro-Psychopharmacology and Biological Psychiatry*. Elsevier, 32(1), pp. 42–48. doi: 10.1016/j.pnpbp.2007.06.031.

Bilder, R. M. *et al.* (2002) 'Neurocognitive effects of clozapine, olanzapine, risperidone, and haloperidol in patients with chronic schizophrenia or schizoaffective disorder', *American Journal of Psychiatry*. Am J Psychiatry, 159(6), pp. 1018–1028. doi: 10.1176/appi.ajp.159.6.1018.

Biswas, S. K. (2016) 'Does the interdependence between oxidative stress and inflammation explain the antioxidant paradox?', *Oxidative Medicine and Cellular Longevity*. Hindawi Publishing Corporation, 2016. doi: 10.1155/2016/5698931.

Bitanihirwe, B. K. Y. and Woo, T. U. W. (2011) 'Oxidative stress in schizophrenia: An integrated approach', *Neuroscience and Biobehavioral Reviews*, 35(3), pp. 878–893. doi: 10.1016/j.neubiorev.2010.10.008.

Blasko, I. *et al.* (2004) 'How chronic inflammation can affect the brain and support the development of Alzheimer's disease in old age: The role of microglia and astrocytes', *Aging Cell*, pp. 169–176.

doi: 10.1111/j.1474-9728.2004.00101.x.

Blesa, J. *et al.* (2015) 'Oxidative stress and Parkinson's disease', *Frontiers in Neuroanatomy*. Frontiers Research Foundation, 9. doi: 10.3389/fnana.2015.00091.

Bonini, M. G. and Malik, A. B. (2014) 'Regulating the regulator of ROS production', *Cell Research*. Nature Publishing Group, 24(8), pp. 908–909. doi: 10.1038/cr.2014.66.

Brenman, J. E. and Bredt, D. S. (1997) 'Synaptic signaling by nitric oxide', *Current Opinion in Neurobiology*. Elsevier Ltd, 7(3), pp. 374–378. doi: 10.1016/S0959-4388(97)80065-7.

Brisch, R. *et al.* (2014) 'The role of dopamine in schizophrenia from a neurobiological and evolutionary perspective: Old fashioned, but still in vogue', *Frontiers in Psychiatry*. Frontiers Media S.A., 5, p. 47. doi: 10.3389/fpsyt.2014.00047.

Browne, C. J. *et al.* (2019) 'Dorsal raphe serotonin neurons inhibit operant responding for reward via inputs to the ventral tegmental area but not the nucleus accumbens: evidence from studies combining optogenetic stimulation and serotonin reuptake inhibition', *Neuropsychopharmacology*. Nature Publishing Group, 44(4), pp. 793–804. doi: 10.1038/s41386-018-0271-x.

Cabungcal, J. H. *et al.* (2006) 'Glutathione deficit during development induces anomalies in the rat anterior cingulate GABAergic neurons: Relevance to schizophrenia', *Neurobiology of Disease*. Academic Press, 22(3), pp. 624–637. doi: 10.1016/j.nbd.2006.01.003.

Calcia, M. A. *et al.* (2016) 'Stress and neuroinflammation: A systematic review of the effects of stress on microglia and the implications for mental illness', *Psychopharmacology*. Springer Verlag, 233(9), pp. 1637–1650. doi: 10.1007/s00213-016-4218-9.

Campo-Soria, C., Chang, Y. and Weiss, D. S. (2006) 'Mechanism of action of benzodiazepines on GABA A receptors', *British Journal of Pharmacology*. Wiley-Blackwell, 148(7), pp. 984–990. doi: 10.1038/sj.bjp.0706796.

Cecchi, C. *et al.* (2008) 'Replicating neuroblastoma cells in different cell cycle phases display different vulnerability to amyloid toxicity', *Journal of Molecular Medicine*. J Mol Med (Berl), 86(2), pp. 197–209. doi: 10.1007/s00109-007-0265-3.

Cekanaviciute, E. and Buckwalter, M. S. (2016) 'Astrocytes: Integrative regulators of neuroinflammation in stroke and other neurological diseases', *Neurotherapeutics*. Springer New York LLC, 13(4), pp. 685–701. doi: 10.1007/s13311-016-0477-8.

Chen, J. *et al.* (2010) 'The Behavioral and Pharmacological Actions of NMDA Receptor Antagonism are Conserved in Zebrafish Larvae.', *International journal of comparative psychology*. NIH Public Access, 23(1), pp. 82–90. Available at: http://www.ncbi.nlm.nih.gov/pubmed/21278812 (Accessed: 24 February 2021).

Cherry, J. D., Olschowka, J. A. and O'Banion, M. K. (2014) 'Neuroinflammation and M2 microglia: The good, the bad, and the inflamed', *Journal of Neuroinflammation*. BioMed Central Ltd., 11(1). doi: 10.1186/1742-2094-11-98.

Chittiprol, S. *et al.* (2010) 'Oxidative stress and neopterin abnormalities in schizophrenia: A

longitudinal study', *Journal of Psychiatric Research*. Pergamon, 44(5), pp. 310–313. doi: 10.1016/j.jpsychires.2009.09.002.

Choi, Y. B., Chen, H. S. V. and Lipton, S. A. (2001) 'Three pairs of cysteine residues mediate both redox and ZN2+ modulation of the NMDA receptor', *Journal of Neuroscience*. Society for Neuroscience, 21(2), pp. 392–400. doi: 10.1523/jneurosci.21-02-00392.2001.

Chouinard, G. *et al.* (2017) 'Antipsychotic-induced dopamine supersensitivity psychosis: pharmacology, criteria, and therapy', *Psychotherapy and Psychosomatics*. S. Karger AG, 86(4), pp. 189–219. doi: 10.1159/000477313.

Corcoran, C. *et al.* (2002) 'Could stress cause psychosis in individuals vulnerable to schizophrenia?', *CNS Spectrums*. CNS Spectr, 7(1), p. 42. doi: 10.1017/S1092852900022240.

Corson, P. W. *et al.* (1999) 'Change in basal ganglia volume over 2 years in patients with schizophrenia: Typical versus atypical neuroleptics', *The American Journal of Psychiatry*, 156(8), pp. 1200–1204.

Curran, K. P. and Chalasani, S. H. (2012) 'Serotonin circuits and anxiety: What can invertebrates teach us?', *Invertebrate Neuroscience*. Springer, 12(2), pp. 81–92. doi: 10.1007/s10158-012-0140-y.

Czepiel, M. *et al.* (2011) 'Differentiation of induced pluripotent stem cells into functional oligodendrocytes', *Glia*. John Wiley & Sons, Ltd, 59(6), pp. 882–892. doi: 10.1002/glia.21159.

Das, I. *et al.* (1995) 'Elevated platelet calcium mobilization and nitric oxide synthase activity may reflect abnormalities in schizophrenic brain', *Biochemical and Biophysical Research Communications*. Biochem Biophys Res Commun, 212(2), pp. 375–380. doi: 10.1006/bbrc.1995.1980.

Davies, S. J. C. *et al.* (2004) 'Potential for drug interactions involving cytochromes P450 2D6 and 3A4 on general adult psychiatric and functional elderly psychiatric wards', *British Journal of Clinical Pharmacology*. Wiley-Blackwell, 57(4), pp. 464–472. doi: 10.1111/j.1365-2125.2003.02040.x.

Debnath, M. and Berk, M. (2014) 'Th17 pathway-mediated immunopathogenesis of schizophrenia: Mechanisms and implications', *Schizophrenia Bulletin*, 40(6), pp. 1412–1421. doi: 10.1093/schbul/sbu049.

Dichtl, S. *et al.* (2018) 'Dopamine promotes cellular iron accumulation and oxidative stress responses in macrophages', *Biochemical Pharmacology*. Elsevier Inc., 148, pp. 193–201. doi: 10.1016/j.bcp.2017.12.001.

DiSabato, D. J., Quan, N. and Godbout, J. P. (2016) 'Neuroinflammation: the devil is in the details', *Journal of Neurochemistry*. Blackwell Publishing Ltd, 139(Suppl 2), pp. 136–153. doi: 10.1111/jnc.13607.

Do, K. Q. *et al.* (2000) 'Schizophrenia: Glutathione deficit in cerebrospinal fluid and prefrontal cortex in vivo', *European Journal of Neuroscience*. John Wiley & Sons, Ltd, 12(10), pp. 3721–3728. doi: 10.1046/j.1460-9568.2000.00229.x.

Do, K. Q. *et al.* (2009) 'Redox dysregulation, neurodevelopment, and schizophrenia', *Current Opinion in Neurobiology*. Curr Opin Neurobiol, 19(2), pp. 220–230. doi: 10.1016/j.conb.2009.05.001.

Domenicotti, C. *et al.* (2003) 'Role of PKC-δ activity in glutathione-depleted neuroblastoma cells', *Free Radical Biology and Medicine*. Elsevier Inc., 35(5), pp. 504–516. doi: 10.1016/S0891-5849(03)00332-0.

Dringen, R. (2000) 'Metabolism and functions of glutathione in brain', *Progress in Neurobiology*. Pergamon, 62(6), pp. 649–671. doi: 10.1016/S0301-0082(99)00060-X.

Dringen, R., Pawlowski, P. G. and Hirrlinger, J. (2005) 'Peroxide detoxification by brain cells', *Journal of Neuroscience Research*. John Wiley & Sons, Ltd, 79(1–2), pp. 157–165. doi: 10.1002/jnr.20280.

Dubbelaar, M. L. *et al.* (2018) 'The kaleidoscope of microglial phenotypes', *Frontiers in immunology*. NLM (Medline), 9, p. 1753. doi: 10.3389/fimmu.2018.01753.

Dükel, M. *et al.* (2019) 'Protein kinase C inhibitors selectively modulate dynamics of cell adhesion molecules and cell death in human colon cancer cells', *Cell Adhesion and Migration*. Taylor and Francis Inc., 13(1), pp. 83–97. doi: 10.1080/19336918.2018.1530933.

Egerton, A. *et al.* (2017) 'Neuroimaging studies of GABA in schizophrenia: A systematic review with meta-analysis', *Translational Psychiatry*. Nature Publishing Group, 7(6). doi: 10.1038/tp.2017.124.

Ek, F. *et al.* (2016) 'Behavioral analysis of dopaminergic activation in zebrafish and rats reveals similar phenotypes', *ACS Chemical Neuroscience*. American Chemical Society, 7(5), pp. 633–646. doi: 10.1021/acschemneuro.6b00014.

Emdad, L. *et al.* (2012) 'Efficient differentiation of human embryonic and induced pluripotent stem cells into functional astrocytes', *Stem Cells and Development*. Mary Ann Liebert, Inc. 140 Huguenot Street, 3rd Floor New Rochelle, NY 10801 USA , 21(3), pp. 404–410. doi: 10.1089/scd.2010.0560.

Erritzoe, D. *et al.* (2008) 'Cortical and subcortical 5-HT2A receptor binding in neuroleptic-naive first-episode schizophrenic patients', *Neuropsychopharmacology*. Neuropsychopharmacology, 33(10), pp. 2435–2441. doi: 10.1038/sj.npp.1301656.

Esposito, E. and Cuzzocrea, S. (2011) 'Anti-TNF therapy in the injured spinal cord', *Trends in Pharmacological Sciences*. Elsevier Current Trends, 32(2), pp. 107–115. doi: 10.1016/j.tips.2010.11.009.

Farrell, T. C. *et al.* (2011) 'Evaluation of spontaneous propulsive movement as a screening tool to detect rescue of Parkinsonism phenotypes in zebrafish models', *Neurobiology of Disease*, 44(1), pp. 9–18. doi: 10.1016/j.nbd.2011.05.016.

Flatow, J., Buckley, P. and Miller, B. J. (2013) 'Meta-analysis of oxidative stress in schizophrenia', *Biological Psychiatry*. NIH Public Access, 74(6), pp. 400–409. doi: 10.1016/j.biopsych.2013.03.018.

Da Frota, M. L. C. *et al.* (2011) 'In vitro optimization of retinoic acid-induced neuritogenesis and TH endogenous expression in human SH-SY5Y neuroblastoma cells by the antioxidant Trolox', *Molecular and Cellular Biochemistry*. Kluwer Academic Publishers, 358(1–2), pp. 325–334. doi: 10.1007/s11010-011-0983-2.

Fujimoto, T. *et al.* (1992) 'Study of chronic schizophrenics using ^{31} P magnetic resonance chemical shift imaging', *Acta Psychiatrica Scandinavica*. John Wiley & Sons, Ltd, 86(6), pp. 455–462. doi: 10.1111/j.1600-0447.1992.tb03297.x.

Gaddum, J. H. and Hameed, K. A. (1954) 'Drugs which antagonize 5-hydroxytryptamine', *British journal of pharmacology and chemotherapy*. Wiley-Blackwell, 9(2), pp. 240–248. doi: 10.1111/j.1476-5381.1954.tb00848.x.

Gaignard, P. *et al.* (2018) 'Sex differences in brain mitochondrial metabolism: influence of endogenous steroids and stroke', *Journal of Neuroendocrinology*. Blackwell Publishing Ltd, 30(2). doi: 10.1111/jne.12497.

Gandal, M. J. *et al.* (2018) 'Transcriptome-wide isoform-level dysregulation in ASD, schizophrenia, and bipolar disorder', *Science*. American Association for the Advancement of Science, 362(6420). doi: 10.1126/science.aat8127.

Gawryluk, J. W. *et al.* (2011) 'Decreased levels of glutathione, the major brain antioxidant, in post-mortem prefrontal cortex from patients with psychiatric disorders', *International Journal of Neuropsychopharmacology*. Int J Neuropsychopharmacol, 14(1), pp. 123–130. doi: 10.1017/S1461145710000805.

Genc, K. and Genc, S. (2009) 'Oxidative stress and dysregulated Nrf2 activation in the pathogenesis of schizophrenia', *Bioscience Hypotheses*. Elsevier, 2(1), pp. 16–18. doi: 10.1016/j.bihy.2008.10.005.

Geyer, M. A. and Ellenbroek, B. (2003) 'Animal behavior models of the mechanisms underlying antipsychotic atypicality', *Progress in Neuro-Psychopharmacology and Biological Psychiatry*. Elsevier Inc., 27(7), pp. 1071–1079. doi: 10.1016/j.pnpbp.2003.09.003.

Gibbs, S. M. (2003) 'Regulation of neuronal proliferation and differentiation by nitric oxide', *Molecular Neurobiology*. Humana Press, 27(2), pp. 107–120. doi: 10.1385/MN:27:2:107.

Gill, R., Tsung, A. and Billiar, T. (2010) 'Linking oxidative stress to inflammation: Toll-like receptors', *Free Radical Biology and Medicine*. Pergamon, 48(9), pp. 1121–1132. doi: 10.1016/j.freeradbiomed.2010.01.006.

Goldsmith, P. (2004) 'Zebrafish as a pharmacological tool: The how, why and when', *Current Opinion in Pharmacology*. Elsevier, 4(5), pp. 504–512. doi: 10.1016/j.coph.2004.04.005.

Goldstone, J. V. *et al.* (2010) 'Identification and developmental expression of the full complement of Cytochrome P450 genes in Zebrafish', *BMC Genomics*. BioMed Central, 11(1), pp. 1–21. doi: 10.1186/1471-2164-11-643.

Gómez, L. J. *et al.* (2019) 'In-vitro antioxidant capacity and cytoprotective/cytotoxic effects upon Caco-2 cells of red tilapia (Oreochromis spp.) viscera hydrolysates', *Food Research International*. Elsevier Ltd, 120, pp. 52–61. doi: 10.1016/j.foodres.2019.02.029.

De Gregorio, D. *et al.* (2016) 'D-lysergic acid diethylamide (LSD) as a model of psychosis: Mechanism of action and pharmacology', *International Journal of Molecular Sciences*. MDPI AG,

17(11). doi: 10.3390/ijms17111953.

Grima, G. *et al.* (2003) 'Dopamine-induced oxidative stress in neurons with glutathione deficit: Implication for schizophrenia', *Schizophrenia Research*. Elsevier, 62(3), pp. 213–224. doi: 10.1016/S0920-9964(02)00405-X.

Grohmann, R. *et al.* (2014) 'Flupentixol use and adverse reactions in comparison with other common first- and second-generation antipsychotics: Data from the AMSP study', *European Archives of Psychiatry and Clinical Neuroscience*. Eur Arch Psychiatry Clin Neurosci, 264(2), pp. 131–141. doi: 10.1007/s00406-013-0419-y.

Gupta, P., Khobragade, S. B. and Shingatgeri, V. M. (2014) 'Effect of various antiepileptic drugs in zebrafish PTZ-seizure model', *Indian Journal of Pharmaceutical Sciences*. Medknow Publications, 76(2), pp. 157–163. Available at: /pmc/articles/PMC4023285/ (Accessed: 22 April 2021).

Gysin, R. *et al.* (2007) 'Impaired glutathione synthesis in schizophrenia: Convergent genetic and functional evidence', *Proceedings of the National Academy of Sciences of the United States of America*. National Academy of Sciences, 104(42), pp. 16621–16626. doi: 10.1073/pnas.0706778104.

Haddad, P. M. and Correll, C. U. (2018) 'Therapeutic advances in psychopharmacology the acute efficacy of antipsychotics in schizophrenia: A review of recent meta-analyses', *Ther Adv Psychopharmacol*, 8(11), pp. 303–318. doi: 10.1177/2045125318781475.

Halliwell, B. (2006) 'Phagocyte-derived reactive species: salvation or suicide?', *Trends in Biochemical Sciences*. Elsevier Current Trends, 31(9), pp. 509–515. doi: 10.1016/J.TIBS.2006.07.005.

Han, X. *et al.* (2020) 'TNF-α-dependent lung inflammation upregulates superoxide dismutase-2 to promote tumor cell proliferation in lung adenocarcinoma', *Molecular Carcinogenesis*. John Wiley and Sons Inc., 59(9), pp. 1088–1099. doi: 10.1002/mc.23239.

Hanisch, U. K. (2013) 'Functional diversity of microglia - How heterogeneous are they to begin with?', *Frontiers in Cellular Neuroscience*, 7, pp. 1–18. doi: 10.3389/fncel.2013.00065.

Hardingham, G. E. and Bading, H. (2010) 'Synaptic versus extrasynaptic NMDA receptor signalling: Implications for neurodegenerative disorders', *Nature Reviews Neuroscience*. Europe PMC Funders, 11(10), pp. 682–696. doi: 10.1038/nrn2911.

Hasan, A. *et al.* (2012) 'World Federation of Societies of Biological Psychiatry (WFSBP) guidelines for biological treatment of schizophrenia, part 1: Update 2012 on the acute treatment of schizophrenia and the management of treatment resistance', *World Journal of Biological Psychiatry*. Informa Healthcare, 13(5), pp. 318–378. doi: 10.3109/15622975.2012.696143.

Hasan Mohajeri, M. *et al.* (2018) 'Relationship between the gut microbiome and brain function', *Nutrition Reviews*. Oxford University Press, 76(7), pp. 481–496. doi: 10.1093/nutrit/nuy009.

Hayden, M. S. and Ghosh, S. (2004) 'Signaling to NF-κB', *Genes and Development*. Genes Dev, 18(18), pp. 2195–2224. doi: 10.1101/gad.1228704.

De Hert, M., Detraux, J. and Vancampfort, D. (2018) 'The intriguing relationship between coronary heart disease and mental disorders', *Dialogues in Clinical Neuroscience*. Les Laboratoires Seriver, 20(1), pp. 31–40. doi: 10.31887/dcns.2018.20.1/mdehert.

Hölscher, C. and Rose, S. P. R. (1992) 'An inhibitor of nitric oxide synthesis prevents memory formation in the chick', *Neuroscience Letters*. Elsevier, 145(2), pp. 165–167. doi: 10.1016/0304-3940(92)90012-V.

Hovatta, I. *et al.* (2005) 'Glyoxalase 1 and glutathione reductase 1 regulate anxiety in mice', *Nature*. Nature Publishing Group, 438(7068), pp. 662–666. doi: 10.1038/nature04250.

Howe, K. *et al.* (2013) 'The zebrafish reference genome sequence and its relationship to the human genome', *Nature*. Nature Publishing Group, 496(7446), pp. 498–503. doi: 10.1038/nature12111.

Howes, O. D. *et al.* (2012) 'The nature of dopamine dysfunction in schizophrenia and what this means for treatment: Meta-analysisof imaging studies', *Archives of General Psychiatry*. Europe PMC Funders, 69(8), pp. 776–786. doi: 10.1001/archgenpsychiatry.2012.169.

Howes, O. D. and Kapur, S. (2009) 'The dopamine hypothesis of schizophrenia: Version III - The final common pathway', *Schizophrenia Bulletin*. Schizophr Bull, 35(3), pp. 549–562. doi: 10.1093/schbul/sbp006.

Hroudová, J. and Fišar, Z. (2013) 'Control mechanisms in mitochondrial oxidative phosphorylation', *Neural Regeneration Research*. Wolters Kluwer -- Medknow Publications, 8(4), pp. 363–375. doi: 10.3969/j.issn.1673-5374.2013.04.009.

Huang, R.-Q. *et al.* (2001) 'Pentylenetetrazole-induced inhibition of recombinant-aminobutyric acid type A (GABA A) receptors: Mechanism and site of action', *J Pharmacol Exp*, 298(3), pp. 986–985.

Huang, X. *et al.* (2017) 'Role of tandospirone, a 5-HT1A receptor partial agonist, in the treatment of central nervous system disorders and the underlying mechanisms', *Oncotarget*. Impact Journals LLC, 8(60), pp. 102705–102720. doi: 10.18632/oncotarget.22170.

Irons, T. D. *et al.* (2013a) 'Acute administration of dopaminergic drugs has differential effects on locomotion in larval zebrafish', *Pharmacology Biochemistry and Behavior*. Elsevier, 103(4), pp. 792–813. doi: 10.1016/j.pbb.2012.12.010.

Irons, T. D. *et al.* (2013b) 'Acute administration of dopaminergic drugs has differential effects on locomotion in larval zebrafish', *Pharmacology Biochemistry and Behavior*. Elsevier, 103(4), pp. 792–813. doi: 10.1016/j.pbb.2012.12.010.

Iside, C. *et al.* (2020) 'SIRT1 activation by natural phytochemicals: An overview', *Frontiers in Pharmacology*. Frontiers Media S.A., 11, p. 1225. doi: 10.3389/fphar.2020.01225.

James, S. L. *et al.* (2018) 'Global, regional, and national incidence, prevalence, and years lived with disability for 354 diseases and injuries for 195 countries and territories, 1990–2017: A systematic analysis for the Global Burden of Disease Study 2017', *The Lancet*. Lancet Publishing Group, 392(10159), pp. 1789–1858. doi: 10.1016/S0140-6736(18)32279-7.

Jeong, J. Y. *et al.* (2008) 'Functional and developmental analysis of the blood-brain barrier in

zebrafish', *Brain Research Bulletin*, 75(5), pp. 619–628. doi: 10.1016/j.brainresbull.2007.10.043.

Jørgensen, A. (1980) 'Pharmacokinetic studies in volunteers of intravenous and oral cis (Z)-flupentixol and intramuscular cis (Z)-flupentixol decanoate in viscoleo®', *European Journal of Clinical Pharmacology*. Springer-Verlag, 18(4), pp. 355–360. doi: 10.1007/BF00561395.

Joubert, F. P. *et al.* (2021) 'Extrapyramidal side effects in first-episode schizophrenia treated with flupenthixol decanoate', *South African Journal of Psychiatry*. AOSIS (pty) Ltd, 27, pp. 1–7. doi: 10.4102/sajpsychiatry.v27i0.1568.

Joyce, E. M. and Roiser, J. P. (2007) 'Cognitive heterogeneity in schizophrenia', *Current Opinion in Psychiatry*. Lippincott Williams and Wilkins, 20(3), pp. 268–272. doi: 10.1097/YCO.0b013e3280ba4975.

Kaatz, G. W. *et al.* (2003) 'Phenothiazines and thioxanthenes inhibit multidrug efflux pump activity in Staphylococcus aureus', *Antimicrobial Agents and Chemotherapy*. American Society for Microbiology (ASM), 47(2), pp. 719–726. doi: 10.1128/AAC.47.2.719-726.2003.

Kalueff, A. V., Stewart, A. M. and Gerlai, R. (2014) 'Zebrafish as an emerging model for studying complex brain disorders', *Trends in Pharmacological Sciences*. Trends Pharmacol Sci, 35(2), pp. 63–75. doi: 10.1016/j.tips.2013.12.002.

Kanji, S. *et al.* (2018) 'The microbiome-gut-brain axis: Implications for schizophrenia and antipsychotic induced weight gain', *European Archives of Psychiatry and Clinical Neuroscience*, 268, pp. 3–15. doi: 10.1007/s00406-017-0820-z.

Kapur, S. and Mamo, D. (2003) 'Half a century of antipsychotics and still a central role for dopamine D2 receptors', *Progress in Neuro-Psychopharmacology and Biological Psychiatry*. Elsevier Inc., 27(7), pp. 1081–1090. doi: 10.1016/j.pnpbp.2003.09.004.

Keefe, R. S. E. *et al.* (2004) 'Comparative effect of atypical and conventional antipsychotic drugs on neurocognition in first-episode psychosis: A randomized, double-blind trial of olanzapine versus low doses of haloperidol', *American Journal of Psychiatry*. Am J Psychiatry, 161(6), pp. 985–995. doi: 10.1176/appi.ajp.161.6.985.

Kegeles, L. S. *et al.* (2010) 'Increased synaptic dopamine function in associative regions of the striatum in schizophrenia', *Archives of General Psychiatry*, 67(3), pp. 231–239. doi: 10.1001/archgenpsychiatry.2010.10.

Kegeles, L. S., Humaran, T. J. and Mann, J. J. (1998) 'In vivo neurochemistry of the brain in schizophrenia as revealed by magnetic resonance spectroscopy', *Biological Psychiatry*. Biol Psychiatry, 44(6), pp. 382–398. doi: 10.1016/S0006-3223(97)00425-3.

Khoury, R. and Nasrallah, H. A. (2018) 'Inflammatory biomarkers in individuals at clinical high risk for psychosis (CHR-P): State or trait?' doi: 10.1016/j.schres.2018.04.017.

Kim, J. and Song, J.-H. (2016) 'Molecular and cellular pharmacology Thioxanthenes, chlorprothixene and flupentixol inhibit proton currents in BV2 microglial cells'. doi: 10.1016/j.ejphar.2016.03.009.

Kim, J. and Song, J. H. (2016) 'Thioxanthenes, chlorprothixene and flupentixol inhibit proton currents

in BV2 microglial cells', *European Journal of Pharmacology*. Elsevier B.V., 779, pp. 31–37. doi: 10.1016/j.ejphar.2016.03.009.

Kim, M. *et al.* (2014) 'Using citrate-functionalized TiO 2 nanoparticles to study the effect of particle size on zebrafish embryo toxicity'. doi: 10.1039/c3an01966g.

Kokel, D. *et al.* (2010) 'Rapid behavior-based identification of neuroactive small molecules in the zebrafish', *Nature Chemical Biology*. Nature Publishing Group, 6(3), pp. 231–237. doi: 10.1038/nchembio.307.

Kowalski, J., Labuzek, K. and Herman, Z. S. (2003) 'Flupentixol and trifluperidol reduce secretion of tumor necrosis factor-α and nitric oxide by rat microglial cells', *Neurochemistry International*. Neurochem Int, 43(2), pp. 173–178. doi: 10.1016/S0197-0186(02)00163-8.

Kowalski, J., Labuzek, K. and Herman, Z. S. (2004) 'Flupentixol and trifluperidol reduce interleukin-1b and interleukin-2 release by rat mixed glial and microglial cell cultures', *Polish Journal of Pharmacology Pol. J. Pharmacol*, 56, pp. 563–570.

Kroeze, W. K. *et al.* (2003) 'H1-histamine receptor affinity predicts short-term weight gain for typical and atypical antipsychotic drugs', *Neuropsychopharmacology*, 28, pp. 519–526. doi: 10.1038/sj.npp.1300027.

Kropp, S. *et al.* (2005) 'Oxidative stress during treatment with first- and second-generation antipsychotics', *Journal of Neuropsychiatry and Clinical Neurosciences*. American Psychiatric Publishing Inc., 17(2), pp. 227–231. doi: 10.1176/jnp.17.2.227.

Kyzar, E. J. *et al.* (2012) 'Effects of hallucinogenic agents mescaline and phencyclidine on zebrafish behavior and physiology', *Progress in Neuro-Psychopharmacology and Biological Psychiatry*. Prog Neuropsychopharmacol Biol Psychiatry, 37(1), pp. 194–202. doi: 10.1016/j.pnpbp.2012.01.003.

Laursen, T. M., Nordentoft, M. and Mortensen, P. B. (2014) 'Excess early mortality in schizophrenia', *Annual Review of Clinical Psychology*. Annual Reviews, 10(1), pp. 425–448. doi: 10.1146/annurev-clinpsy-032813-153657.

Lee, S. and Lee, D. K. (2018) 'Multiple comparison test and its imitations what is the proper way to apply the multiple comparison test?', *Korean J Anesthesiol*, (5), pp. 353–360. doi: 10.4097/kja.d.18.00242.

Leucht, S. *et al.* (2009) 'Second-generation versus first-generation antipsychotic drugs for schizophrenia: a meta-analysis', *The Lancet*. Lancet, 373(9657), pp. 31–41. doi: 10.1016/S0140-6736(08)61764-X.

Li, L. H. *et al.* (2020) 'Action of trichostatin A on Alzheimer's disease-like pathological changes in SH-SY5Y neuroblastoma cells', *Neural Regeneration Research*. Wolters Kluwer Medknow Publications, 15(2), pp. 293–301. doi: 10.4103/1673-5374.265564.

Li, Q. *et al.* (2011) 'Alsin and SOD1 G93A proteins regulate endosomal reactive oxygen species production by glial cells and proinflammatory pathways responsible for neurotoxicity', *Journal of Biological Chemistry*. J Biol Chem, 286(46), pp. 40151–40162. doi: 10.1074/jbc.M111.279711.

Lin, C.-P. *et al.* (2004) 'Effects of root-end filling materials and eugenol on mitochondrial dehydrogenase activity and cytotoxicity to human periodontal ligament fibroblasts', *Journal of Biomedical Materials Research*. John Wiley & Sons, Ltd, 71B(2), pp. 429–440. doi: 10.1002/jbm.b.30107.

Lin, T. Y. *et al.* (2015) 'Lipopolysaccharide-promoted proliferation of Caco-2 cells is mediated by c-Src induction and ERK activation', *BioMedicine (Netherlands)*, 5(1), pp. 33–38. doi: 10.7603/s40681-015-0005-x.

Liu, Y. P., Lin, H. I. and Tzeng, S. F. (2005) 'Tumor necrosis factor-α and interleukin-18 modulate neuronal cell fate in embryonic neural progenitor culture', *Brain Research*. Brain Res, 1054(2), pp. 152–158. doi: 10.1016/j.brainres.2005.06.085.

Liu, Z. *et al.* (2017) 'Oxidative stress in neurodegenerative diseases: from molecular mechanisms to clinical applications', *Oxidative Medicine and Cellular Longevity*. Hindawi, 2017. doi: 10.1155/2017/2525967.

Loboda, A. *et al.* (2016) 'Role of Nrf2/HO-1 system in development, oxidative stress response and diseases: an evolutionarily conserved mechanism', *Cellular and Molecular Life Sciences*. Birkhauser Verlag AG, 73(17), pp. 3221–3247. doi: 10.1007/s00018-016-2223-0.

Lonart, G., Wang, J. and Johnson, K. M. (1992) 'Nitric oxide induces neurotransmitter release from hippocampal slices', *European Journal of Pharmacology*. Eur J Pharmacol, 220(2–3), pp. 271–272. doi: 10.1016/0014-2999(92)90759-W.

Lü, L. *et al.* (2004) 'Effect of clozapine and risperidone on serum cytokine levels in patients with first-episode paranoid schizophrenia', *International Immunopharmacology*, 6, pp. 666–671.

Luo, Y. *et al.* (2019) 'Changes in serum TNF-α, IL-18, and IL-6 concentrations in patients with chronic schizophrenia at admission and at discharge'. doi: 10.1016/j.comppsych.2019.01.003.

Marder, S. R. and Cannon, T. D. (2019) 'Schizophrenia', *New England Journal of Medicine*. Edited by A. H. Ropper. N Engl J Med, 381(18), pp. 1753–1761. doi: 10.1056/NEJMra1808803.

Markus, T. *et al.* (2018) 'Neuroprotective dobutamine treatment upregulates superoxide dismutase 3, anti-oxidant and survival genes and attenuates genes mediating inflammation', *BMC Neuroscience*. BioMed Central Ltd., 19(1), p. 9. doi: 10.1186/s12868-018-0415-2.

Martin, P., Carlsson, M. L. and Hjorth, S. (1998) 'Systemic PCP treatment elevates brain extracellular 5-HT: A microdialysis study in awake rats', *NeuroReport*. Lippincott Williams and Wilkins, 9(13), pp. 2985–2988. doi: 10.1097/00001756-199809140-00012.

Martin, S. J., Grimwood, P. D. and Morris, R. G. M. (2000) 'Synaptic plasticity and memory: An evaluation of the hypothesis', *Annual Review of Neuroscience*. Annual Reviews 4139 El Camino Way, P.O. Box 10139, Palo Alto, CA 94303-0139, USA, 23(1), pp. 649–711. doi: 10.1146/annurev.neuro.23.1.649.

Martins, M. R. *et al.* (2008) 'Antipsychotic-induced oxidative stress in rat brain', *Neurotoxicity Research*. Springer, 13(1), pp. 63–69. doi: 10.1007/BF03033368.

Masaki, T. *et al.* (2001) 'Targeted disruption of histamine H 1-receptor attenuates regulatory effects of leptin on feeding, adiposity, and UCP family in mice', *Diabetes*, 50.

Masood, A. *et al.* (2008) 'Reversal of oxidative stress-induced anxiety by inhibition of phosphodiesterase-2 in mice', *The Journal of pharmacology and experimental therapeutics*. NIH Public Access, 326(2), p. 369. doi: 10.1124/JPET.108.137208.

Matigian, N. *et al.* (2010) 'Disease-specific, neurosphere-derived cells as models for brain disorders', *DMM Disease Models and Mechanisms*, 3(11–12), pp. 785–798. doi: 10.1242/dmm.005447.

Maurer, I., Zierz, S. and Möller, H. J. (2001) 'Evidence for a mitochondrial oxidative phosphorylation defect in brains from patients with schizophrenia', *Schizophrenia Research*. Schizophr Res, 48(1), pp. 125–136. doi: 10.1016/S0920-9964(00)00075-X.

McCutcheon, R. *et al.* (2018) 'Defining the locus of dopaminergic dysfunction in schizophrenia: A meta-analysis and test of the mesolimbic hypothesis', *Schizophrenia Bulletin*. Oxford University Press, 44(6), pp. 1301–1311. doi: 10.1093/schbul/sbx180.

McCutcheon, R. A., Abi-Dargham, A. and Howes, O. D. (2019) 'Schizophrenia, Dopamine and the Striatum: From Biology to Symptoms', *Trends in Neurosciences*. Elsevier Ltd, 42(3), pp. 205–220. doi: 10.1016/j.tins.2018.12.004.

Meltzer, H. Y. *et al.* (2003) 'Clozapine treatment for suicidality in schizophrenia: International Suicide Prevention Trial (InterSePT)', *Archives of General Psychiatry*, 60(1), pp. 82–91. doi: 10.1001/archpsyc.60.1.82.

Mendieta-Serrano, M. A. *et al.* (2019) 'NADPH-Oxidase-derived reactive oxygen species are required for cytoskeletal organization, proper localization of E-cadherin and cell motility during zebrafish epiboly', *Free Radical Biology and Medicine*. Elsevier Inc., 130, pp. 82–98. doi: 10.1016/j.freeradbiomed.2018.10.416.

Mishara, A. L. and Goldberg, T. E. (2004) 'A meta-analysis and critical review of the effects of conventional neuroleptic treatment on cognition in schizophrenia: Opening a closed book', *Biological Psychiatry*. Elsevier USA, 55(10), pp. 1013–1022. doi: 10.1016/j.biopsych.2004.01.027.

Mishra, A., Singh, S. and Shukla, S. (2018) 'Physiological and functional basis of dopamine receptors and their role in neurogenesis: Possible implication for Parkinson's disease', *Journal of Experimental Neuroscience*. SAGE Publications Ltd, 12. doi: 10.1177/1179069518779829.

Miyaoka, T. *et al.* (2007) 'Possible antipsychotic effects of minocycline in patients with schizophrenia', *Progress in Neuro-Psychopharmacology and Biological Psychiatry*. Elsevier, 31(1), pp. 304–307. doi: 10.1016/j.pnpbp.2006.08.013.

Miyaoka, T. *et al.* (2008) 'Minocycline as adjunctive therapy for schizophrenia', *Clinical Neuropharmacology*, 31(5), pp. 287–292. doi: 10.1097/WNF.0b013e3181593d45.

Miyazaki, I. and Asanuma, M. (2008) 'Dopaminergic neuron-specific oxidative stress caused by dopamine itself', *Acta Miedica Okayama*, 62(3), pp. 141–150.

Momtazmanesh, S. *et al.* (2019) 'Cytokine alterations in schizophrenia: An updated review', *Frontiers*

in Psychiatry, 10, p. 892. doi: 10.3389/fpsyt.2019.00892.

Monji, A., Kato, T. and Kanba, S. (2009) 'Cytokines and schizophrenia: Microglia hypothesis of schizophrenia', *Psychiatry and Clinical Neurosciences*. Wiley-Blackwell, 63(3), pp. 257–265. doi: 10.1111/j.1440-1819.2009.01945.x.

Monkkonen, T. and Debnath, J. (2018) 'Inflammatory signaling cascades and autophagy in cancer', *Autophagy*. Taylor and Francis Inc., 14(2), pp. 190–198. doi: 10.1080/15548627.2017.1345412.

Moradi-Afrapoli, F. *et al.* (2017) 'HPLC-based activity profiling for GABA A receptor modulators in Searsia pyroides using a larval zebrafish locomotor assay', *Planta Medica*. Georg Thieme Verlag, 83(14–15), pp. 1169–1175. doi: 10.1055/s-0043-110768.

Mostafa, I. M. *et al.* (2018) 'Benzofurazan-based fluorophore for the selective determination of flupentixol dihydrochloride: Application to content uniformity testing', *Luminescence*. John Wiley and Sons Ltd, 33(6), pp. 1026–1032. doi: 10.1002/bio.3503.

Müller, N. *et al.* (2005) 'Clinical effects of COX-2 inhibitors on cognition in schizophrenia', *European Archives of Psychiatry and Clinical Neuroscience*. Springer, 255(2), pp. 149–151. doi: 10.1007/s00406-004-0548-4.

Mussulini, B. H. M. *et al.* (2013) 'Seizures induced by pentylenetetrazole in the adult zebrafish: A detailed behavioral characterization', *PLoS ONE*. Edited by P. Callaerts. Public Library of Science, 8(1). doi: 10.1371/journal.pone.0054515.

Nakagawa, Y. and Chiba, K. (2014) 'Role of microglial M1/M2 polarization in relapse and remission of psychiatric disorders and diseases', *Pharmaceuticals*, 7, p. 7. doi: 10.3390/ph7121028.

Nakano, Y. *et al.* (2010) 'Association between plasma nitric oxide metabolites levels and negative symptoms of schizophrenia: A pilot study', *Human Psychopharmacology: Clinical and Experimental*. John Wiley & Sons, Ltd, 25(2), pp. 139–144. doi: 10.1002/hup.1102.

Nakazawa, K. and Sapkota, K. (2020) 'The origin of NMDA receptor hypofunction in schizophrenia', *Pharmacology and Therapeutics*. Elsevier Inc., 205, p. 107426. doi: 10.1016/j.pharmthera.2019.107426.

Narayanan, R. *et al.* (2005) 'Trypan blue: Effect on retinal pigment epithelial and neurosensory retinal cells', *Investigative Ophthalmology and Visual Science*. The Association for Research in Vision and Ophthalmology, 46(1), pp. 304–309. doi: 10.1167/iovs.04-0703.

Newell, D. W. *et al.* (1995) 'Glutamate and non-glutamate receptor mediated toxicity caused by oxygen and glucose deprivation in organotypic hippocampal cultures', *Journal of Neuroscience*. Society for Neuroscience, 15(11), pp. 7702–7711. doi: 10.1523/jneurosci.15-11-07702.1995.

Ng, F. *et al.* (2008) 'Oxidative stress in psychiatric disorders: Evidence base and therapeutic implications', *International Journal of Neuropsychopharmacology*. Int J Neuropsychopharmacol, 11(6), pp. 851–876. doi: 10.1017/S1461145707008401.

Niedzielska, E. *et al.* (2016) 'Oxidative stress in neurodegenerative diseases', *Molecular Neurobiology*. Springer, 53(6), pp. 4094–4125. doi: 10.1007/s12035-015-9337-5.

Niu, X. *et al.* (2021) 'Toxic effects of the dinoflagellate Karenia mikimotoi on zebrafish (Danio rerio) larval behavior', *Harmful Algae*. Elsevier B.V., 103, p. 101996. doi: 10.1016/j.hal.2021.101996.

Nordberg, J. and Arnér, E. S. J. (2001) 'Reactive oxygen species, antioxidants, and the mammalian thioredoxin system', *Free Radical Biology and Medicine*. Free Radic Biol Med, 31(11), pp. 1287–1312. doi: 10.1016/S0891-5849(01)00724-9.

Nucifora, L. G. *et al.* (2017) 'Reduction of plasma glutathione in psychosis associated with schizophrenia and bipolar disorder in translational psychiatry', *Translational psychiatry*. Nature Publishing Group, 7(8), p. e1215. doi: 10.1038/tp.2017.178.

Obuchowicz, E. *et al.* (2017) 'Different influence of antipsychotics on the balance between pro- and anti-inflammatory cytokines depends on glia activation: An in vitro study', *Cytokine*. Academic Press, 94, pp. 37–44. doi: 10.1016/j.cyto.2017.04.004.

Ochoa-Repáraz, J. and Kasper, L. H. (2016) 'The second brain: Is the gut microbiota a link between obesity and central nervous system disorders?', *Current obesity reports*. NIH Public Access, 5(1), pp. 51–64. doi: 10.1007/s13679-016-0191-1.

Oja, S. S. *et al.* (2000) 'Modulation of glutamate receptor functions by glutathione', *Neurochemistry International*. Elsevier Ltd, 37(2–3), pp. 299–306. doi: 10.1016/S0197-0186(00)00031-0.

Okubo, Y. *et al.* (2000) 'Serotonin 5-HT2 receptors in schizophrenic patients studied by positron emission tomography', *Life Sciences*. Pergamon, 66(25), pp. 2455–2464. doi: 10.1016/S0024-3205(00)80005-3.

de Oliveira, M. R. *et al.* (2007) 'Oxidative stress in the hippocampus, anxiety-like behavior and decreased locomotory and exploratory activity of adult rats: Effects of sub acute vitamin A supplementation at therapeutic doses', *NeuroToxicology*. Neurotoxicology, 28(6), pp. 1191–1199. doi: 10.1016/j.neuro.2007.07.008.

Oliveri, A. N. and Levin, E. D. (2019) 'Dopamine D 1 and D 2 receptor antagonism during development alters later behavior in zebrafish', *Behavioural Brain Research*. Elsevier B.V., 356, pp. 250–256. doi: 10.1016/j.bbr.2018.08.028.

Oriach, C. S. *et al.* (2016) 'Food for thought: The role of nutrition in the microbiota-gut-brain axis', *Clinical Nutrition Experimental*. Elsevier Ltd, 6, pp. 25–38. doi: 10.1016/j.yclnex.2016.01.003.

Osmond, H. and Smythies, J. (1952) 'Schizophrenia: A new approach', *The Journal of mental science*. Cambridge University Press, 98(411), pp. 309–315. doi: 10.1192/bjp.98.411.309.

Ousman, S. S. and Kubes, P. (2012) 'Immune surveillance in the central nervous system', *Nature Neuroscience*. Nature Publishing Group, 15(8), pp. 1096–1101. doi: 10.1038/nn.3161.

Papadia, S. *et al.* (2008) 'Synaptic NMDA receptor activity boosts intrinsic antioxidant defenses', *Nature Neuroscience*. Nature Publishing Group, 11(4), pp. 476–487. doi: 10.1038/nn2071.

Papadimitriou, C. *et al.* (2018) '3D culture method for Alzheimer's disease modeling reveals interleukin-4 rescues Aβ42-induced loss of human neural stem cell plasticity', *Developmental Cell*. Cell Press, 46(1), pp. 85-101.e8. doi: 10.1016/j.devcel.2018.06.005.

Parsons, M. J. *et al.* (2004) 'The -1438A/G polymorphism in the 5-hydroxytryptamine type 2A receptor gene affects promoter activity', *Biological Psychiatry*. Elsevier, 56(6), pp. 406–410. doi: 10.1016/j.biopsych.2004.06.020.

Pedraz-Petrozzi, B. *et al.* (2020) 'Effects of inflammation on the kynurenine pathway in schizophrenia - A systematic review', *Journal of Neuroinflammation*. BioMed Central Ltd., 17(1), p. 56. doi: 10.1186/s12974-020-1721-z.

Perkins, D. O., Jeffries, C. D. and Do, K. Q. (2020) 'Potential Roles of Redox Dysregulation in the Development of Schizophrenia', *Biological Psychiatry*. Elsevier Inc., pp. 326–336. doi: 10.1016/j.biopsych.2020.03.016.

Perry, V. H. and Teeling, J. (2013) 'Microglia and macrophages of the central nervous system: The contribution of microglia priming and systemic inflammation to chronic neurodegeneration', *Seminars in Immunopathology*. Semin Immunopathol, 35(5), pp. 601–612. doi: 10.1007/s00281-013-0382-8.

Petersen, K. S. and Smith, C. (2016) 'Ageing-associated oxidative stress and inflammation are alleviated by products from grapes', *Oxidative Medicine and Cellular Longevity*. Hindawi Limited, 2016. doi: 10.1155/2016/6236309.

Platt, S. R. (2007) 'The role of glutamate in central nervous system health and disease - A review', *Veterinary Journal*. Vet J, 173(2), pp. 278–286. doi: 10.1016/j.tvjl.2005.11.007.

Pocock, J. M. and Kettenmann, H. (2007) 'Neurotransmitter receptors on microglia', *Trends in Neurosciences*, 30(10), pp. 527–535. doi: 10.1016/j.tins.2007.07.007.

Poon, K. L. *et al.* (2017) 'Humanizing the zebrafish liver shifts drug metabolic profiles and improves pharmacokinetics of CYP3A4 substrates', *Archives of Toxicology*. Springer Verlag, 91(3), pp. 1187–1197. doi: 10.1007/s00204-016-1789-5.

Pribiag, H. and Stellwagen, D. (2013) 'Tnf-α downregulates inhibitory neurotransmission through protein phosphatase 1-dependent trafficking of GABAA receptors', *Journal of Neuroscience*. Society for Neuroscience, 33(40), pp. 15879–15893. doi: 10.1523/JNEUROSCI.0530-13.2013.

Quednow, B. B., Geyer, M. A. and Halberstadt, A. L. (2010) 'Serotonin and schizophrenia', in *Handbook of Behavioral Neuroscience*. Elsevier, pp. 585–620. doi: 10.1016/S1569-7339(10)70102-8.

Quednow, B. B., Geyer, M. A. and Halberstadt, A. L. (2020) 'Serotonin and schizophrenia', in *Handbook of Behavioral Neuroscience*. Elsevier B.V., pp. 711–743. doi: 10.1016/B978-0-444-64125-0.00039-6.

Querobino, S. M., Ribeiro, C. A. J. and Alberto-Silva, C. (2018) 'Bradykinin-potentiating PEPTIDE-10C, an argininosuccinate synthetase activator, protects against H2O2 -induced oxidative stress in SH-SY5Y neuroblastoma cells', *Peptides*. Elsevier Inc., 103, pp. 90–97. doi: 10.1016/j.peptides.2018.03.017.

Raffa, M. *et al.* (2009) 'Decreased glutathione levels and antioxidant enzyme activities in untreated and treated schizophrenic patients', *Progress in Neuro-Psychopharmacology and Biological*

Psychiatry, 33(7), pp. 1178–1183. doi: 10.1016/j.pnpbp.2009.06.018.

Reddy, R., Keshavan, M. and Yao, J. K. (2003) 'Reduced plasma antioxidants in first-episode patients with schizophrenia', *Schizophrenia Research*. Elsevier, 62(3), pp. 205–212. doi: 10.1016/S0920-9964(02)00407-3.

Reimold, M. *et al.* (2007) 'Occupancy of dopamine D1, D2 and serotonin 2A receptors in schizophrenic patients treated with flupentixol in comparison with risperidone and haloperidol', *Psychopharmacology*, 190(2), pp. 241–249. doi: 10.1007/s00213-006-0611-0.

Reis, L. V. de C. *et al.* (2020) 'Evaluation of cytotoxicity of nanolipid carriers with structured Buriti oil in the Caco-2 and HepG2 cell lines', *Bioprocess and Biosystems Engineering*. Springer, 43(6), pp. 1105–1118. doi: 10.1007/s00449-020-02308-6.

Remington, G. *et al.* (2016) 'Treating negative symptoms in schizophrenia: An update', *Current Treatment Options in Psychiatry*. Springer, 3(2), pp. 133–150. doi: 10.1007/s40501-016-0075-8.

Rënyi, L. *et al.* (2001) 'The pharmacological profile of (R)-3,4-dihydro-N-isopropyl-3-(N-isopropyl-N-propylamino)-2H-1-benzopyran-5-carboxamide, a selective 5-hydroxytryptamine1A receptor agonist', *Journal of Pharmacology and Experimental Therapeutics*, 299(3).

Revier, C. J. *et al.* (2015) 'Ten-year outcomes of first-episode psychoses in the MRC ÆSOP-10 study', *The Journal of Nervous and Mental Disease*. Lippincott Williams and Wilkins, 203(5), pp. 379–386. doi: 10.1097/NMD.0000000000000295.

Reynolds, G. P., Zhang, Z. J. and Zhang, X. Bin (2002) 'Association of antipsychotic drug-induced weight gain with a 5-HT2C receptor gene polymorphism', *Lancet*, 359(9323), pp. 2086–2087. doi: 10.1016/S0140-6736(02)08913-4.

Rico, E. P. *et al.* (2011) 'Zebrafish neurotransmitter systems as potential pharmacological and toxicological targets', *Neurotoxicology and Teratology*, 33, pp. 608–617. doi: 10.1016/j.ntt.2011.07.007.

Ridaura, V. and Belkaid, Y. (2015) 'Gut microbiota: The link to your second brain', *Cell*. Cell Press, 161(2), pp. 193–194. doi: 10.1016/j.cell.2015.03.033.

Rihel, J. and Schier, A. F. (2012) 'Behavioral screening for neuroactive drugs in zebrafish', *Developmental Neurobiology*. John Wiley & Sons, Ltd, 72(3), pp. 373–385. doi: 10.1002/dneu.20910.

Ripke, S. *et al.* (2014) 'Biological insights from 108 schizophrenia-associated genetic loci', *Nature*. Nature Publishing Group, 511(7510), pp. 421–427. doi: 10.1038/nature13595.

Rodrigues-Amorim, D. *et al.* (2018) 'Cytokines dysregulation in schizophrenia: A systematic review of psychoneuroimmune relationship', *Schizophrenia Research*. Elsevier B.V., pp. 19–33. doi: 10.1016/j.schres.2017.11.023.

Rodriguez-Antona, C. and Ingelman-Sundberg, M. (2006) 'Cytochrome P450 pharmacogenetics and cancer', *Oncogene*. Nature Publishing Group, 25(11), pp. 1679–1691. doi: 10.1038/sj.onc.1209377.

Ronaldson, A. *et al.* (2018) 'The effects of six-day SSRI administration on diurnal cortisol secretion

in healthy volunteers', *Psychopharmacology*. Springer Verlag, 235(12), pp. 3415–3422. doi: 10.1007/s00213-018-5050-1.

Ross, K. S., Powrie, Y. S. L. and Smith, C. (2020) 'Accelerated ageing profile in inflammatory arthritis is unique and tissue compartment specific', *Inflammopharmacology*. Springer, 28(4), pp. 967–977. doi: 10.1007/s10787-020-00731-5.

Salim, S. *et al.* (2010) 'Oxidative stress: A potential recipe for anxiety, hypertension and insulin resistance', *Brain research*. NIH Public Access, 1359, p. 178. doi: 10.1016/J.BRAINRES.2010.08.093.

Salim, S. (2014) 'Oxidative stress and psychological disorders', *Current Neuropharmacology*. Bentham Science Publishers, 12, pp. 140–147.

Sallinen, V. *et al.* (2009) 'Hyperserotonergic phenotype after monoamine oxidase inhibition in larval zebrafish', *Journal of Neurochemistry*, 109(2), pp. 403–415. doi: 10.1111/j.1471-4159.2009.05986.x.

Salminen, A., Kaarniranta, K. and Kauppinen, A. (2013) 'Crosstalk between oxidative stress and SIRT1: Impact on the aging process', *International Journal of Molecular Sciences*. Multidisciplinary Digital Publishing Institute, 14(2), pp. 3834–3859. doi: 10.3390/ijms14023834.

Scarcello, E. *et al.* (2020) 'Mind your assays: Misleading cytotoxicity with the WST-1 assay in the presence of manganese', *PLOS ONE*. Edited by S. Hussain. Public Library of Science, 15(4), p. e0231634. doi: 10.1371/journal.pone.0231634.

Scherz-Shouval, R. and Elazar, Z. (2007) 'ROS, mitochondria and the regulation of autophagy', *Trends in Cell Biology*. Trends Cell Biol, 17(9), pp. 422–427. doi: 10.1016/j.tcb.2007.07.009.

Schizophrenia (2019) *WHO*. World Health Organization. Available at: https://www.who.int/news-room/fact-sheets/detail/schizophrenia (Accessed: 26 June 2020).

Schmitt, A. *et al.* (2018) 'Effects of aerobic exercise on metabolic syndrome, cardiorespiratory fitness, and symptoms in schizophrenia include decreased mortality', *Frontiers in Psychiatry*. Frontiers Media S.A., p. 690. doi: 10.3389/fpsyt.2018.00690.

Scigliano, G. and Ronchetti, G. (2013) 'Antipsychotic-induced metabolic and cardiovascular side effects in schizophrenia: A novel mechanistic hypothesis', *CNS Drugs*. Springer, 27(4), pp. 249–257. doi: 10.1007/s40263-013-0054-1.

Seeman, P. *et al.* (1975) 'Brain receptors for antipsychotic drugs and dopamine: Direct binding assays', 72(11), pp. 4376–4380.

Seeman, P. *et al.* (2005) 'Dopamine supersensitivity correlates with D2High states, implying many paths to psychosis', *Proceedings of the National Academy of Sciences of the United States of America*. National Academy of Sciences, 102(9), pp. 3513–3518. doi: 10.1073/pnas.0409766102.

Seibt, K. J. *et al.* (2010) 'Antipsychotic drugs prevent the motor hyperactivity induced by psychotomimetic MK-801 in zebrafish (Danio rerio)', *Behavioural Brain Research*. Behav Brain Res, 214(2), pp. 417–422. doi: 10.1016/j.bbr.2010.06.014.

Selvaraj, S. *et al.* (2014) 'Alterations in the serotonin system in schizophrenia: A systematic review

and meta-analysis of postmortem and molecular imaging studies', *Neuroscience and Biobehavioral Reviews*. Elsevier Ltd, 45, pp. 233–245. doi: 10.1016/j.neubiorev.2014.06.005.

Shabab, T. *et al.* (2017) 'Neuroinflammation pathways: A general review', *International Journal of Neuroscience*. Taylor and Francis Ltd, 127(7), pp. 624–633. doi: 10.1080/00207454.2016.1212854.

Sher, L. and Kahn, R. S. (2019) 'Suicide in schizophrenia: An educational overview', *Medicina (Lithuania)*. MDPI AG, p. 361. doi: 10.3390/medicina55070361.

Shin, H. W. and Chung, S. J. (2012) 'Drug-Induced parkinsonism', *Journal of Clinical Neurology (Korea)*. Korean Neurological Association, 8(1), pp. 15–21. doi: 10.3988/jcn.2012.8.1.15.

da Silva Alves, F. *et al.* (2008) 'The revised dopamine hypothesis of schizophrenia: Evidence from pharmacological MRI studies with atypical antipsychotic medication', *Psychopharmacology bulletin*, 41(1), pp. 121–132. doi: 10.1016/s0920-9964(08)70291-3.

Slifstein, M. *et al.* (2015) 'Deficits in prefrontal cortical and extrastriatal dopamine release in schizophrenia a positron emission tomographic functional magnetic resonance imaging study', *JAMA Psychiatry*. American Medical Association, 72(4), pp. 316–324. doi: 10.1001/jamapsychiatry.2014.2414.

Smieskova, R. *et al.* (2009) 'The effects of antipsychotics on the brain: What have we learnt from structural imaging of schizophrenia? – A systematic review', *Current Pharmaceutical Design*. Bentham Science Publishers Ltd., 15(22), pp. 2535–2549. doi: 10.2174/138161209788957456.

Sökmen, T. Ö. *et al.* (2020) 'Polystyrene nanoplastics (20 nm) are able to bioaccumulate and cause oxidative DNA damages in the brain tissue of zebrafish embryo (Danio rerio)', *NeuroToxicology*. Elsevier B.V., 77, pp. 51–59. doi: 10.1016/j.neuro.2019.12.010.

Solmi, M. *et al.* (2017) 'Safety, tolerability, and risks associated with first-and second-generation antipsychotics: A state-of-the-art clinical review', *Therapeutics and Clinical Risk Management*. Dove Medical Press Ltd., 13, pp. 757–777. doi: 10.2147/TCRM.S117321.

Stahl, S. M. (2018) 'Beyond the dopamine hypothesis of schizophrenia to three neural networks of psychosis: Dopamine, serotonin, and glutamate', *CNS Spectrums*. Cambridge University Press, 23(3), pp. 187–191. doi: 10.1017/S1092852918001013.

Stargardt, T. *et al.* (2011) 'Effectiveness and costs of flupentixol compared to other first- and second-generation antipsychotics in the treatment of schizophrenia', *Psychopharmacology*. Springer Verlag, 216(4), pp. 579–587. doi: 10.1007/s00213-011-2256-x.

Steullet, P. *et al.* (2006) 'Synaptic plasticity impairment and hypofunction of NMDA receptors induced by glutathione deficit: Relevance to schizophrenia', *Neuroscience*. Neuroscience, 137(3), pp. 807–819. doi: 10.1016/j.neuroscience.2005.10.014.

Steullet, P. *et al.* (2017) 'Oxidative stress-driven parvalbumin interneuron impairment as a common mechanism in models of schizophrenia', *Molecular Psychiatry*. Nature Publishing Group, pp. 936–943. doi: 10.1038/mp.2017.47.

Steullet, P. *et al.* (2018) 'The thalamic reticular nucleus in schizophrenia and bipolar disorder: role of

parvalbumin-expressing neuron networks and oxidative stress', *Molecular Psychiatry*. Nature Publishing Group, 23(10), pp. 2057–2065. doi: 10.1038/mp.2017.230.

Sudo, N. (2019) 'Role of gut microbiota in brain function and stress-related pathology', *Bioscience of Microbiota, Food and Health*. BMFH Press, 38(3), pp. 75–80. doi: 10.12938/bmfh.19-006.

Sun, H. Q. *et al.* (2016) 'Diurnal neurobiological alterations after exposure to clozapine in first-episode schizophrenia patients', *Psychoneuroendocrinology*. Elsevier Ltd, 64, pp. 108–116. doi: 10.1016/j.psyneuen.2015.11.013.

Sun, Y. and Oberley, L. W. (1996) 'Redox regulation of transcriptional activators', *Free Radical Biology and Medicine*. Elsevier Inc., 21(3), pp. 335–348. doi: 10.1016/0891-5849(96)00109-8.

Takeuchi, O. and Akira, S. (2010) 'Pattern recognition receptors and inflammation', *Cell*. Cell Press, 140(6), pp. 805–820. doi: 10.1016/j.cell.2010.01.022.

Tamminga, C. A. and Holcomb, H. H. (2005) 'Phenotype of schizophrenia: A review and formulation', *Molecular Psychiatry*. Nature Publishing Group, 10(1), pp. 27–39. doi: 10.1038/sj.mp.4001563.

Tandon, R. *et al.* (2013) 'Definition and description of schizophrenia in the DSM-5', *Schizophrenia Research*. Elsevier, pp. 3–10. doi: 10.1016/j.schres.2013.05.028.

Tang, Y. and Le, W. (2016) 'Differential roles of M1 and M2 microglia in neurodegenerative diseases', *Molecular Neurobiology*. Humana Press Inc., 53(2), pp. 1181–1194. doi: 10.1007/s12035-014-9070-5.

Terrando, N. *et al.* (2011) 'Resolving postoperative neuroinflammation and cognitive decline', *Annals of Neurology*. John Wiley & Sons, Ltd, 70(6), pp. 986–995. doi: 10.1002/ana.22664.

Tewari, M. and Seth, P. (2016) 'Astrocytes in neuroinflammation and neuronal disorders: Shifting the focus from neurons', in *Inflammation: The Common Link in Brain Pathologies*. Springer Singapore, pp. 43–70. doi: 10.1007/978-981-10-1711-7_3.

Thameem Dheen, S., Kaur, C. and Ling, E.-A. (2007) 'Microglial activation and its implications in the brain diseases', *Current Medicinal Chemistry*. Bentham Science Publishers Ltd., 14(11), pp. 1189–1197. doi: 10.2174/092986707780597961.

Toimela, T. and Tähti, H. (2004) 'Mitochondrial viability and apoptosis induced by aluminum, mercuric mercury and methylmercury in cell lines of neural origin', *Archives of Toxicology*. Springer, 78(10), pp. 565–574. doi: 10.1007/s00204-004-0575-y.

Trichard, C. *et al.* (1998) 'No serotonin 5-HT(2A) receptor density abnormality in the cortex of schizophrenic patients studied with PET', *Schizophrenia Research*. Elsevier, 31(1), pp. 13–17. doi: 10.1016/S0920-9964(98)00014-0.

Tschopp, J. (2011) 'Mitochondria: Sovereign of inflammation?', *European Journal of Immunology*. Eur J Immunol, 41(5), pp. 1196–1202. doi: 10.1002/eji.201141436.

Uchida, H. *et al.* (2011) 'Dopamine D2 receptor occupancy and clinical effects', *Journal of Clinical Psychopharmacology*, 31(4), pp. 497–502. doi: 10.1097/JCP.0b013e3182214aad.

Uranova, N. *et al.* (2001) 'Electron microscopy of oligodendroglia in severe mental illness', *Brain Research Bulletin*. Brain Res Bull, 55(5), pp. 597–610. doi: 10.1016/S0361-9230(01)00528-7.

Usai, A. *et al.* (2020) 'A model of a zebrafish avatar for co-clinical trials', *Cancers*. MDPI AG, 12(3). doi: 10.3390/cancers12030677.

Vašíček, O., Lojek, A. and Číž, M. (2020) 'Serotonin and its metabolites reduce oxidative stress in murine RAW264.7 macrophages and prevent inflammation', *Journal of Physiology and Biochemistry*. Springer, 76(1), pp. 49–60. doi: 10.1007/s13105-019-00714-3.

Vaz, R. L., Outeiro, T. F. and Ferreira, J. J. (2018) 'Zebrafish as an animal model for drug discovery in Parkinson's disease and other movement disorders: A systematic review', *Frontiers in Neurology*. Frontiers Media S.A., 9, p. 347. doi: 10.3389/fneur.2018.00347.

Verhoeff, N. P. L. G. *et al.* (2000) 'A voxel-by-voxel analysis of [18F]setoperone PET data shows no substantial serotonin 5-HT(2A) receptor changes in schizophrenia', *Psychiatry Research - Neuroimaging*. Psychiatry Res, 99(3), pp. 123–135. doi: 10.1016/S0165-1781(00)00198-0.

Waade, R. B., Solhaug, V. and Høiseth, G. (2020) 'Impact of CYP2D6 on serum concentrations of flupentixol, haloperidol, perphenazine and zuclopenthixol', *British Journal of Clinical Pharmacology*. Blackwell Publishing Ltd. doi: 10.1111/bcp.14626.

Wang, D. *et al.* (2020) 'A comprehensive analysis of the effect of SIRT1 variation on the risk of schizophrenia and depressive symptoms', *Frontiers in Genetics*. Frontiers Media S.A., 11, p. 832. doi: 10.3389/fgene.2020.00832.

Wang, H. L. *et al.* (2019) 'Dorsal Raphe Dual Serotonin-Glutamate Neurons Drive Reward by Establishing Excitatory Synapses on VTA Mesoaccumbens Dopamine Neurons', *Cell Reports*. Elsevier B.V., 26(5), pp. 1128-1142.e7. doi: 10.1016/j.celrep.2019.01.014.

Wang, X. *et al.* (2019) 'Evaluation of development, locomotor behavior, oxidative stress, immune responses and apoptosis in developing zebrafish (Danio rerio) exposed to TBECH (tetrabromoethylcyclohexane)', *Comparative Biochemistry and Physiology Part - C: Toxicology and Pharmacology*. Elsevier Inc., 217, pp. 106–113. doi: 10.1016/j.cbpc.2018.12.004.

Wasel, O. and Freeman, J. L. (2020) 'Chemical and genetic zebrafish models to define mechanisms of and treatments for dopaminergic neurodegeneration', *International Journal of Molecular Sciences*. MDPI AG, 21(17), pp. 1–14. doi: 10.3390/ijms21175981.

Watanabe, Y., Someya, T. and Nawa, H. (2010) 'Cytokine hypothesis of schizophrenia pathogenesis: Evidence from human studies and animal models', *Psychiatry and Clinical Neurosciences*, 64(3), pp. 217–230.

Weaver, I. C. G. *et al.* (2004) 'Epigenetic programming by maternal behavior', *Nature Neuroscience*. Nature Publishing Group, 7(8), pp. 847–854. doi: 10.1038/nn1276.

Weinberger, D. R. and Laruelle, M. (2002) 'Neurochemical and neuropharmacological imaging in schizophrenia', *Neuropsychopharmacology*.

Whatley, S. A. *et al.* (1998) 'Superoxide, neuroleptics and the ubiquinone and cytochrome b 5

reductases in brain and lymphocytes from normals and schizophrenic patients', *Molecular Psychiatry*, 3, pp. 227–237.

Wieck, A. and Haddad, P. (2002) 'Hyperprolactinaemia caused by antipsychotic drugs', *British Medical Journal*. BMJ Publishing Group, 324(7332), pp. 250–252. doi: 10.1136/bmj.324.7332.250.

Wong, D., Dorovini-Zis, K. and Vincent, S. R. (2004) 'Cytokines, nitric oxide, and cGMP modulate the permeability of an in vitro model of the human blood-brain barrier', *Experimental Neurology*. Exp Neurol, 190(2), pp. 446–455. doi: 10.1016/j.expneurol.2004.08.008.

Woolley, D. W. and Shaw, E. (1954) 'Some neurophysiological aspects of serotonin', *British Medical Journal*. BMJ Publishing Group, 2(4880), pp. 122–126. doi: 10.1136/bmj.2.4880.122.

Xie, J. *et al.* (2010) 'A novel transgenic zebrafish model for blood-brain and blood-retinal barrier development', *BMC Developmental Biology*. BioMed Central, 10(1), p. 76. doi: 10.1186/1471-213X-10-76.

Xie, N. *et al.* (2014) 'Stability of casein antioxidant peptide fractions during in vitro digestion/Caco-2 cell model: Characteristics of the resistant peptides', *European Food Research and Technology*. Springer Verlag, 239(4), pp. 577–586. doi: 10.1007/s00217-014-2253-5.

Yang, L. *et al.* (2018) 'The roles of hypoxia-inducible Factor-1 and iron regulatory protein 1 in iron uptake induced by acute hypoxia', *Biochemical and Biophysical Research Communications*. Elsevier B.V., 507(1–4), pp. 128–135. doi: 10.1016/j.bbrc.2018.10.185.

Yang, Y. *et al.* (2019) 'Recent advances in the mechanisms of NLRP3 inflammasome activation and its inhibitors', *Cell Death and Disease*. Nature Publishing Group, 10(2), pp. 1–11. doi: 10.1038/s41419-019-1413-8.

Yao, J. K. and Keshavan, M. S. (2011) 'Antioxidants, redox signaling, and pathophysiology in schizophrenia: An integrative view', *Antioxidants and Redox Signaling*. Mary Ann Liebert, Inc. 140 Huguenot Street, 3rd Floor New Rochelle, NY 10801 USA, 15(7), pp. 2011–2035. doi: 10.1089/ars.2010.3603.

Yao, J. K., Leonard, S. and Reddy, R. (2006) 'Altered glutathione redox state in schizophrenia', *Disease Markers*. IOS Press, 22, pp. 83–93.

Yao, J. K., Leonard, S. and Reddy, R. D. (2004) 'Increased nitric oxide radicals in postmortem brain from patients with schizophrenia', *Schizophrenia Bulletin*. Oxford University Press, 30(4), pp. 923–934. doi: 10.1093/oxfordjournals.schbul.a007142.

Yildirim, O. *et al.* (2011) 'Serum cortisol and dehydroepiandrosterone-sulfate levels in schizophrenic patients and their first-degree relatives', *Psychiatry and Clinical Neurosciences*. Psychiatry Clin Neurosci, 65(6), pp. 584–591. doi: 10.1111/j.1440-1819.2011.02252.x.

Yong, H. Y. F. *et al.* (2019) 'The benefits of neuroinflammation for the repair of the injured central nervous system', *Cellular and Molecular Immunology*. Chinese Soc Immunology, 16(6), pp. 540–546. doi: 10.1038/s41423-019-0223-3.

Yoon, J. H. *et al.* (2013) 'Impaired prefrontal-basal ganglia functional connectivity and substantia

nigra hyperactivity in schizophrenia', *Biological Psychiatry*. Elsevier USA, 74(2), pp. 122–129. doi: 10.1016/j.biopsych.2012.11.018.

Youdim, M. B. H. (2018) 'Monoamine oxidase inhibitors, and iron chelators in depressive illness and neurodegenerative diseases', *Journal of Neural Transmission*. Springer-Verlag Wien, 125(11), pp. 1719–1733. doi: 10.1007/s00702-018-1942-9.

Young, E. (2012) 'Gut instincts: The secrets of your second brain', *New Scientist*. Reed Business Information, 216(2895), pp. 38–42. doi: 10.1016/S0262-4079(12)63204-7.

Zakhary, S. M. *et al.* (2011) 'A behavioral and molecular analysis of ketamine in zebrafish', *Synapse*. NIH Public Access, 65(2), pp. 160–167. doi: 10.1002/syn.20830.

Zhang, M. *et al.* (2010) 'A meta-analysis of oxidative stress markers in schizophrenia', *Sci China Life Sci*, 53(1), pp. 112–124. doi: 10.1007/s11427-010-0013-8.

Zhang, S. (2019) 'Microglial activation after ischaemic stroke', *Stroke and Vascular Neurology*. BMJ Publishing Group, 4(2), pp. 71–74. doi: 10.1136/svn-2018-000196.

Zhang, X. Y. *et al.* (2003) 'The effect of risperidone treatment on superoxide dismutase in schizophrenia', *Journal of Clinical Psychopharmacology*, 23(2), pp. 128–131. doi: 10.1097/00004714-200304000-00004.

Zhong, H. J. *et al.* (2014) 'Discovery of a natural product-like iNOS inhibitor by molecular docking with potential neuroprotective effects in vivo', *PLoS ONE*. Public Library of Science, 9(4), p. 92905. doi: 10.1371/journal.pone.0092905.

Zhong, Y. and Shahidi, F. (2015) 'Methods for the assessment of antioxidant activity in foods', in *Handbook of Antioxidants for Food Preservation*. Elsevier Inc., pp. 287–333. doi: 10.1016/B978-1-78242-089-7.00012-9.

Zuo, L. *et al.* (2015) 'Biological and physiological role of reactive oxygen species - the good, the bad and the ugly', *Acta Physiologica*. Blackwell Publishing Ltd, 214(3), pp. 329–348. doi: 10.1111/apha.12515.

Appendices

Appendix A: Thiobarbituric acid reactive substances (Malondialdehyde) protocol

TBARS (MDA) Assay protocol

(Adapted from Ross *et al.* (2020))

Reagents:

1. Absolute ethanol
2. 2 mM MDA standard stock (Must be made fresh*):
   - 0.0125408 g (12.5408 mg) MDA in 20 ml 40% ethanol.
3. 4 mM BHT (butylated hydroxytoluene) (Must be made fresh*):
   - 0.008814 g (8.814 mg) BHT in 10 ml abs ethanol.
4. 0.2 M ortho-phosphoric acid (OPA)
5. 0.1 M NaOH
6. 0.11 M TBA (2-thiobarbituric acid) (must be made fresh*):
   - 0.159 g (158.565 mg) in 10 mL 0.1 M NaOH
7. N-butanol
8. NaCl (saturated)

Standards preparation: Just did a serial dilution from 2000uM concentration 500ul dH2O with 500ul previous std

	MDA (ul of stock)	dH_2O (ul)	Concentration (µM)
Std K	1000	0 ul	2000
Std J	500	500	1000
Std I	250	750	500
Std H	125	875	250
Std G	62.5	937.5	125
Std F	31.25	968.75	62.5
Std E	15.625	984.375	31.25
Std D	7.8125	992.1875	15.625
Std C	3.4	996.6	7.8125
Std B	1.7	998.3	3.9
Std A	0.85	999.15	1.95
Blank	0	1000	0

Blank	A	B	C	D	E	F	G	H	I	J	K
Blank	A	B	C	D	E	F	G	H	I	J	K
Blank	A	B	C	D	E	F	G	H	I	J	K
x	x	x	x	x	x	x	x	x	x	x	x
x	V	1	2	3	4	5	6	7	8	x	x
x	V	1	2	3	4	5	6	7	8	x	x
x	V	1	2	3	4	5	6	7	8	x	x
x	x	x	x	x	x	x	x	x	x	x	x

V= PBS

1= Control	5= Control + LPS
2= 3 mg/d Flu	6= 3 mg/d Flu + LPS
3= 10 mg/d Flu	7= 10 mg/d Flu + LPS
4= 30 mg/d Flu	8= 30 mg/d Flu + LPS

Assay Protocol:

- Thaw samples on ice (takes an hour); make up reagents and label tubes, grab a coffee
- Lyse samples 3x pulses for 15 seconds on amp 5 with 20 second intervals (program 1)
- Add 100 µl of sample/stdin into 2 ml Eppendorf tube
- Add 12.5 µl of 4 mM BHT (reagent 4)
- Add 100 µl of 0.2 M OPA (reagent 5)
- Vortex for 10 secs
- Add 12.5 µl TBA (reagent 7)
- Heat at 90°C for 45 mins
- Put on ice for 2 mins
- Keep at room temperature for 5 minutes
- Add 1 mL n-butanol (reagent 8)
- Add 100 µl saturated NaCl (reagent 9)
- Vortex for 10 seconds
- Centrifuge at 6000 rpm for 5 mins at 4°C
- Aliquot 300 µl of supernatant (top layer only) into 96 well plate in triplicate
- transferred into fresh eppi and homogenised before plating (extracted 980 ul)
- Read at 532-572 nm

Reagents:

- Malondialdehyde tetrabutylammonium salt (MDA)
  Molecular Weight: 313.52
  2 mM Stock
  = 0.0125408 g (12.5408 mg) MDA in 20 ml abs ethanol.

- BHT (butylated hydroxytoluene)
  MW: 220.35
  4 mM stock
  = 0.008814 g (8.814 mg) BHT in 10 ml abs ethanol.

- Ortho-phosphoric acid (OPA)
  MW: 97.99
  0.2 M stock
  =9.799 g OPA in 500 ml dH_2O

- Sodium hydroxide (NaOH)

MW: 40
0.1 M stock
= 2 g NaOH in 500 ml dH_2O

- 2-thiobarbituric acid (TBA)

MW: 144.15
0.11 M TBA stock
= 0.158565 g (158.565 mg) in 10 mL 0.1 M NaOH

Appendix B: Protocol for hydrogen peroxide kit from Elabscience optimised by Lesha Pretorius to a 96-well plate and adapted for my experiments

Hydrogen Peroxide (H_2O_2) Assay Kit (Elabscience®, E-BC-K102)

Operation table

	Blank tube	Standard tube	Sample tube
Reagent 1 (mL)	1	1	1
Preheat at 37°C for 10 min.			
Distilled water (mL)	0.1		
60 mmol/L H_2O_2 standard solution (mL)		0.1	
Sample (mL)			0.1
Reagent 2 (mL)	1	1	1
Mix fully, set to zero with double-distilled water, then measure the OD values of each tube at 405 nm with 1 cm optical path quartz cuvette.			

Protocol (adapted for 96-well microtiter plate):

1. Calculate the actual concentration of Reagent 3 (hydrogen peroxide). Dilute reagent 3 from '1 mol/L' to 10 mmol/L (100x dilution). Measure the optical density of the '10 mmol/L' solution using a quartz cuvette at 240 nm.
    - The actual concentration of Reagent 3 is: **22,94 x A_{240} x 100 ÷ 1000**

2. Make up solutions for the standard curve. This step requires you to calculate dilution factors for each concentration of hydrogen peroxide standard you wish to incorporate into the standard curve, according to the actual concentration of Reagent 3.
    - Concentrations (mmol/L) for the standard curve are recommended to be 150, 100, 80, 60, 40, 20 and 0.

3. Deposit 100 µL of Reagent 1 (buffer solution) into each well. Place the plate into a 37°C incubator for 10 min.

4. Add 10 µL of hydrogen peroxide standard, or 10 µL sample, or an appropriate blank into an appropriate well.

5. Add 100 µL of Reagent 2 (ammonium molybdate) to each well.

6. Measure optical density on a plate reader at 405 nm.

7. Use the linear formula of the standard curve to calculate the concentration of hydrogen peroxide in samples.

Appendix C: Trolox-equivalent antioxidant capacity (TEAC) assay protocol ABTS (TEAC) ASSAY

(Adapted from Ross et al. (2020))

Reagents:

1. ABTS (2,2'-Azino-bis(3-ethylbenzothiazoline-6-sulfonic acid) Diammonium salt: 7 mM (Sigma Cat nr.: A1888).
    a. Weigh 0.0192 g of ABTS (Fridge) in a 15 mL screw cap tube and add 5 mL distilled water. Mix until dissolve. Prepare fresh.

2. Potassium-peroxodisulphate: 140mM (Merck Cat Nr.: 105091)
    a. Weigh 0.1892 g $K_2S_2O_8$ (Reagent rack) in a 15 mL screw cap tube and add 5 mL distilled water. Mix until dissolve. Prepare fresh.

3. ABTS mix (This must be done 16 hours before starting the assay):
    a. Add 88 µl of the potassium-peroxodisulphate solution to 5 mL of the ABTS solution in a 15 mL screw cap tube. Mix well. Leave in the dark at room temperature for 16 hours before use.

4. Standard (Trolox also known as 6-Hydrox-2,5,7,8-tetramethylchroman-2-carboxylic acid):1.0 mM (Aldrich Cat nr.: 238831)
    a. Weigh 0.0125 g Trolox in a 50 mL screw cap tube and add 50 mL of Ethanol (Saarchem Cat Nr: 2233540LP). Mix until dissolved. Prepare fresh. Use this solution as the stock standard. (Check: When diluted 5x with ethanol this solution should give an absorbance of 0.650 ±0.015 at 289 nm.)

Protocol:

a) Ensure that the plate reader is set to read at 734 nm and the temperature is set at 25°C.

b) Thaw cells on ice for hour (during which make and plate standards)

c) Sonicate cells on ice (amp of 5 for 5 seconds x3 pulses with 20 second intervals).

d) Centrifuge cells at 4 degrees Celsius at 12000 rpm for 15 minutes. Transferred supernatants to labelled eppis

e) Preparation of standard series – Take 13 eppendorf tubes and label A-M. Add the amount of standard stock solution and diluents to each tube as described in the table below. Dilute the stock solution as follows to make a series of standards:

Tube	Trolox standard µl	Ethanol µl	Trolox conc. µM	Well number
A	0	1000	0	A1, B1, C1
B	0.5	999.5	0.5	A2, B2, C2

C	1	999	1	A3, B3, C3
D	1.5	998.5	1.5	A4, B4, C4
E	2.5	997.5	2.5	A5, B5, C5
F	5	995	5	A6, B6, C6
G	10	990	10	A7, B7, C7
H	15	985	15	A8, B8, C8
I	25	975	25	A9, B9, C9
J	50	950	50	A10, B10, C10
K	100	900	100	A11, B11, C11
L	150	850	150	A12, B12, C12
M	250	750	250	E1, F1, G1

f) Trolox standard wells – add 25 μl of standard per well in the designated wells in a clear well plate.

g) Control wells – add 25 μl of the control to the wells (standard A in wells A1. B1, C1).

h) Vector control -add 25 μl of PBS to wells E2, F2, G2

i) Sample wells – add 25 μl of sample IN TRIPLICATE to the wells (E4-11, F4-11, G4-11).

Sample 1 = Control (E4, F4, G4)
Sample 2 = 3 mg/day Flu (E5, F5, G5)
Sample 3 = 10 mg/day Flu (E6, F6, G6)
Sample 4 = 30 mg/day Flu (E7, F7, G7)
Sample 5 = Control + LPS (E8, F8, G8)
Sample 6 = 3 mg/day Flu + LPS (E9, F9, G9)
Sample 7 = 10 mg/day Flu + LPS (E10, F10, G10)
Sample 8 = 30 mg/day Flu + LPS (E11, F11, G11)

j) Dilute the ABTS mix solution with ethanol to read an absorbance of approximately 0.7 (±0.02) (Approximately 1 ml ABTS mix and 99 mL EtOH). Add 300 μl of this ABTS mix to each well using a multichannel pipette.

k) Leave the plate for 30 minutes at room temperature before taking a reading.

l) Run plate

Appendix D: Zebrafish model statistics

Table D.1: Toxicity screen; Two-way repeated measures ANOVA statistics with Bonferroni's multiple comparisons test for distance moved (mm) recorded after acute treatment with Fluanxol. See figure 4.8 A

Two-way RM ANOVA	Matching: Both factors				
Alpha	0,05				
Source of Variation	% of total variation	P value	P value summary	Significant?	
Row Factor	0,5536	0,0409	*	Yes	
Column Factor	5,008	0,8764	ns	No	
Interaction: Row Factor x Column Factor	2,07	0,7465	ns	No	
Interaction: Row Factor x Subjects	1,18				
Interaction: Column Factor x Subjects	71,65				
Subjects	1,469				
ANOVA table	SS	DF	MS	F (DFn, DFd)	P value
Row Factor	91967	3	30656	F (3, 21) = 3,285	P=0,0409
Column Factor	832041	9	92449	F (9, 63) = 0,4893	P=0,8764
Interaction: Row Factor x Column Factor	343867	27	12736	F (27, 189) = 0,8017	P=0,7465
Interaction: Row Factor x Subjects	195960	21	9331		
Interaction: Column Factor x Subjects	11903392	63	188943		
Subjects	243975	7	34854		
Residual	3002526	189	15886		

Bonferroni's multiple comparisons test	**Mean Diff,**	**95,00% CI of diff,**	**Significant?**	**Summary**	**Adjusted P Value**			
10-15 min								
Control vs. 0.25uM Fluanxol	31,21	-145,6 to 208	No	ns	>0,9999			
Control vs. 0.49uM Fluanxol	95,16	-81,62 to 271,9	No	ns	>0,9999			
Control vs. 0.99uM Fluanxol	52,75	-124 to 229,5	No	ns	>0,9999			
Control vs. 1.97uM Fluanxol	-6,834	-183,6 to 169,9	No	ns	>0,9999			
Control vs. 3.94uM Fluanxol	97,89	-78,89 to 274,7	No	ns	>0,9999			

Control vs. 6.16uM Fluanxol	96	-80,78 to 272,8	No	ns	>0,9999			
Control vs. 12.32uM Fluanxol	123,1	-53,64 to 299,9	No	ns	0,4696			
Control vs. 24.63uM Fluanxol	22,88	-153,9 to 199,7	No	ns	>0,9999			
Control vs. 49.27uM Fluanxol	32,99	-143,8 to 209,8	No	ns	>0,9999			
15-20 min								
Control vs. 0.25uM Fluanxol	-6,059	-182,8 to 170,7	No	ns	>0,9999			
Control vs. 0.49uM Fluanxol	69,29	-107,5 to 246,1	No	ns	>0,9999			
Control vs. 0.99uM Fluanxol	63,53	-113,3 to 240,3	No	ns	>0,9999			
Control vs. 1.97uM Fluanxol	-105,6	-282,4 to 71,14	No	ns	0,8581			
Control vs. 3.94uM Fluanxol	54,38	-122,4 to 231,2	No	ns	>0,9999			
Control vs. 6.16uM Fluanxol	87,88	-88,9 to 264,7	No	ns	>0,9999			
Control vs. 12.32uM Fluanxol	19,86	-156,9 to 196,6	No	ns	>0,9999			
Control vs. 24.63uM Fluanxol	7,842	-168,9 to 184,6	No	ns	>0,9999			
Control vs. 49.27uM Fluanxol	-75,96	-252,7 to 100,8	No	ns	>0,9999			
20-25 min								
Control vs. 0.25uM Fluanxol	-37,08	-213,9 to 139,7	No	ns	>0,9999			
Control vs. 0.49uM Fluanxol	4,365	-172,4 to 181,1	No	ns	>0,9999			
Control vs. 0.99uM Fluanxol	-37,61	-214,4 to 139,2	No	ns	>0,9999			
Control vs. 1.97uM Fluanxol	-188,8	-365,5 to -11,98	Yes	*	0,028			
Control vs. 3.94uM Fluanxol	-12,83	-189,6 to 163,9	No	ns	>0,9999			
Control vs. 6.16uM Fluanxol	-7,005	-183,8 to 169,8	No	ns	>0,9999			
Control vs. 12.32uM Fluanxol	-117,8	-294,6 to 58,93	No	ns	0,5672			

Control vs. 24.63uM Fluanxol	-74	-250,8 to 102,8	No	ns	>0,9999			
Control vs. 49.27uM Fluanxol	-135,1	-311,9 to 41,69	No	ns	0,3001			
25-30 min								
Control vs. 0.25uM Fluanxol	-25,69	-202,5 to 151,1	No	ns	>0,9999			
Control vs. 0.49uM Fluanxol	-46,97	-223,7 to 129,8	No	ns	>0,9999			
Control vs. 0.99uM Fluanxol	-79,82	-256,6 to 96,96	No	ns	>0,9999			
Control vs. 1.97uM Fluanxol	-171,5	-348,2 to 5,323	No	ns	0,0641			
Control vs. 3.94uM Fluanxol	-14,62	-191,4 to 162,2	No	ns	>0,9999			
Control vs. 6.16uM Fluanxol	2,135	-174,6 to 178,9	No	ns	>0,9999			
Control vs. 12.32uM Fluanxol	-68	-244,8 to 108,8	No	ns	>0,9999			
Control vs. 24.63uM Fluanxol	-208,8	-385,6 to -32,02	Yes	**	0,0099			
Control vs. 49.27uM Fluanxol	-161,3	-338,1 to 15,48	No	ns	0,1014			

Table D.2: Toxicity screen; Two-way repeated measures ANOVA statistics with Bonferroni's multiple comparisons test for distance moved (mm) recorded 3 hours after treatment with Fluanxol. See figure 4.8 B

Two-way RM ANOVA	Matching: Both factors				
Alpha	0,05				
Source of Variation	% of total variation	P value	P value summary	Significant?	
Row Factor	2,236	0,0005	***	Yes	
Column Factor	2,834	0,949	ns	No	
Interaction: Row Factor x Column Factor	4,168	0,5552	ns	No	
Interaction: Row Factor x Subjects	1,764				
Interaction: Column Factor x Subjects	54,87				
Subjects	3,073				
ANOVA table	SS	DF	MS	F (DFn, DFd)	P value
Row Factor	433999	3	144666	F (3, 21) = 8,871	P=0,0005

Column Factor	550037	9	61115	F (9, 63) = 0,3615	P=0,9490
Interaction: Row Factor x Column Factor	809092	27	29966	F (27, 189) = 0,9396	P=0,5552
Interaction: Row Factor x Subjects	342470	21	16308		
Interaction: Column Factor x Subjects	10651996	63	169079		
Subjects	596454	7	85208		
Residual	6027776	189	31893		

Bonferroni's multiple comparisons test	**Mean Diff,**	**95,00% CI of diff,**	**Significant?**	**Summary**	**Adjusted P Value**			
10-15 min								
Control vs. 0.25uM Fluanxol	-136,2	-386,7 to 114,3	No	ns	>0,9999			
Control vs. 0.49uM Fluanxol	-40,4	-290,9 to 210,1	No	ns	>0,9999			
Control vs. 0.99uM Fluanxol	-34,89	-285,4 to 215,6	No	ns	>0,9999			
Control vs. 1.97uM Fluanxol	-24,92	-275,4 to 225,6	No	ns	>0,9999			
Control vs. 3.94uM Fluanxol	-140,7	-391,1 to 109,8	No	ns	>0,9999			
Control vs. 6.16uM Fluanxol	57,51	-193 to 308	No	ns	>0,9999			
Control vs. 12.32uM Fluanxol	22,99	-227,5 to 273,5	No	ns	>0,9999			
Control vs. 24.63uM Fluanxol	59,58	-190,9 to 310,1	No	ns	>0,9999			
Control vs. 49.27uM Fluanxol	-28,84	-279,3 to 221,6	No	ns	>0,9999			
15-20 min								
Control vs. 0.25uM Fluanxol	-80,32	-330,8 to 170,2	No	ns	>0,9999			
Control vs. 0.49uM Fluanxol	-86,15	-336,6 to 164,3	No	ns	>0,9999			
Control vs. 0.99uM Fluanxol	-91,45	-341,9 to 159	No	ns	>0,9999			
Control vs. 1.97uM Fluanxol	-40,22	-290,7 to 210,3	No	ns	>0,9999			
Control vs. 3.94uM Fluanxol	-80,26	-330,7 to 170,2	No	ns	>0,9999			

Control vs. 6.16uM Fluanxol	42,03	-208,4 to 292,5	No	ns	>0,9999			
Control vs. 12.32uM Fluanxol	-135,9	-386,4 to 114,5	No	ns	>0,9999			
Control vs. 24.63uM Fluanxol	13,35	-237,1 to 263,8	No	ns	>0,9999			
Control vs. 49.27uM Fluanxol	12,95	-237,5 to 263,4	No	ns	>0,9999			
20-25 min								
Control vs. 0.25uM Fluanxol	-7,011	-257,5 to 243,5	No	ns	>0,9999			
Control vs. 0.49uM Fluanxol	-42,74	-293,2 to 207,7	No	ns	>0,9999			
Control vs. 0.99uM Fluanxol	-81,65	-332,1 to 168,8	No	ns	>0,9999			
Control vs. 1.97uM Fluanxol	-42,14	-292,6 to 208,3	No	ns	>0,9999			
Control vs. 3.94uM Fluanxol	-2,305	-252,8 to 248,2	No	ns	>0,9999			
Control vs. 6.16uM Fluanxol	65,54	-184,9 to 316	No	ns	>0,9999			
Control vs. 12.32uM Fluanxol	59,6	-190,9 to 310,1	No	ns	>0,9999			
Control vs. 24.63uM Fluanxol	-211,5	-462 to 38,98	No	ns	0,1698			
Control vs. 49.27uM Fluanxol	-10,25	-260,7 to 240,2	No	ns	>0,9999			
25-30 min								
Control vs. 0.25uM Fluanxol	-0,7631	-251,2 to 249,7	No	ns	>0,9999			
Control vs. 0.49uM Fluanxol	-47,34	-297,8 to 203,1	No	ns	>0,9999			
Control vs. 0.99uM Fluanxol	22,4	-228,1 to 272,9	No	ns	>0,9999			
Control vs. 1.97uM Fluanxol	33,79	-216,7 to 284,3	No	ns	>0,9999			
Control vs. 3.94uM Fluanxol	-88,42	-338,9 to 162,1	No	ns	>0,9999			
Control vs. 6.16uM Fluanxol	96,77	-153,7 to 347,2	No	ns	>0,9999			
Control vs. 12.32uM Fluanxol	86,49	-164 to 337	No	ns	>0,9999			

Control vs. 24.63uM Fluanxol	-93,58	-344,1 to 156,9	No	ns	>0,9999			
Control vs. 49.27uM Fluanxol	59,25	-191,2 to 309,7	No	ns	>0,9999			

Table D.3: Toxicity screen; Two-way repeated measures ANOVA statistics for distance moved (mm) recorded 9 hours after treatment with Fluanxol. See figure 4.8 C

Two-way RM ANOVA	Matching: Both factors				
Alpha	0,05				
Source of Variation	% of total variation	P value	P value summary	Significant?	
Row Factor	0,3008	0,5907	ns	No	
Column Factor	7,086	0,6631	ns	No	
Interaction: Row Factor x Column Factor	1,624	0,8612	ns	No	
Interaction: Row Factor x Subjects	3,231				
Interaction: Column Factor x Subjects	66,24				
Subjects	5,331				
ANOVA table	SS	DF	MS	F (DFn, DFd)	P value
Row Factor	35073	3	11691	F (3, 21) = 0,6518	P=0,5907
Column Factor	826165	9	91796	F (9, 63) = 0,7488	P=0,6631
Interaction: Row Factor x Column Factor	189296	27	7011	F (27, 189) = 0,7021	P=0,8612
Interaction: Row Factor x Subjects	376676	21	17937		
Interaction: Column Factor x Subjects	7723548	63	122596		
Subjects	621548	7	88793		
Residual	1887252	189	9985		

Table D.4: Toxicity screen; Two-way repeated measures ANOVA statistics for distance moved (mm) recorded 18 hours after treatment with Fluanxol. See figure 4.8 D

Two-way RM ANOVA	Matching: Both factors				
Alpha	0,05				
Source of Variation	% of total variation	P value	P value summary	Significant?	
Row Factor	0,6467	0,2734	ns	No	
Column Factor	6,429	0,6349	ns	No	

Interaction: Row Factor x Column Factor	4,541	0,0556	ns	No	
Interaction: Row Factor x Subjects	3,256				
Interaction: Column Factor x Subjects	57,66				
Subjects	6,614				
ANOVA table	SS	DF	MS	F (DFn, DFd)	P value
Row Factor	86530	3	28843	F (3, 21) = 1,39	P=0,2734
Column Factor	860174	9	95575	F (9, 63) = 0,7805	P=0,6349
Interaction: Row Factor x Column Factor	607561	27	22502	F (27, 189) = 1,524	P=0,0556
Interaction: Row Factor x Subjects	435651	21	20745		
Interaction: Column Factor x Subjects	7714149	63	122447		
Subjects	884876	7	126411		
Residual	2790590	189	14765		

Table D.5: Toxicity screen; Two-way repeated measures ANOVA statistics with Bonferroni's multiple comparisons test for velocity (mm/sec) recorded after acute treatment with Fluanxol. See figure 4.9 A

Two-way RM ANOVA	Matching: Both factors				
Alpha	0,05				
Source of Variation	% of total variation	P value	P value summary	Significant?	
Row Factor	0,5589	0,0397	*	Yes	
Column Factor	5,008	0,8764	ns	No	
Interaction: Row Factor x Column Factor	2,07	0,7463	ns	No	
Interaction: Row Factor x Subjects	1,179				
Interaction: Column Factor x Subjects	71,64				
Subjects	1,468				
ANOVA table	SS	DF	MS	F (DFn, DFd)	P value
Row Factor	1,033	3	0,3442	F (3, 21) = 3,317	P=0,0397
Column Factor	9,254	9	1,028	F (9, 63) = 0,4893	P=0,8764
Interaction: Row Factor x Column Factor	3,825	27	0,1417	F (27, 189) = 0,8018	P=0,7463
Interaction: Row Factor x Subjects	2,179	21	0,1038		
Interaction: Column Factor x Subjects	132,4	63	2,101		

Subjects	2,713	7	0,3876		
Residual	33,39	189	0,1767		

Bonferroni's multiple comparisons test	**Mean Diff,**	**95,00% CI of diff,**	**Significant ?**	**Summary**	**Adjusted P Value**			
10-15 min								
Control vs. 0.25uM Fluanxol	0,104	-0,4855 to 0,6936	No	ns	>0,9999			
Control vs. 0.49uM Fluanxol	0,3173	-0,2722 to 0,9068	No	ns	>0,9999			
Control vs. 0.99uM Fluanxol	0,1759	-0,4137 to 0,7654	No	ns	>0,9999			
Control vs. 1.97uM Fluanxol	-0,02278	-0,6123 to 0,5668	No	ns	>0,9999			
Control vs. 3.94uM Fluanxol	0,3264	-0,2631 to 0,9159	No	ns	>0,9999			
Control vs. 6.16uM Fluanxol	0,3201	-0,2695 to 0,9096	No	ns	>0,9999			
Control vs. 12.32uM Fluanxol	0,4106	-0,179 to 1	No	ns	0,47			
Control vs. 24.63uM Fluanxol	0,0763	-0,5132 to 0,6658	No	ns	>0,9999			
Control vs. 49.27uM Fluanxol	0,11	-0,4795 to 0,6995	No	ns	>0,9999			
15-20 min								
Control vs. 0.25uM Fluanxol	-0,02021	-0,6097 to 0,5693	No	ns	>0,9999			
Control vs. 0.49uM Fluanxol	0,2311	-0,3584 to 0,8206	No	ns	>0,9999			
Control vs. 0.99uM Fluanxol	0,2119	-0,3777 to 0,8014	No	ns	>0,9999			
Control vs. 1.97uM Fluanxol	-0,3523	-0,9419 to 0,2372	No	ns	0,8578			
Control vs. 3.94uM Fluanxol	0,1814	-0,4082 to 0,7709	No	ns	>0,9999			
Control vs. 6.16uM Fluanxol	0,2931	-0,2964 to 0,8826	No	ns	>0,9999			
Control vs. 12.32uM Fluanxol	0,06625	-0,5233 to 0,6558	No	ns	>0,9999			
Control vs. 24.63uM Fluanxol	0,02615	-0,5634 to 0,6157	No	ns	>0,9999			

Control vs. 49.27uM Fluanxol	-0,2533	-0,8429 to 0,3362	No	ns	>0,9999			
20-25 min								
Control vs. 0.25uM Fluanxol	-0,1237	-0,7132 to 0,4659	No	ns	>0,9999			
Control vs. 0.49uM Fluanxol	0,01456	-0,575 to 0,6041	No	ns	>0,9999			
Control vs. 0.99uM Fluanxol	-0,1254	-0,715 to 0,4641	No	ns	>0,9999			
Control vs. 1.97uM Fluanxol	-0,6296	-1,219 to -0,04002	Yes	*	0,028			
Control vs. 3.94uM Fluanxol	-0,04279	-0,6323 to 0,5467	No	ns	>0,9999			
Control vs. 6.16uM Fluanxol	-0,02336	-0,6129 to 0,5662	No	ns	>0,9999			
Control vs. 12.32uM Fluanxol	-0,393	-0,9826 to 0,1965	No	ns	0,5671			
Control vs. 24.63uM Fluanxol	-0,2468	-0,8363 to 0,3427	No	ns	>0,9999			
Control vs. 49.27uM Fluanxol	-0,4505	-1,04 to 0,139	No	ns	0,3			
25-30 min								
Control vs. 0.25uM Fluanxol	-0,08569	-0,6752 to 0,5038	No	ns	>0,9999			
Control vs. 0.49uM Fluanxol	-0,1566	-0,7462 to 0,4329	No	ns	>0,9999			
Control vs. 0.99uM Fluanxol	-0,2662	-0,8557 to 0,3233	No	ns	>0,9999			
Control vs. 1.97uM Fluanxol	-0,5718	-1,161 to 0,01771	No	ns	0,0641			
Control vs. 3.94uM Fluanxol	-0,04877	-0,6383 to 0,5408	No	ns	>0,9999			
Control vs. 6.16uM Fluanxol	0,007121	-0,5824 to 0,5967	No	ns	>0,9999			
Control vs. 12.32uM Fluanxol	-0,2268	-0,8163 to 0,3628	No	ns	>0,9999			
Control vs. 24.63uM Fluanxol	-0,6964	-1,286 to -0,1068	Yes	**	0,0099			
Control vs. 49.27uM Fluanxol	-0,538	-1,127 to 0,05158	No	ns	0,1013			

Table D.6: Toxicity screen; Two-way repeated measures ANOVA statistics for velocity (mm/sec) recorded 3 hours after treatment with Fluanxol. See figure 4.9 B

Two-way RM ANOVA	Matching: Both factors				
Alpha	0,05				
Source of Variation	% of total variation	P value	P value summary	Significant?	
Row Factor	1,077	0,1575	ns	No	
Column Factor	4,399	0,6296	ns	No	
Interaction: Row Factor x Column Factor	5,995	0,4595	ns	No	
Interaction: Row Factor x Subjects	3,928				
Interaction: Column Factor x Subjects	39,15				
Subjects	3,836				
ANOVA table	SS	DF	MS	F (DFn, DFd)	P value
Row Factor	40,32	3	13,44	F (3, 21) = 1,918	P=0,1575
Column Factor	164,8	9	18,31	F (9, 63) = 0,7865	P=0,6296
Interaction: Row Factor x Column Factor	224,5	27	8,315	F (27, 189) = 1,008	P=0,4595
Interaction: Row Factor x Subjects	147,1	21	7,005		
Interaction: Column Factor x Subjects	1466	63	23,28		
Subjects	143,7	7	20,53		
Residual	1558	189	8,245		

Table D.7: Toxicity screen; Two-way repeated measures ANOVA statistics for velocity (mm/sec) recorded 9 hours after treatment with Fluanxol. See figure 4.9 C

Two-way RM ANOVA	Matching: Both factors				
Alpha	0,05				
Source of Variation	% of total variation	P value	P value summary	Significant?	
Row Factor	0,3027	0,5882	ns	No	
Column Factor	7,085	0,6632	ns	No	
Interaction: Row Factor x Column Factor	1,623	0,8613	ns	No	
Interaction: Row Factor x Subjects	3,23				
Interaction: Column Factor x Subjects	66,24				
Subjects	5,331				
ANOVA table	SS	DF	MS	F (DFn, DFd)	P value

Row Factor	0,3925	3	0,1308	F (3, 21) = 0,656	P=0,5882
Column Factor	9,188	9	1,021	F (9, 63) = 0,7487	P=0,6632
Interaction: Row Factor x Column Factor	2,105	27	0,07796	F (27, 189) = 0,702	P=0,8613
Interaction: Row Factor x Subjects	4,189	21	0,1995		
Interaction: Column Factor x Subjects	85,9	63	1,363		
Subjects	6,913	7	0,9875		
Residual	20,99	189	0,1111		

Table D.8: Toxicity screen; Two-way repeated measures ANOVA statistics with Bonferroni's multiple comparisons test for velocity (mm/sec) recorded 18 hours after treatment with Fluanxol. See figure 4.9 D

Two-way RM ANOVA	Matching: Both factors				
Alpha	0,05				
Source of Variation	% of total variation	P value	P value summary	Significant?	
Row Factor	0,004273	0,2281	ns	No	
Column Factor	10,94	0,4854	ns	No	
Interaction: Row Factor x Column Factor	0,03498	0,0229	*	Yes	
Interaction: Row Factor x Subjects	0,01914				
Interaction: Column Factor x Subjects	80,19				
Subjects	8,669				
ANOVA table	SS	DF	MS	F (DFn, DFd)	P value
Row Factor	1,29	3	0,43	F (3, 21) = 1,563	P=0,2281
Column Factor	3302	9	366,9	F (9, 63) = 0,9548	P=0,4854
Interaction: Row Factor x Column Factor	10,56	27	0,3912	F (27, 189) = 1,694	P=0,0229
Interaction: Row Factor x Subjects	5,778	21	0,2752		
Interaction: Column Factor x Subjects	24208	63	384,3		
Subjects	2617	7	373,9		
Residual	43,65	189	0,231		

Bonferroni's multiple comparisons test	Mean Diff,	95,00% CI of diff,	Significant?	Summary	Adjusted P Value			
10-15 min								
Control vs. 0.25uM Fluanxol	-11,29	-11,97 to -10,62	Yes	****	<0,0001			
Control vs. 0.49uM Fluanxol	0,2129	-0,4611 to 0,887	No	ns	>0,9999			
Control vs. 0.99uM Fluanxol	0,2659	-0,4082 to 0,94	No	ns	>0,9999			
Control vs. 1.97uM Fluanxol	-0,1005	-0,7746 to 0,5735	No	ns	>0,9999			
Control vs. 3.94uM Fluanxol	-0,4345	-1,109 to 0,2396	No	ns	0,6495			
Control vs. 6.16uM Fluanxol	-0,1821	-0,8561 to 0,492	No	ns	>0,9999			
Control vs. 12.32uM Fluanxol	-0,2673	-0,9414 to 0,4068	No	ns	>0,9999			
Control vs. 24.63uM Fluanxol	-0,1656	-0,8397 to 0,5085	No	ns	>0,9999			
Control vs. 49.27uM Fluanxol	-0,3332	-1,007 to 0,3408	No	ns	>0,9999			
15-20 min								
Control vs. 0.25uM Fluanxol	-10,89	-11,56 to -10,22	Yes	****	<0,0001			
Control vs. 0.49uM Fluanxol	-0,3016	-0,9756 to 0,3725	No	ns	>0,9999			
Control vs. 0.99uM Fluanxol	-0,07052	-0,7446 to 0,6036	No	ns	>0,9999			
Control vs. 1.97uM Fluanxol	-0,3119	-0,986 to 0,3622	No	ns	>0,9999			
Control vs. 3.94uM Fluanxol	-0,0921	-0,7662 to 0,582	No	ns	>0,9999			
Control vs. 6.16uM Fluanxol	-0,6639	-1,338 to 0,01019	No	ns	0,0567			
Control vs. 12.32uM Fluanxol	-0,4932	-1,167 to 0,1809	No	ns	0,3737			
Control vs. 24.63uM Fluanxol	-0,3842	-1,058 to 0,2899	No	ns	>0,9999			
Control vs. 49.27uM Fluanxol	-0,5678	-1,242 to 0,1063	No	ns	0,1724			
20-25 min								

Control vs. 0.25uM Fluanxol	-10,41	-11,08 to -9,735	Yes	****	<0,0001			
Control vs. 0.49uM Fluanxol	-0,5112	-1,185 to 0,1628	No	ns	0,3121			
Control vs. 0.99uM Fluanxol	-0,1096	-0,7837 to 0,5645	No	ns	>0,9999			
Control vs. 1.97uM Fluanxol	-0,1307	-0,8048 to 0,5433	No	ns	>0,9999			
Control vs. 3.94uM Fluanxol	0,2101	-0,464 to 0,8841	No	ns	>0,9999			
Control vs. 6.16uM Fluanxol	-0,5933	-1,267 to 0,08078	No	ns	0,1299			
Control vs. 12.32uM Fluanxol	-0,3688	-1,043 to 0,3052	No	ns	>0,9999			
Control vs. 24.63uM Fluanxol	-0,2645	-0,9386 to 0,4096	No	ns	>0,9999			
Control vs. 49.27uM Fluanxol	-0,5285	-1,203 to 0,1456	No	ns	0,2616			
25-30 min								
Control vs. 0.25uM Fluanxol	-10,86	-11,53 to -10,18	Yes	****	<0,0001			
Control vs. 0.49uM Fluanxol	-0,02011	-0,6942 to 0,654	No	ns	>0,9999			
Control vs. 0.99uM Fluanxol	0,3294	-0,3447 to 1,003	No	ns	>0,9999			
Control vs. 1.97uM Fluanxol	0,1427	-0,5314 to 0,8167	No	ns	>0,9999			
Control vs. 3.94uM Fluanxol	0,1895	-0,4845 to 0,8636	No	ns	>0,9999			
Control vs. 6.16uM Fluanxol	-0,404	-1,078 to 0,2701	No	ns	0,8493			
Control vs. 12.32uM Fluanxol	0,2415	-0,4325 to 0,9156	No	ns	>0,9999			
Control vs. 24.63uM Fluanxol	-0,146	-0,8201 to 0,528	No	ns	>0,9999			
Control vs. 49.27uM Fluanxol	-0,2434	-0,9174 to 0,4307	No	ns	>0,9999			

Table D.9: PTZ psychosis model; Two-way repeated measures ANOVA statistics with Bonferroni's multiple comparisons test for distance (mm) recorded after acute treatment with Fluanxol (See figure 4.10 A).

Two-way RM ANOVA	Matching: Both factors				
Alpha	0,05				

Source of Variation	% of total variation	P value	P value summary	Significant?	
Row Factor	5,681	<0,0001	****	Yes	
Column Factor	31,59	<0,0001	****	Yes	
Interaction: Row Factor x Column Factor	8,325	<0,0001	****	Yes	
Interaction: Row Factor x Subjects	3,822				
Interaction: Column Factor x Subjects	25				
Subjects	4,698				
ANOVA table	SS	DF	MS	F (DFn, DFd)	P value
Row Factor	2686850	5	537370	F (5, 35) = 10,4	P<0,0001
Column Factor	14940217	10	1494022	F (10, 70) = 8,845	P<0,0001
Interaction: Row Factor x Column Factor	3937098	50	78742	F (50, 350) = 2,79	P<0,0001
Interaction: Row Factor x Subjects	1807716	35	51649		
Interaction: Column Factor x Subjects	11824214	70	168917		
Subjects	2221802	7	317400		
Residual	9877207	350	28221		

Bonferroni's multiple comparisons test	**Mean Diff,**	**95,00% CI of diff,**	**Significant?**	**Summary**	**Adjusted P Value**
10-15 min					
Control vs. PTZ	-224,8	-462,1 to 12,48	No	ns	0,0779
Control vs. Diazepam	-138	-375,2 to 99,32	No	ns	>0,9999
Control vs. 0.3uM Fluanxol	-185,5	-422,7 to 51,83	No	ns	0,279
Control vs. 0.6uM Fluanxol	-243,9	-481,2 to -6,626	Yes	*	0,0392
Control vs. 1.2uM Fluanxol	-260,7	-498 to -23,42	Yes	*	0,0207
Control vs. 2.5uM Fluanxol	-205,3	-442,5 to 32,02	No	ns	0,1503
Control vs. 5uM Fluanxol	-191,7	-429 to 45,58	No	ns	0,2307
Control vs. 10uM Fluanxol	-201,1	-438,4 to 36,18	No	ns	0,1718
Control vs. 25uM Fluanxol	-31,71	-269 to 205,6	No	ns	>0,9999
Control vs. 50uM Fluanxol	-60,45	-297,7 to 176,8	No	ns	>0,9999
15-20 min					
Control vs. PTZ	-333,2	-570,5 to -95,95	Yes	***	0,0009
Control vs. Diazepam	-183,3	-420,6 to 53,96	No	ns	0,2973

Control vs. 0.3uM Fluanxol	-248,6	-485,9 to -11,35	Yes	*	0,0329
Control vs. 0.6uM Fluanxol	-361	-598,3 to -123,8	Yes	***	0,0002
Control vs. 1.2uM Fluanxol	-357,5	-594,8 to -120,3	Yes	***	0,0003
Control vs. 2.5uM Fluanxol	-241,5	-478,7 to -4,186	Yes	*	0,0429
Control vs. 5uM Fluanxol	-267,2	-504,5 to -29,93	Yes	*	0,016
Control vs. 10uM Fluanxol	-188,3	-425,6 to 48,99	No	ns	0,2561
Control vs. 25uM Fluanxol	-101,6	-338,9 to 135,7	No	ns	>0,9999
Control vs. 50uM Fluanxol	-119	-356,3 to 118,3	No	ns	>0,9999
20-25 min					
Control vs. PTZ	-441,7	-678,9 to -204,4	Yes	****	<0,0001
Control vs. Diazepam	-177,9	-415,2 to 59,36	No	ns	0,3486
Control vs. 0.3uM Fluanxol	-467	-704,3 to -229,7	Yes	****	<0,0001
Control vs. 0.6uM Fluanxol	-410,4	-647,6 to -173,1	Yes	****	<0,0001
Control vs. 1.2uM Fluanxol	-533,5	-770,8 to -296,2	Yes	****	<0,0001
Control vs. 2.5uM Fluanxol	-264,7	-502 to -27,39	Yes	*	0,0177
Control vs. 5uM Fluanxol	-407,7	-644,9 to -170,4	Yes	****	<0,0001
Control vs. 10uM Fluanxol	-270,4	-507,7 to -33,11	Yes	*	0,0141
Control vs. 25uM Fluanxol	-215,1	-452,4 to 22,17	No	ns	0,1086
Control vs. 50uM Fluanxol	-220,7	-458 to 16,57	No	ns	0,0898
25-30 min					
Control vs. PTZ	-500,5	-737,7 to -263,2	Yes	****	<0,0001
Control vs. Diazepam	-69,82	-307,1 to 167,5	No	ns	>0,9999
Control vs. 0.3uM Fluanxol	-526,3	-763,6 to -289	Yes	****	<0,0001
Control vs. 0.6uM Fluanxol	-394,1	-631,4 to -156,8	Yes	****	<0,0001
Control vs. 1.2uM Fluanxol	-513,3	-750,5 to -276	Yes	****	<0,0001
Control vs. 2.5uM Fluanxol	-288,8	-526 to -51,49	Yes	**	0,0066
Control vs. 5uM Fluanxol	-423	-660,3 to -185,7	Yes	****	<0,0001
Control vs. 10uM Fluanxol	-286,9	-524,2 to -49,6	Yes	**	0,0071
Control vs. 25uM Fluanxol	-253,7	-491 to -16,47	Yes	*	0,027

Control vs. 50uM Fluanxol	-277,7	-515 to -40,46	Yes	*	0,0104
30-35 min					
Control vs. PTZ	-791,9	-1029 to -554,6	Yes	****	<0,0001
Control vs. Diazepam	-166,8	-404,1 to 70,47	No	ns	0,4782
Control vs. 0.3uM Fluanxol	-763,2	-1000 to -525,9	Yes	****	<0,0001
Control vs. 0.6uM Fluanxol	-687,4	-924,7 to -450,1	Yes	****	<0,0001
Control vs. 1.2uM Fluanxol	-738,3	-975,6 to -501	Yes	****	<0,0001
Control vs. 2.5uM Fluanxol	-435,8	-673 to -198,5	Yes	****	<0,0001
Control vs. 5uM Fluanxol	-767,1	-1004 to -529,8	Yes	****	<0,0001
Control vs. 10uM Fluanxol	-551,1	-788,4 to -313,8	Yes	****	<0,0001
Control vs. 25uM Fluanxol	-420,5	-657,8 to -183,2	Yes	****	<0,0001
Control vs. 50uM Fluanxol	-444,5	-681,8 to -207,2	Yes	****	<0,0001
35-40 min					
Control vs. PTZ	-909	-1146 to -671,7	Yes	****	<0,0001
Control vs. Diazepam	-180,8	-418,1 to 56,45	No	ns	0,3201
Control vs. 0.3uM Fluanxol	-844,9	-1082 to -607,6	Yes	****	<0,0001
Control vs. 0.6uM Fluanxol	-796,7	-1034 to -559,5	Yes	****	<0,0001
Control vs. 1.2uM Fluanxol	-889,6	-1127 to -652,3	Yes	****	<0,0001
Control vs. 2.5uM Fluanxol	-697,5	-934,8 to -460,2	Yes	****	<0,0001
Control vs. 5uM Fluanxol	-820,6	-1058 to -583,3	Yes	****	<0,0001
Control vs. 10uM Fluanxol	-606,1	-843,4 to -368,8	Yes	****	<0,0001
Control vs. 25uM Fluanxol	-430,7	-668 to -193,4	Yes	****	<0,0001
Control vs. 50uM Fluanxol	-480,8	-718,1 to -243,5	Yes	****	<0,0001

Table D.10: PTZ psychosis model; Two-way repeated measures ANOVA statistics with Bonferroni's multiple comparisons test for velocity (mm/sec) recorded after acute treatment with Fluanxol (See figure 4.10 B).

Table Analyzed	PTZ acute v				
Two-way RM ANOVA	Matching: Both factors				
Alpha	0,05				
Source of Variation	% of total variation	P value	P value summary	Significant?	
Row Factor	5,676	<0,0001	****	Yes	
Column Factor	31,59	<0,0001	****	Yes	

Interaction: Row Factor x Column Factor	8,324	<0,0001	****	Yes	
Interaction: Row Factor x Subjects	3,822				
Interaction: Column Factor x Subjects	25				
Subjects	4,698				
ANOVA table	SS	DF	MS	F (DFn, DFd)	P value
Row Factor	29,85	5	5,97	F (5, 35) = 10,39	P<0,0001
Column Factor	166,1	10	16,61	F (10, 70) = 8,844	P<0,0001
Interaction: Row Factor x Column Factor	43,78	50	0,8755	F (50, 350) = 2,79	P<0,0001
Interaction: Row Factor x Subjects	20,1	35	0,5743		
Interaction: Column Factor x Subjects	131,5	70	1,879		
Subjects	24,71	7	3,53		
Residual	109,8	350	0,3138		

Bonferroni's multiple comparisons test	**Mean Diff,**	**95,00% CI of diff,**	**Significant?**	**Summary**	**Adjusted P Value**
10-15 min					
Control vs. PTZ	-0,7495	-1,541 to 0,04174	No	ns	0,078
Control vs. Diazepam	-0,46	-1,251 to 0,3313	No	ns	>0,9999
Control vs. 0.3uM Fluanxol	-0,6183	-1,41 to 0,1729	No	ns	0,2792
Control vs. 0.6uM Fluanxol	-0,8132	-1,605 to -0,02197	Yes	*	0,0393
Control vs. 1.2uM Fluanxol	-0,8692	-1,661 to -0,07796	Yes	*	0,0207
Control vs. 2.5uM Fluanxol	-0,6844	-1,476 to 0,1069	No	ns	0,1505
Control vs. 5uM Fluanxol	-0,6392	-1,43 to 0,1521	No	ns	0,2309
Control vs. 10uM Fluanxol	-0,6705	-1,462 to 0,1208	No	ns	0,172
Control vs. 25uM Fluanxol	-0,1057	-0,897 to 0,6855	No	ns	>0,9999
Control vs. 50uM Fluanxol	-0,2016	-0,9928 to 0,5897	No	ns	>0,9999
15-20 min					
Control vs. PTZ	-1,111	-1,903 to -0,3201	Yes	***	0,0009
Control vs. Diazepam	-0,6114	-1,403 to 0,1799	No	ns	0,2971
Control vs. 0.3uM Fluanxol	-0,8292	-1,62 to -0,03794	Yes	*	0,0328
Control vs. 0.6uM Fluanxol	-1,204	-1,995 to -0,4128	Yes	***	0,0002
Control vs. 1.2uM Fluanxol	-1,192	-1,984 to -0,4012	Yes	***	0,0003

Control vs. 2.5uM Fluanxol	-0,8053	-1,597 to -0,01405	Yes	*	0,0429
Control vs. 5uM Fluanxol	-0,8912	-1,682 to -0,09991	Yes	*	0,016
Control vs. 10uM Fluanxol	-0,628	-1,419 to 0,1633	No	ns	0,2559
Control vs. 25uM Fluanxol	-0,3389	-1,13 to 0,4523	No	ns	>0,9999
Control vs. 50uM Fluanxol	-0,3969	-1,188 to 0,3944	No	ns	>0,9999
20-25 min					
Control vs. PTZ	-1,473	-2,264 to -0,6817	Yes	****	<0,0001
Control vs. Diazepam	-0,5934	-1,385 to 0,1979	No	ns	0,3484
Control vs. 0.3uM Fluanxol	-1,558	-2,349 to -0,7663	Yes	****	<0,0001
Control vs. 0.6uM Fluanxol	-1,369	-2,16 to -0,5773	Yes	****	<0,0001
Control vs. 1.2uM Fluanxol	-1,779	-2,571 to -0,988	Yes	****	<0,0001
Control vs. 2.5uM Fluanxol	-0,8827	-1,674 to -0,09143	Yes	*	0,0177
Control vs. 5uM Fluanxol	-1,36	-2,151 to -0,5683	Yes	****	<0,0001
Control vs. 10uM Fluanxol	-0,9018	-1,693 to -0,1105	Yes	*	0,014
Control vs. 25uM Fluanxol	-0,7174	-1,509 to 0,07386	No	ns	0,1085
Control vs. 50uM Fluanxol	-0,7361	-1,527 to 0,05518	No	ns	0,0897
25-30 min					
Control vs. PTZ	-1,669	-2,46 to -0,8778	Yes	****	<0,0001
Control vs. Diazepam	-0,2329	-1,024 to 0,5584	No	ns	>0,9999
Control vs. 0.3uM Fluanxol	-1,755	-2,547 to -0,964	Yes	****	<0,0001
Control vs. 0.6uM Fluanxol	-1,314	-2,106 to -0,5231	Yes	****	<0,0001
Control vs. 1.2uM Fluanxol	-1,712	-2,503 to -0,9205	Yes	****	<0,0001
Control vs. 2.5uM Fluanxol	-0,9631	-1,754 to -0,1718	Yes	**	0,0066
Control vs. 5uM Fluanxol	-1,411	-2,202 to -0,6195	Yes	****	<0,0001
Control vs. 10uM Fluanxol	-0,9568	-1,748 to -0,1655	Yes	**	0,0071
Control vs. 25uM Fluanxol	-0,8463	-1,638 to -0,055	Yes	*	0,027
Control vs. 50uM Fluanxol	-0,9263	-1,718 to -0,135	Yes	*	0,0104
30-35 min					
Control vs. PTZ	-2,641	-3,432 to -1,85	Yes	****	<0,0001
Control vs. Diazepam	-0,5563	-1,348 to 0,235	No	ns	0,478
Control vs. 0.3uM Fluanxol	-2,545	-3,337 to -1,754	Yes	****	<0,0001
Control vs. 0.6uM Fluanxol	-2,293	-3,084 to -1,501	Yes	****	<0,0001
Control vs. 1.2uM Fluanxol	-2,462	-3,254 to -1,671	Yes	****	<0,0001
Control vs. 2.5uM Fluanxol	-1,453	-2,245 to -0,662	Yes	****	<0,0001
Control vs. 5uM Fluanxol	-2,558	-3,35 to -1,767	Yes	****	<0,0001
Control vs. 10uM Fluanxol	-1,838	-2,629 to -1,047	Yes	****	<0,0001

Control vs. 25uM Fluanxol	-1,402	-2,194 to -0,6112	Yes	****	<0,0001
Control vs. 50uM Fluanxol	-1,482	-2,274 to -0,6912	Yes	****	<0,0001
35-40 min					
Control vs. PTZ	-3,031	-3,822 to -2,24	Yes	****	<0,0001
Control vs. Diazepam	-0,6029	-1,394 to 0,1884	No	ns	0,3204
Control vs. 0.3uM Fluanxol	-2,817	-3,608 to -2,026	Yes	****	<0,0001
Control vs. 0.6uM Fluanxol	-2,656	-3,448 to -1,865	Yes	****	<0,0001
Control vs. 1.2uM Fluanxol	-2,966	-3,757 to -2,175	Yes	****	<0,0001
Control vs. 2.5uM Fluanxol	-2,326	-3,117 to -1,534	Yes	****	<0,0001
Control vs. 5uM Fluanxol	-2,736	-3,527 to -1,945	Yes	****	<0,0001
Control vs. 10uM Fluanxol	-2,021	-2,812 to -1,23	Yes	****	<0,0001
Control vs. 25uM Fluanxol	-1,436	-2,227 to -0,6448	Yes	****	<0,0001
Control vs. 50uM Fluanxol	-1,603	-2,394 to -0,8119	Yes	****	<0,0001

Table D.11: PTZ psychosis model; Two-way repeated measures ANOVA statistics with Bonferroni's multiple comparisons test for distance (mm) recorded 18 hours after treatment with Fluanxol (See figure 4.11 A).

Two-way RM ANOVA	Matching: Both factors				
Alpha	0,05				
Source of Variation	% of total variation	P value	P value summary	Significant?	
Row Factor	1,576	<0,0001	****	Yes	
Column Factor	44,75	<0,0001	****	Yes	
Interaction: Row Factor x Column Factor	5,21	0,0005	***	Yes	
Interaction: Row Factor x Subjects	1,517				
Interaction: Column Factor x Subjects	26,33				
Subjects	1,489				
ANOVA table	SS	DF	MS	F (DFn, DFd)	P value
Row Factor	1052641	5	210528	F (5, 35) = 7,27	P<0,0001
Column Factor	29890212	10	2989021	F (10, 70) = 11,9	P<0,0001
Interaction: Row Factor x Column Factor	3480237	50	69605	F (50, 350) = 1,906	P=0,0005
Interaction: Row Factor x Subjects	1013601	35	28960		
Interaction: Column Factor x Subjects	17584786	70	251211		
Subjects	994791	7	142113		
Residual	12778366	350	36510		

Bonferroni's multiple comparisons test	Mean Diff,	95,00% CI of diff,	Significant?	Summary	Adjusted P Value
10-15 min					
Control vs. PTZ	-262,8	-532,7 to 7,073	No	ns	0,0625
Control vs. Diazepam	179,3	-90,54 to 449,2	No	ns	0,6131
Control vs. 0.3uM Fluanxol	38,64	-231,2 to 308,5	No	ns	>0,9999
Control vs. 0.6uM Fluanxol	-199,3	-469,2 to 70,59	No	ns	0,3769
Control vs. 1.2uM Fluanxol	10,49	-259,4 to 280,4	No	ns	>0,9999
Control vs. 2.5uM Fluanxol	-150,7	-420,6 to 119,2	No	ns	>0,9999
Control vs. 5uM Fluanxol	-192,7	-462,6 to 77,22	No	ns	0,4449
Control vs. 10uM Fluanxol	-382,1	-652 to -112,3	Yes	***	0,0008
Control vs. 25uM Fluanxol	205,2	-64,68 to 475,1	No	ns	0,324
Control vs. 50uM Fluanxol	305,5	35,58 to 575,4	Yes	*	0,0151
15-20 min					
Control vs. PTZ	-450	-719,9 to -180,1	Yes	****	<0,0001
Control vs. Diazepam	-83,37	-353,3 to 186,5	No	ns	>0,9999
Control vs. 0.3uM Fluanxol	-157,4	-427,3 to 112,5	No	ns	>0,9999
Control vs. 0.6uM Fluanxol	-372	-641,8 to -102,1	Yes	**	0,0012
Control vs. 1.2uM Fluanxol	-217	-486,9 to 52,88	No	ns	0,2372
Control vs. 2.5uM Fluanxol	-334,2	-604,1 to -64,32	Yes	**	0,0053
Control vs. 5uM Fluanxol	-452,8	-722,7 to -183	Yes	****	<0,0001
Control vs. 10uM Fluanxol	-430,5	-700,4 to -160,7	Yes	****	<0,0001
Control vs. 25uM Fluanxol	76,55	-193,3 to 346,4	No	ns	>0,9999
Control vs. 50uM Fluanxol	91,24	-178,6 to 361,1	No	ns	>0,9999
20-25 min					
Control vs. PTZ	-625,2	-895,1 to -355,4	Yes	****	<0,0001
Control vs. Diazepam	-129,8	-399,6 to 140,1	No	ns	>0,9999
Control vs. 0.3uM Fluanxol	-47,66	-317,6 to 222,2	No	ns	>0,9999
Control vs. 0.6uM Fluanxol	-470,4	-740,3 to -200,5	Yes	****	<0,0001

Control vs. 1.2uM Fluanxol	-293,8	-563,7 to -23,93	Yes	*	0,0227
Control vs. 2.5uM Fluanxol	-389,8	-659,7 to -119,9	Yes	***	0,0006
Control vs. 5uM Fluanxol	-432,1	-702 to -162,2	Yes	****	<0,0001
Control vs. 10uM Fluanxol	-435,9	-705,7 to -166	Yes	****	<0,0001
Control vs. 25uM Fluanxol	91,63	-178,3 to 361,5	No	ns	>0,9999
Control vs. 50uM Fluanxol	18,08	-251,8 to 288	No	ns	>0,9999
25-30 min					
Control vs. PTZ	-776,2	-1046 to -506,3	Yes	****	<0,0001
Control vs. Diazepam	-190,4	-460,3 to 79,49	No	ns	0,4705
Control vs. 0.3uM Fluanxol	-187	-456,9 to 82,87	No	ns	0,5107
Control vs. 0.6uM Fluanxol	-528,8	-798,7 to -258,9	Yes	****	<0,0001
Control vs. 1.2uM Fluanxol	-227,8	-497,7 to 42,04	No	ns	0,1761
Control vs. 2.5uM Fluanxol	-480,7	-750,6 to -210,8	Yes	****	<0,0001
Control vs. 5uM Fluanxol	-475,2	-745,1 to -205,3	Yes	****	<0,0001
Control vs. 10uM Fluanxol	-442,8	-712,7 to -172,9	Yes	****	<0,0001
Control vs. 25uM Fluanxol	53,8	-216,1 to 323,7	No	ns	>0,9999
Control vs. 50uM Fluanxol	-23,6	-293,5 to 246,3	No	ns	>0,9999
30-35 min					
Control vs. PTZ	-872,2	-1142 to -602,3	Yes	****	<0,0001
Control vs. Diazepam	-167,5	-437,4 to 102,4	No	ns	0,805
Control vs. 0.3uM Fluanxol	-380,9	-650,8 to -111	Yes	***	0,0008
Control vs. 0.6uM Fluanxol	-562,3	-832,2 to -292,4	Yes	****	<0,0001
Control vs. 1.2uM Fluanxol	-457	-726,9 to -187,1	Yes	****	<0,0001
Control vs. 2.5uM Fluanxol	-702,6	-972,5 to -432,7	Yes	****	<0,0001
Control vs. 5uM Fluanxol	-572,4	-842,3 to -302,5	Yes	****	<0,0001
Control vs. 10uM Fluanxol	-517,2	-787 to -247,3	Yes	****	<0,0001
Control vs. 25uM Fluanxol	-4,7	-274,6 to 265,2	No	ns	>0,9999
Control vs. 50uM Fluanxol	-63,21	-333,1 to 206,7	No	ns	>0,9999

35-40 min					
Control vs. PTZ	-939	-1209 to -669,1	Yes	****	<0,0001
Control vs. Diazepam	-112,2	-382,1 to 157,7	No	ns	>0,9999
Control vs. 0.3uM Fluanxol	-419,9	-689,8 to -150	Yes	***	0,0001
Control vs. 0.6uM Fluanxol	-509,4	-779,3 to -239,5	Yes	****	<0,0001
Control vs. 1.2uM Fluanxol	-519	-788,9 to -249,1	Yes	****	<0,0001
Control vs. 2.5uM Fluanxol	-724,5	-994,4 to -454,6	Yes	****	<0,0001
Control vs. 5uM Fluanxol	-486,4	-756,3 to -216,5	Yes	****	<0,0001
Control vs. 10uM Fluanxol	-434,7	-704,6 to -164,8	Yes	****	<0,0001
Control vs. 25uM Fluanxol	77,89	-192 to 347,8	No	ns	>0,9999
Control vs. 50uM Fluanxol	86,64	-183,2 to 356,5	No	ns	>0,9999

Table D.12: PTZ psychosis model; Two-way repeated measures ANOVA statistics with Bonferroni's multiple comparisons test for velocity (mm/sec) recorded 18 hours after treatment with Fluanxol (See figure 4.11 B).

Two-way RM ANOVA	Matching: Both factors				
Alpha	0,05				
Source of Variation	% of total variation	P value	P value summary	Significant?	
Row Factor	1,574	<0,0001	****	Yes	
Column Factor	44,75	<0,0001	****	Yes	
Interaction: Row Factor x Column Factor	5,21	0,0005	***	Yes	
Interaction: Row Factor x Subjects	1,518				
Interaction: Column Factor x Subjects	26,33				
Subjects	1,489				
ANOVA table	SS	DF	MS	F (DFn, DFd)	P value
Row Factor	11,69	5	2,338	F (5, 35) = 7,26	P<0,0001
Column Factor	332,4	10	33,24	F (10, 70) = 11,9	P<0,0001
Interaction: Row Factor x Column Factor	38,7	50	0,7741	F (50, 350) = 1,906	P=0,0005
Interaction: Row Factor x Subjects	11,27	35	0,3221		
Interaction: Column Factor x Subjects	195,6	70	2,794		
Subjects	11,06	7	1,581		

Residual	142,1	350	0,406		

Bonferroni's multiple comparisons test	**Mean Diff,**	**95,00% CI of diff,**	**Significant?**	**Summary**	**Adjusted P Value**
10-15 min					
Control vs. PTZ	-0,8765	-1,777 to 0,02354	No	ns	0,0625
Control vs. Diazepam	0,5981	-0,3019 to 1,498	No	ns	0,613
Control vs. 0.3uM Fluanxol	0,1289	-0,7712 to 1,029	No	ns	>0,9999
Control vs. 0.6uM Fluanxol	-0,6647	-1,565 to 0,2354	No	ns	0,3768
Control vs. 1.2uM Fluanxol	0,035	-0,8651 to 0,935	No	ns	>0,9999
Control vs. 2.5uM Fluanxol	-0,5027	-1,403 to 0,3974	No	ns	>0,9999
Control vs. 5uM Fluanxol	-0,6426	-1,543 to 0,2575	No	ns	0,4448
Control vs. 10uM Fluanxol	-1,275	-2,175 to -0,3745	Yes	***	0,0008
Control vs. 25uM Fluanxol	0,6844	-0,2157 to 1,584	No	ns	0,324
Control vs. 50uM Fluanxol	1,019	0,1187 to 1,919	Yes	*	0,0151
15-20 min					
Control vs. PTZ	-1,501	-2,401 to -0,6008	Yes	****	<0,0001
Control vs. Diazepam	-0,278	-1,178 to 0,622	No	ns	>0,9999
Control vs. 0.3uM Fluanxol	-0,5248	-1,425 to 0,3752	No	ns	>0,9999
Control vs. 0.6uM Fluanxol	-1,24	-2,141 to -0,3404	Yes	**	0,0012
Control vs. 1.2uM Fluanxol	-0,7238	-1,624 to 0,1763	No	ns	0,2372
Control vs. 2.5uM Fluanxol	-1,115	-2,015 to -0,2146	Yes	**	0,0053
Control vs. 5uM Fluanxol	-1,51	-2,41 to -0,6102	Yes	****	<0,0001
Control vs. 10uM Fluanxol	-1,436	-2,336 to -0,5358	Yes	****	<0,0001
Control vs. 25uM Fluanxol	0,2553	-0,6447 to 1,155	No	ns	>0,9999
Control vs. 50uM Fluanxol	0,3043	-0,5958 to 1,204	No	ns	>0,9999
20-25 min					
Control vs. PTZ	-2,085	-2,985 to -1,185	Yes	****	<0,0001
Control vs. Diazepam	-0,4327	-1,333 to 0,4673	No	ns	>0,9999
Control vs. 0.3uM Fluanxol	-0,159	-1,059 to 0,7411	No	ns	>0,9999
Control vs. 0.6uM Fluanxol	-1,569	-2,469 to -0,6687	Yes	****	<0,0001
Control vs. 1.2uM Fluanxol	-0,9799	-1,88 to -0,07985	Yes	*	0,0227
Control vs. 2.5uM Fluanxol	-1,3	-2,2 to -0,3999	Yes	***	0,0006
Control vs. 5uM Fluanxol	-1,441	-2,341 to -0,5409	Yes	****	<0,0001
Control vs. 10uM Fluanxol	-1,454	-2,354 to -0,5536	Yes	****	<0,0001
Control vs. 25uM Fluanxol	0,3056	-0,5945 to 1,206	No	ns	>0,9999

Control vs. 50uM Fluanxol	0,0603	-0,8398 to 0,9604	No	ns	>0,9999
25-30 min					
Control vs. PTZ	-2,589	-3,489 to -1,689	Yes	****	<0,0001
Control vs. Diazepam	-0,635	-1,535 to 0,265	No	ns	0,4703
Control vs. 0.3uM Fluanxol	-0,6237	-1,524 to 0,2763	No	ns	0,5106
Control vs. 0.6uM Fluanxol	-1,764	-2,664 to -0,8635	Yes	****	<0,0001
Control vs. 1.2uM Fluanxol	-0,7599	-1,66 to 0,1402	No	ns	0,1761
Control vs. 2.5uM Fluanxol	-1,603	-2,503 to -0,7031	Yes	****	<0,0001
Control vs. 5uM Fluanxol	-1,585	-2,485 to -0,6848	Yes	****	<0,0001
Control vs. 10uM Fluanxol	-1,477	-2,377 to -0,5766	Yes	****	<0,0001
Control vs. 25uM Fluanxol	0,1794	-0,7206 to 1,079	No	ns	>0,9999
Control vs. 50uM Fluanxol	-0,07873	-0,9788 to 0,8213	No	ns	>0,9999
30-35 min					
Control vs. PTZ	-2,908	-3,808 to -2,008	Yes	****	<0,0001
Control vs. Diazepam	-0,5584	-1,458 to 0,3417	No	ns	0,8056
Control vs. 0.3uM Fluanxol	-1,27	-2,17 to -0,3701	Yes	***	0,0008
Control vs. 0.6uM Fluanxol	-1,875	-2,775 to -0,9747	Yes	****	<0,0001
Control vs. 1.2uM Fluanxol	-1,524	-2,424 to -0,6237	Yes	****	<0,0001
Control vs. 2.5uM Fluanxol	-2,343	-3,243 to -1,443	Yes	****	<0,0001
Control vs. 5uM Fluanxol	-1,909	-2,809 to -1,008	Yes	****	<0,0001
Control vs. 10uM Fluanxol	-1,724	-2,624 to -0,8243	Yes	****	<0,0001
Control vs. 25uM Fluanxol	-0,01567	-0,9157 to 0,8844	No	ns	>0,9999
Control vs. 50uM Fluanxol	-0,2108	-1,111 to 0,6893	No	ns	>0,9999
35-40 min					
Control vs. PTZ	-3,132	-4,032 to -2,232	Yes	****	<0,0001
Control vs. Diazepam	-0,3741	-1,274 to 0,5259	No	ns	>0,9999
Control vs. 0.3uM Fluanxol	-1,4	-2,3 to -0,5004	Yes	***	0,0001
Control vs. 0.6uM Fluanxol	-1,699	-2,599 to -0,7989	Yes	****	<0,0001
Control vs. 1.2uM Fluanxol	-1,731	-2,631 to -0,831	Yes	****	<0,0001
Control vs. 2.5uM Fluanxol	-2,416	-3,316 to -1,516	Yes	****	<0,0001
Control vs. 5uM Fluanxol	-1,622	-2,522 to -0,722	Yes	****	<0,0001
Control vs. 10uM Fluanxol	-1,45	-2,35 to -0,5496	Yes	****	<0,0001
Control vs. 25uM Fluanxol	0,2598	-0,6403 to 1,16	No	ns	>0,9999
Control vs. 50uM Fluanxol	0,289	-0,6111 to 1,189	No	ns	>0,9999